

# **AN APPROACH ON MIGRATION MODELLING**

## **FOR JÁSZSÁG-BASIN, HUNGARY**

**MASTER'S THESIS**

**SZILÁRD DÉNES**

**SUPERVISOR: Assoc. Prof. Dr. habil FERENC L. FORRAY**

**BABEŞ-BOLYAI UNIVERSITY,  
DEPARTMENT OF GEOLOGY,  
CLUJ-NAPOCA, ROMANIA**

**CO-SUPERVISOR: Dr. habil ZOLTÁN UNGER**

**UNIVERSITY OF WEST HUNGARY,  
SAVARIA CAMPUS, SZOMBATHELY  
GEOGRAPHICAL- AND ENVIRONMENTAL INSTITUTE  
GEOLOGICAL DEPARTMENT**

**DEPARTMENT OF GEOLOGY, BABEŞ-BOLYAI UNIVERSITY**

**CLUJ-NAPOCA, 2016**



## **ACKNOWLEDGEMENTS**

This master thesis was accomplished with the approval and support of **OIL&GAS DEVELOPMENT**. I would like to express my gratitude to Abhi Manerikar, Ákos Boros and Gábor Varga, those people from company who allowed this work and helped with professional comments.

I would like to say thank you to Zoltán Unger and Ferenc L. Forray, who supervised and corrected with academic attitude this work. Many thanks to Steve Cloutier and Attila Bartha who gave me advices based on them basin modeler experience. I say thank you to Zhiyong He, who allowed the temporary free use of Genesis software.

Special thanks to **MIGRI TEAM**: Øyvind Sylta, Matthias Daszinnies, Are Tømmerås and Davide Mencaroni, who not just lead me technically in building the Migri model, but supported all the time with their answers and ideas. Thank you for allowing me the free use of Migri during this thesis.

## TABLE OF CONTENTS

<b>1. INTRODUCTION .....</b>	<b>1</b>
<b>2. GEOLOGICAL BACKGROUND.....</b>	<b>2</b>
<b>2.1 The Pannonian Basin.....</b>	<b>2</b>
<b>2.2 Syn-rift sediments of Jászság-basin.....</b>	<b>6</b>
<b>2.3 The hydrocarbon system of Jászság-basin .....</b>	<b>11</b>
<b>3. DATA AND METHODS.....</b>	<b>12</b>
<b>4. GEOMODEL .....</b>	<b>16</b>
<b>4.1 Genesis Workflow-1D modelling .....</b>	<b>18</b>
<b>4.1.1 Data Input .....</b>	<b>18</b>
<b>4.1.2 Heat Flow and Calibration .....</b>	<b>21</b>
<b>4.1.3 Organic Geochemistry .....</b>	<b>29</b>
<b>4.1.4 Results of 1D modelling .....</b>	<b>33</b>
<b>4.2 Migri Workflow-3D modelling .....</b>	<b>44</b>
<b>4.2.1 Data Input .....</b>	<b>44</b>
<b>4.2.2 Calibration and Simulation .....</b>	<b>51</b>
<b>4.2.3 Results of 3D Migration Modelling.....</b>	<b>52</b>
<b>4.3 Probabilistic Approach.....</b>	<b>62</b>
<b>5. CONCLUSIONS .....</b>	<b>68</b>
<b>References .....</b>	<b>70</b>

## **1. INTRODUCTION**

### **The Topic**

As member of research group at University of Babes-Bolyai, Cluj-Napoca, (according to the contract between UBB and Sand Hill Petroleum Romania BV), which project is to investigate the relation of methane and salt in Transylvanian Basin, my task was to model the generation of biogenic gas in basin. Initially this topic seemed to be perfect theme for MSc thesis. Due to lack of data this ought to been cancelled, but remaining alongside the subject of modelling the Jászság-basin was chosen as exploration area. The territory of Jászság-basin recently does not owns any company as concessionary area, thus the data availability was easy and free access. These were the major reasons changing the initial area, and my investigation results are shown in thesis.

### **Aims of Study**

The petroleum industry is increasingly based on computerized methods in exploration for new hydrocarbon fields. The widely prevalent seismic methods completing with the evolving geological model building could be a good source to increase the success of explorations.

The aims of this study are to investigate the methods of modelling the migration of oil and gas through geologic time and to determine the leading forces and parameters of it. In addition the aim of unraveling the role and importance of probabilistic modelling based on 3D basin scale simulation techniques was set.

The thesis has the following main parts:

- (1)** general overview of the studied area;
- (2)** description of data and methods;
- (3)** building of the geological model;
- (4)** introduction to probabilistic modelling;
- (5)** conclusions;

hence targeting the learning of modelling steps and exploring the main ideas of migration based basin modelling and the associated risk-domains.

## 2. GEOLOGICAL BACKGROUND

### 2.1 The Pannonian Basin

The Pannonian basin is an extensional back arc basin situated within the Alpine, Carpathian, and Dinaric mountain belts. The basin system was formed due to lithospheric extension during the Late Early to Late Miocene times (Gábor Tari & Horváth, 1992). Structurally can be divided in two tectonostratigraphic mega units, on the norther part is found the **ALCAPA** mega unit (Faupl, P., Császár, G., Mišik, 1997) (**Alpic-Carpathian-Pannon** region) and the southern part is build up by the Tisza-Dacia Microplate. The Mid-Hungarian Shear Zone can be considered as a wide boundary line between the two mega units. During the early Oligocene, the subduction of Magura Ocean and its roll-back effect (Balla, 1984) allowed the approaching movement of the two microplates realized with a southern hiking of the Tisza-Dacia unit and an eastern hiking of the ALCAPA unit (Csontos, Nagymarosy, Horváth, & Kováč, 1992). The thinned lithosphere due to a mantle upwelling event which led to a series of transtensional and transpressional displacements in the Late Early Miocene (Gábor Tari & Horváth, 1992). This divided morphology is defined by the heights of the substratum and resulted the formation of a bunch of initial sub-basins inside the Pannonian Basin, like the studied Jászság-basin (Figure 1). One of the results of the Early Miocene mantle upwelling is a basin dominated by high surface heat flow ( $80\text{-}120 \text{ mW/m}^2$ ) trough geologic time, compared to the adjacent average continental values ( $50\text{-}60 \text{ mW/m}^2$ ) (Lenkey L., Dövényi P., Horváth F., Cloething & L., 2002). Based on subsidence analysis and geophysical data, in terms of geodynamic the Pannonian Basin can be divided in two main phases. Royden et al. (1982) separated the syn- and post-rift phases, although recent structural analyses revealed a more complex evolution (Fodor, Csontos, Bada, Görfi, & Benkovics, 1999).

The syn-rift phase started (~18 Ma) with a large scaled division of the lithosphere which was accompanied by volcanic activity (G Tari et al., 1999). Next to this the thinning and stretching of the lithosphere –known as the rift phase in the Pannonian Basin– is researched and proved by many authors (Lenkey L., Dövényi P., Horváth F., Cloething & L., 2002; Sclater, J. G., Royden, L., Horváth F., Semken, S., Stegna, 1980). The stretching factor of the crust ( $\beta$ ) and of the crustal lithosphere ( $\delta$ ) respectively the thinning factor ( $1/\beta$ ;  $1/\delta$ ) are derived from the post-rift thicknesses. In the case of Pannonian Basin Sclater et al. (1980) presupposed for the stretching factor a  $\beta=1.8\text{-}2$  value and for the thinning factor a  $\delta \rightarrow \infty$  value, assuming the possibility of disappearance of the crustal lithosphere. This estimated values obtain importance in thermal modelling of the studied area (Chapter 4.1). The syn-rift phase of ~18–12 Ma resulted in the formation of numerous grabens

filled with relatively thin syn-rift sediments of marine to brackish origin, while in the higher structural position situated basin margins were characterized by shallow marine sedimentation with sandstones and limestones (Bérczi, 1988; Vakarcs et al., 1994). The syn-rift crustal extension was followed by the thermal subsidence of the basin as a result of the lithospheric mantle updoming and subsequent thermal contraction (Horváth & Royden, 1981). At the end of the Middle Miocene the cessation of the syn-rift faulting is related to the end of thrusting along the Carpathian arc (Bada et al., 2007). At the same time a series of tectonic events in Alpic-Dinaric region due to a new phase of deformation, determined as inversion of Pannonian Basin (Fodor et al., 1999; Horváth, 1995).

The post-rift (~12–5.3 Ma) subsidence was compensated with the intense sedimentation of the Lake Pannon, which started its evolution around ~11.5 Ma (Piller, Harzhauser, & Mandic, 2004; Uhrin, Magyar, & Sztanó, 2009), age determined by fauna changing events related to the disconnection of Central Paratethys and External Paratethys (Rögl, 1998). The syn-rift sedimentation can be characterized by progressively filled up deltaic to littoral sediments, which sedimentation turned into fluvial by the end of the Miocene (Vakarcs et al., 1994).

The transgression of the Lake Pannon started simultaneously with the thermal subsidence of the basin (Sclater, J. G., Royden, L., Horváth F., Semken, S., Stegna, 1980) obtaining its maximum dimension around 9.8 Ma ago (Sztanó, Magyar, & Horváth, 2007). The combination of divided substratum and thermal subsidence increased the difference between the positive and negative morphologies and due to the formation of deepest sub-basins and highest ridges (G Tari et al., 1999). At the same time started the sedimentation of deep water marls (*Endrődi Formation*) which occurrence on the basin margins can be explained with the high water level covering the structural highs also (Sztanó et al., 2013). The maximal flooding surface was followed by the filling up phase (~6 Ma) of the basin, which sediment input was ensured by the clastic material of the uplifting Alpine region (Sztanó et al., 2013). In the deep basin the deposition of marls continued while in the foreground of prograding slope clinoforms (*Algöyi Formation*) (Pogácsás, 1984; Révész, 1980) turbiditic sediments (*Szolnoki Formation*) were depositing (Juhász, 1994; Uhrin & Sztanó, 2012). The deposition path of the filling sediments from the continental source to deep basin went through on continuously building deltaic systems (*Újfalúi Formation*) situated on the “shelf” margins (Mucsi & Révész, 1975; Révész, 1980; Sztanó et al., 2013). The evolution of the prograding shelf margins from NE-NW to S-SE (Mucsi & Révész, 1975; Sacchi, Horváth, & Magyari, 1999) direction was slowed by the intervening sub-basins. The progradation of shelf margin resulted the

filling up of the basin, and as consequence of the second Miocene/Pliocene inversion related to a compressional field in region (Bada et al., 2007; Uhrin et al., 2009) the present day morphology was formed (Lenkey L., Dövényi P., Horváth F., Cloething & L., 2002). In the background of the prograding deltaic systems the territory was covered by alluvial plains and (*Zagyvai Formation*) (Juhász, 1998) and rivers which during the Pliocene accumulated more than 1000 m sediment. Around 4 Ma ago the shelf margin reached its southern position and the most significant part of the Lake Pannon evolution ended (Magyar, Geary, & Müller, 1999).

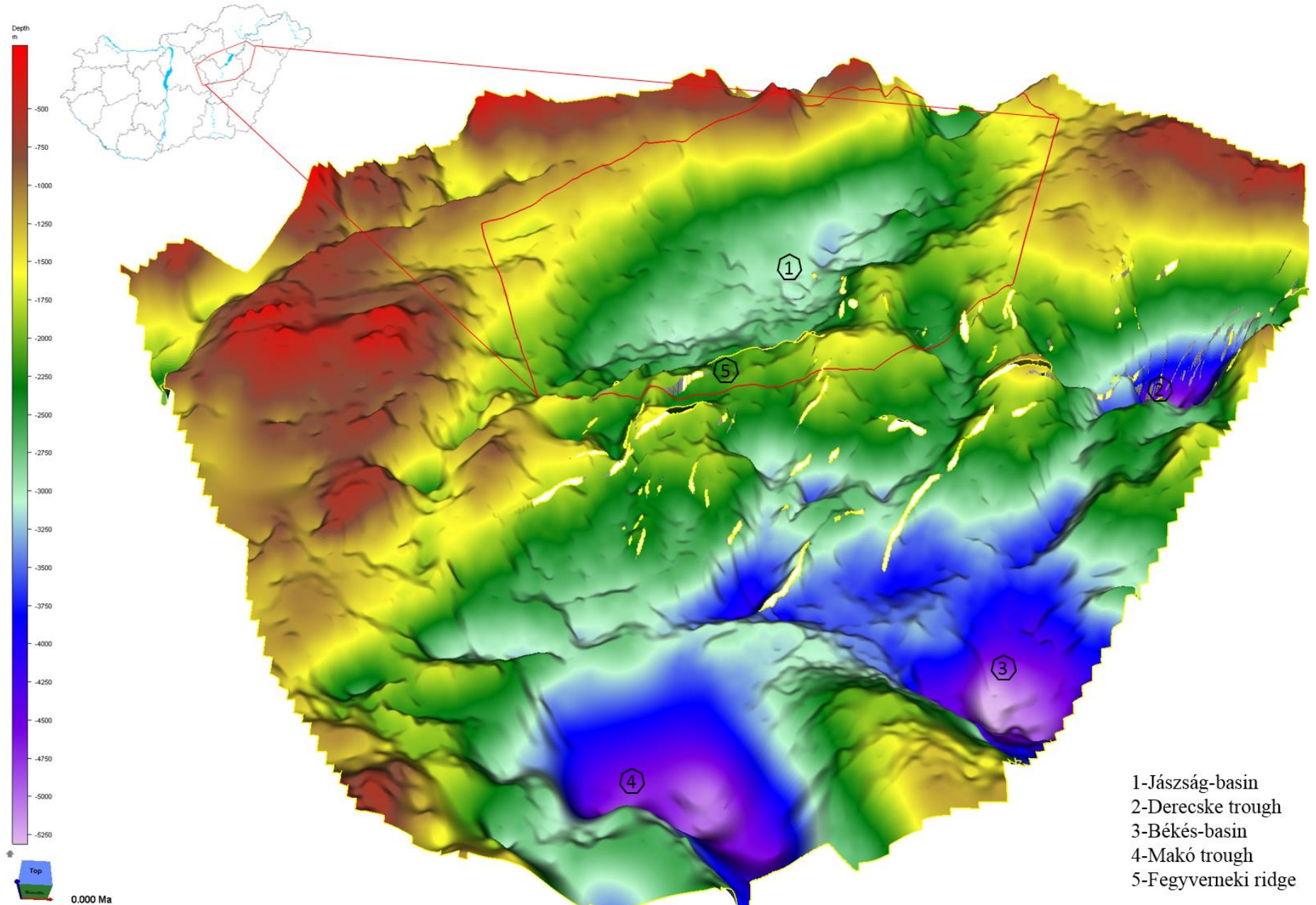


Figure 1: Overview base Pannonian depth map, displayed in 3D view by Migri, highlighting (red lines) the studied area (company data, G.Varga).

## 2.2 Syn-rift Sediments of Jászság-basin

The appearing sedimentary successions of studied area of this work are discussed within the framework of seismic interpretation.

Juhász (1993) identified the presence of both previously discussed main sedimentation input pathways in the case of Jászság-basin. The progress of intermeshing of the sedimentation was intensified by the presence of the Fegyvernek-ridge, which formed a natural barrier and reimbursed the NW-directional sediment input to East and delayed the progradation of north-westward shelf margin (Juhász, 1998).

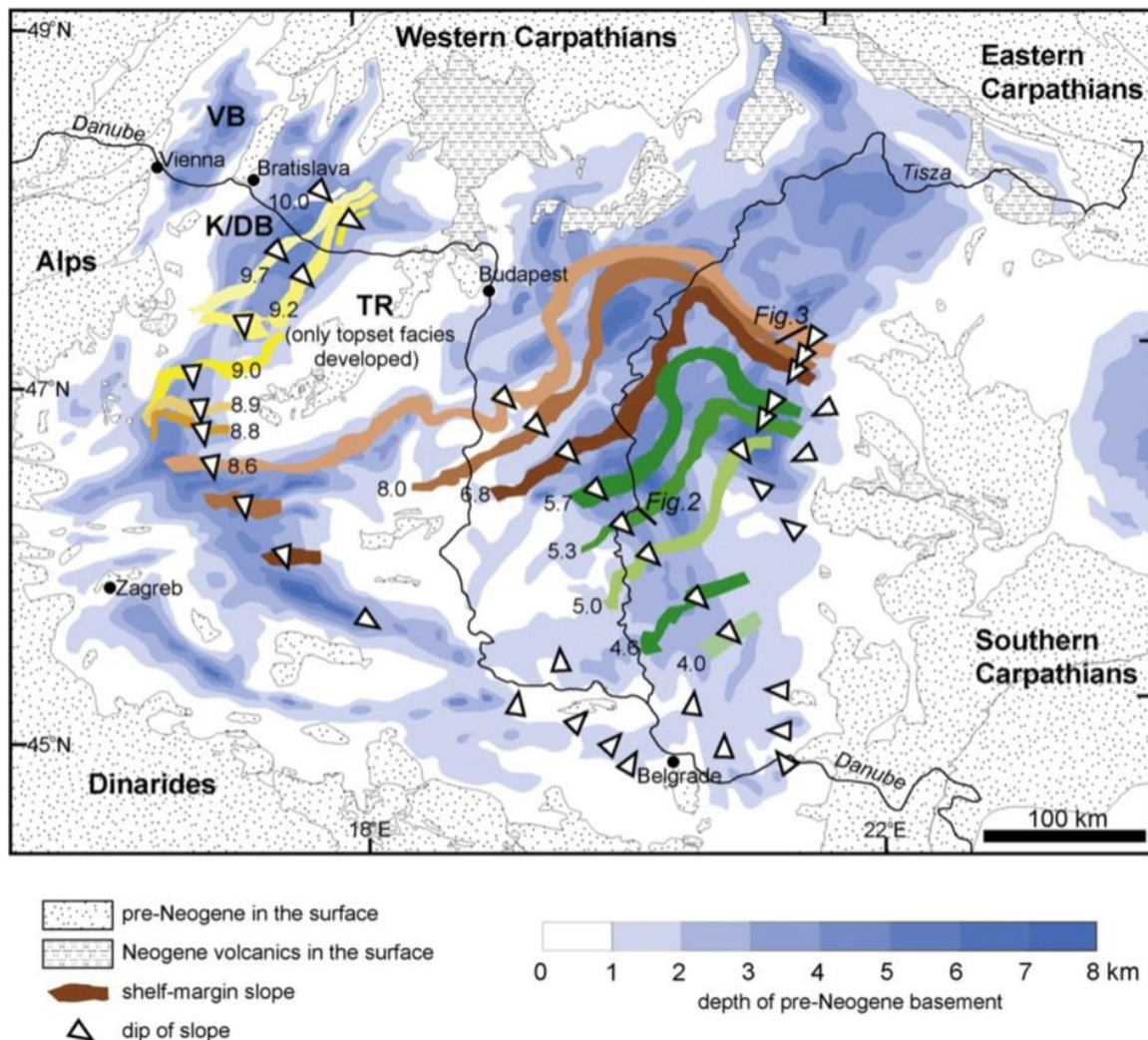


Figure 2: Progradation of the shelf-margin slopes across the Pannonian Basin during Late Miocene and Early Pliocene times (Magyar et al., 1999).

The deposition of sedimentary facieses, besides the changing sediment input and substratum morphology, is widely affected by relative water level changes in the Lake Pannon. This topic in Pannonian Basin is poorly understood and highly contentious by numerous authors, the interpretation/correlation of regional water level changes to global sea level changes representing the subject of debate (Csató, 1993; Juhász, 2007; Sztanó et al., 2013; Sztanó, Magyar, & Horváth, 2007b; Uhrin & Sztanó, 2012; Vakarcs et al., 1994). The importance of sequential stratigraphic interpretation consist in determination of the timing-, thickness- and location of discussed sedimentary facieses. These characteristics are the main input parameters of the modelling work. The age of sedimentation defined by isotopic measurements and based on biostratigraphy can be extended as chronostratigraphic tops/horizons allowing the method of seismic interpretation. A bunch of sequential stratigraphic interpretation were made by Pogácsás et al. (1989, 1994), Vakarcs et al. (1997) and Juhász et al. (2006, 2007) concerning the exploration area i.e. Jászság-basin. The regional seismic interpretation, and in basin scale mapped horizons (used in followings *hAge*; *h*-horizon; *Age*—age associated to horizon) are based on the mentioned works (Figure 3). The data set and the process of seismic interpretation are detailed in Chapter 3. The characterization of the in Jászság-basin deposits are discussed below through formations in the order of chronostratigraphic seismic horizons from the older to younger sequences. Based on the interpretation of Vakarcs (1997) interpretation three 3<sup>rd</sup> order sequence boundary (***Pa-3 – 9.2 Ma***; ***Pa-4 – h6.85 Ma***; ***Pa-5 – h5.3 Ma***), three 4<sup>th</sup> order sequence boundary (***h8.3 Ma***; ***h7.5 Ma***; ***h7 Ma***) horizons were determined. Based on well data the top horizon of *Endrődi Formation* (age assigned with high uncertainty: ***h8.8 Ma–h8.3 Ma***) and the base horizon of the formation (***h12.6 Ma***) was interpreted. The ages assigned to formations in some cases are covering/overlapping each other (Table 1), because of the discussed intermeshing of two directional sediment input and the chronostratigraphic interpretation cannot be related straight to the lithostratigraphic units.

top horizon	from [Ma]	to [Ma]	facies 1	facies 2	facies 3	facies 4
–	2.4	0	<i>Quaternary</i>			
<b><i>h 5.3 Ma</i></b>	5.3	2.4	<i>Zagyvai Fm</i>	<i>Újfalui Fm</i>		
<b><i>h 6.85 Ma</i></b>	6.85	5.3	<i>Zagyvai Fm</i>	<i>Újfalui Fm</i>	<i>Algyői Fm</i>	
<b><i>h 8.3 Ma</i></b>	8.3	6.85	<i>Algyői Fm</i>	<i>Újfalui Fm</i>	<i>Szolnoki Fm</i>	<i>Endrődi Fm</i>
<b><i>h T_Endrődi</i></b>	8.8	7	<i>Szolnoki Fm</i>	<i>Endrődi Fm</i>		
<b><i>h 12.6 Ma</i></b>	12.6	8.8	<i>Endrődi Fm</i>	<i>Szolnoki Fm</i>		

Table 1: The used (highly uncertain) age and formation assignment.

### ***Endrődi Formation-( $\sim$ 12.6 Ma – $\sim$ 8.8 Ma)***

The belonging sediment succession is created by hemipelagic marls. The average thickness of the formation is 200 m with a 700 m maximal thickness. The water depth of the deposition environment is estimated from 15 m to 800 m. The pre-Pannonian bedrock of the formation is dominated by silty tuffs, the cap rock is represented by the *Szolnoki Formation* or *Algyői Formation*. The older sequences were deposited in shallow-water environment containing calcareous marls with a constant transition to deep water marls to younger sequences. The uppermost also younger parts can have intercalated turbidites (Juhász, 1998).

### ***Szolnoki Formation-( $\sim$ 8.8 Ma – $\sim$ 7 Ma)***

The formation is determined as deep water turbiditic succession including all the elements of gravitational sedimentation. It is characterized by the alternation of sandstones with siltstones and clay marls. The sandstone in the lower part of the facies occurs as thick amalgamated units, mostly very fine grained turbiditic sandstone. Well logs indicate that several sandstone units has 30 m thickness representing 50 – 70% of the sequence. In some cases completely can be distinguished on the lower part of formation the distal turbiditic character. The formation with a maximal 1000 m thickness is situated between the *Endrődi Formation* (bedrock) and *Algyői Formation* (caprock) (Juhász, 1998) .

### ***Algyői Formation-( $\sim$ 8.3 Ma – $\sim$ 6.85 Ma)***

This succession of sedimentary beds were deposited in a prodelta-slope environment. The formation is dominated by alternating siltstones with marls intercalated with sandstones. The sandstone beds generally has less than 10 m thickness and represents only 10 – 20% of the sediments. The percentage of the sand fraction is variable and it is most frequent in the lower part of the formation. Due to the variations of the current intensity along the slope the sand bodies are probably discontinuous (Mattick RE, Rumpler J, Ujfalusy A, Szanyi B, 1994). The formation thickness varies between 200 – 1000 m. The upper boundary of formation coincides with the Upper- and Lower Pannonian limit, which age are younger to south-eastern direction in basin (Juhász, 1998). The cap formation is the *Újfalui Formation*, the underneath formation could be the *Szolnoki Formation* or *Endrődi Formation* (Juhász, 1998).

### ***Újfalui Formation-(<sub>h</sub>6.85 Ma –Quaternary)***

The delta-plain and delta-front formation contains fine to medium grained sandstones with marl and siltstone intercalations. The sandstones represent about 50 – 60% of delta plain deposits. The sand bodies occur as distributary-channel sands reaching 20 m thickness, with an average of 10 m. (Mattick RE, Rumppler J, Ujfalusy A, Szanyi B, 1994). The lower boundary of the formation is easily to define from the *Algöi Formation*, in the case of missing *Zagyvai Formation* the covering formation cannot be always delimited.

### ***Zagyvai Formation-(<sub>h</sub>6.85 Ma –Quaternary)***

The alluvial-plain deposits are mostly sandstones and sands. The sand or sandstones represents not more than 50 % of the deposits and generally the bed thickness is less than 5 or 10 m. The rest part of the section is formed by alternating and weakly compacted siltstones and alluvial marls (Juhász, 1998). The average thickness of the formation is 300 – 900 m, the lower boundary being represented always by *Újfalui Formation* and the upper boundary are quaternary sediments (Juhász, 1998).

The closing sediments of the area are determined quaternary succession. This contains alluvial unconsolidated silty clayey sediments which attempt to delimitation in seismic surveys was not made.

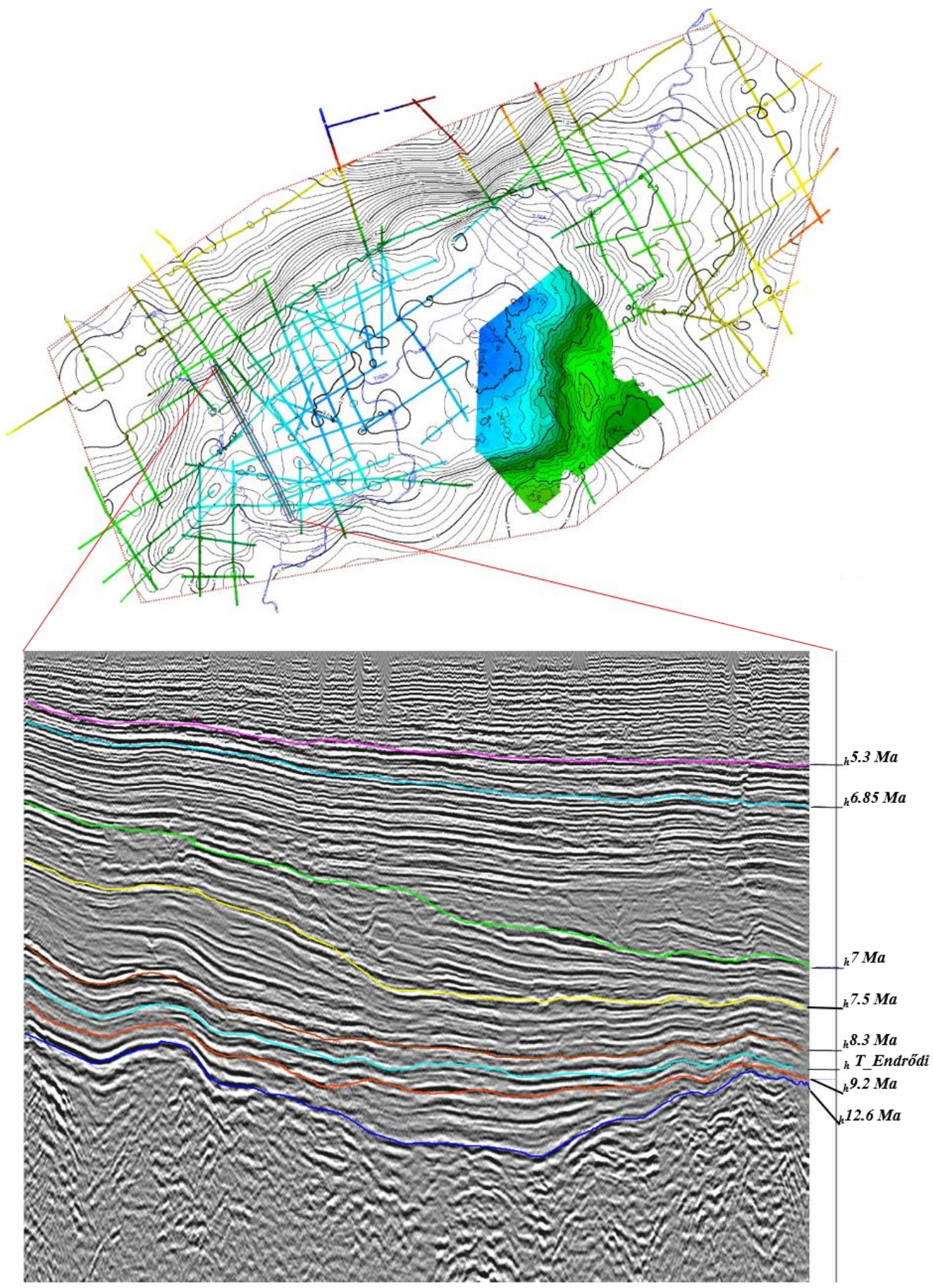


Figure 3: Non scaled map of the interpreted seismic lines from the area of study and an example survey (TWT) showing the discussed horizons.

## **2.3 The Hydrocarbon System of Jászság-basin**

### **Source rocks**

In the Neogene section of the Pannonian Basin the Middle to Late Miocene marls and clay marls are considered as main source rocks and can be characterized with a low quality regarding to TOC% and HI average values (Dolton, 2006). In Jászság-basin the marls and calcareous marls of *Endrődi Formation* are considered as source rocks. This sediments contain Type II-oil generator and Type III gas generator kerogens estimated with a 33% (Type II) 66% (Type III) ratio.(Badics & Vétő 2012). Dolton (2006) and Badics (2012) based on their collected data estimated an average TOC=1.8 % and HI= 280 mgHC/gTOC for the Pannonian Basin. Based on available well data and seismic data considering the mentioned authors estimations the studied area can be endowed with a 1.5% TOC and 180 mgHC/gTOC hydrogen index. In model for source rock thickness a 125 m average can be applied. The oil window started its evolution ~ 8 mA at 2200 m depth, but the thermal history of the basin and the measured Ro% data is not suggesting the possibility of presence of the gas window.

### **Reservoirs**

In Pannonian Basin the Neogene sediments are the most significant reservoirs, representing 80% of all reservoirs from basin (Dolton, 2006). Pannonian reservoirs are the most productive which include shallow water sandstones and conglomerates of fluvial, marine, and lacustrine origin as well as turbidites, marls, algal and freshwater limestones. The average porosities of Neogene syn-rift reservoirs varies from 5% to 30% while the average porosity value of post-rift sediments is 22% and represents a wider varying range between 8% and 40% (Dolton, 2006). In case of Jászság-basin the *Szolnoki Formation* and *Újfalui Formations* can be considered as main reservoirs.

### **Traps and seals**

The depth range of producing traps in the Pannonian Basin varies between 80 and 5000 m, the most oil occurring between 800 a 3000 m the gas somewhat deeper (Dolton, 2006). A great combination of structural and stratigraphic traps is present in basin. The set of structural traps is represented by: fault-closed features, roll-overs associated with growth faults, compaction anticlines over basement highs and closures in flower structures along strike-slip faults. The stratigraphic traps are secondary mostly represented by truncations and unconformities. Seals in basin are provided by fine-grained sediments, particularly middle to upper Miocene shale, clay-marl, and marl (Dolton, 2006). In the case of Jászság-basin the shales of *Algői Formation* and *Zagyvai Formation* are considered as seals.

### **3. DATA AND METHODS**

#### **Seismic Data and Interpretation**

The seismic database used for this study consist ~63 2D seismic lines and one 3D seismic package (Figure 4) with high resolution DRS horizons (horizons generated by **Detailed Reconnaissance Study Workflow**). The seismic interpretation was made in TWT domain supervised by the experts of the company. The objective of this part was to produce time maps by interpreting the available seismic data. In total 8 horizons were interpreted in the studied area based on seismic stratigraphy method considering as starting-point the interpretation work of researchers (Csató, 1993; Juhász, Pogácsás, Magyar, & Vakarcs, 2007; Vakarcs et al., 1994) related to Jászság-basin. The interpretation work was carried in the software IHS Kingdom 2016. The large scaled age-formation assignment shown in the Table 2 was used as layer input during the building of geological model.

#### **Well Data**

The well database contains ~70 wells. The wells were used on the exploration area to specify certain rock-physical/ layer condition parameters. The used input data from the wells can be grouped as follows: temperature data, lithology data, geochemical data (**TOC%, HI, Ro%, Rock-Eval**), hydrocarbon column/accumulation data (well test results). The selected wells, with input data are shown in Figure 4.

#### **Gridding Method**

The goal of gridding is to resample the data points on a regular grid. At each new grid point, this estimation method uses interpolation from the values of the existing nearest data points. The set of interpolation schemes represents a large selection and due to prior experiences the scheme of Kriging (interpolation by a Gaussian process) was generally used in this work. The gridding method was applied in several steps in order to extrapolate data to the uncovered areas. Data extrapolation needed in generation of time maps from the interpreted horizons. The accuracy of time maps depends on the quality of the seismic data, on topography and on the available data density. For this purpose a grid size of 150 x 150 was selected with a medium smoothing process inside the bounding polygon of the area (Figure 4). The method to extrapolate the available well data- situated as point data in different depths in space- consist in two steps: (1) to define the intersection points of well and mapped layers; (2) to calculate average values to the delimited

thicknesses by layers and apply them as XY value of the top layer. For property gridding a grid size of 150\*150 was generally used.

## Depth Conversion

Depth conversion is a process of converting the seismic data and the linked horizons/grid maps from time depth domain into real depth domain. The concept of depth conversion is based on the basic velocity offset defined in the following equation:

$$d = \frac{v * twt}{2},$$

where  $d$  –depth (m),  $v$  –velocity (m/s),  $twt$  – two way travel time (s).

The process of depth conversion is highly stressed with uncertainty which increases with depth, because of major changes in geology. In this work the depth conversion was made through velocities from one well, which satisfies the accuracy of a large scaled basin model with low data coverage. The accuracy of depth conversion in case of sufficient data can be increased with generating velocity maps choosing one from the large range of conversion methods. With this process the time maps generated by gridding method from the interpreted horizons was transformed into depth domain, and used as main layers in 3D geological model.

## TDL-Data

Building a geological model is indispensable the use of data which reflects the conditions for the Time of Deposition of the Layer (used in followings as **TDL**). TDL data were used during the building of 1D model (paleolatitude, paleo water depth, sediment surface) – this mostly linked to research data – and TDL plus modelled/estimated data was extrapolated by gridding and used in the form of property grids building the 3D model. In some cases the modelled or estimated (by other authors) TDL data were checked and corrected by back-calculation methods. An example for the back-calculation is given below in relation to the measured present day TOC% values (the explanation of geochemical data is described in Chapter 4.1):

### Input data:

$TOC_x$  –present day total organic carbon content

$HI_x$  –present day hydrogen index calculated from Rock Eval analysis results

$HI_0$  – original hydrogen index assumed from kerogen type – in this case after Pepper & Corvi (1995): 333 mg/gTOC

$PI_x$  – production index calculated from Rock-Eval analysis results

$PI_0$  – original production index assumed value: 0.02

### **Output data:**

$TOC_0$  – original total organic carbon content

$f$  – transformation ratio

#### **(1) Fractional conversion calculation for measured TOC%**

$$f = 1 - HI_x \cdot \{1200 - [HI_o / (1 - PI_o)]\} / HI_o \cdot \{1200 - [HI_x / (1 - PI_x)]\}$$

#### **(2) Original TOC calculation**

$$TOC_o = 83.33 \cdot HI_x \cdot TOC_x / [HI_o \cdot (1 - f) \cdot (83.33 - TOC_x) + (HI_x \cdot TOC_x)]$$

The above equation after Peters (2005) was used to back-calculate the measured TOC% values from the area of thesis (3 examples below). The results were extrapolated by the method of gridding to the generated depth surface layers.

	$TOC_x$	$HI_0$	$HI_x$	$PI_x$	$PI_0$	$f$	$TOC_o$
<b>Well-1</b>	1.55	333	200	0.2	0.02	0.47179	1.7225
<b>Well-2</b>	4.49	333	180	0.2	0.02	0.5368	5.09259
<b>Well-3</b>	0.66	333	171	0.2	0.02	0.56498	0.75349

Table 2: Examples of back-calculated TOC% values in three wells.

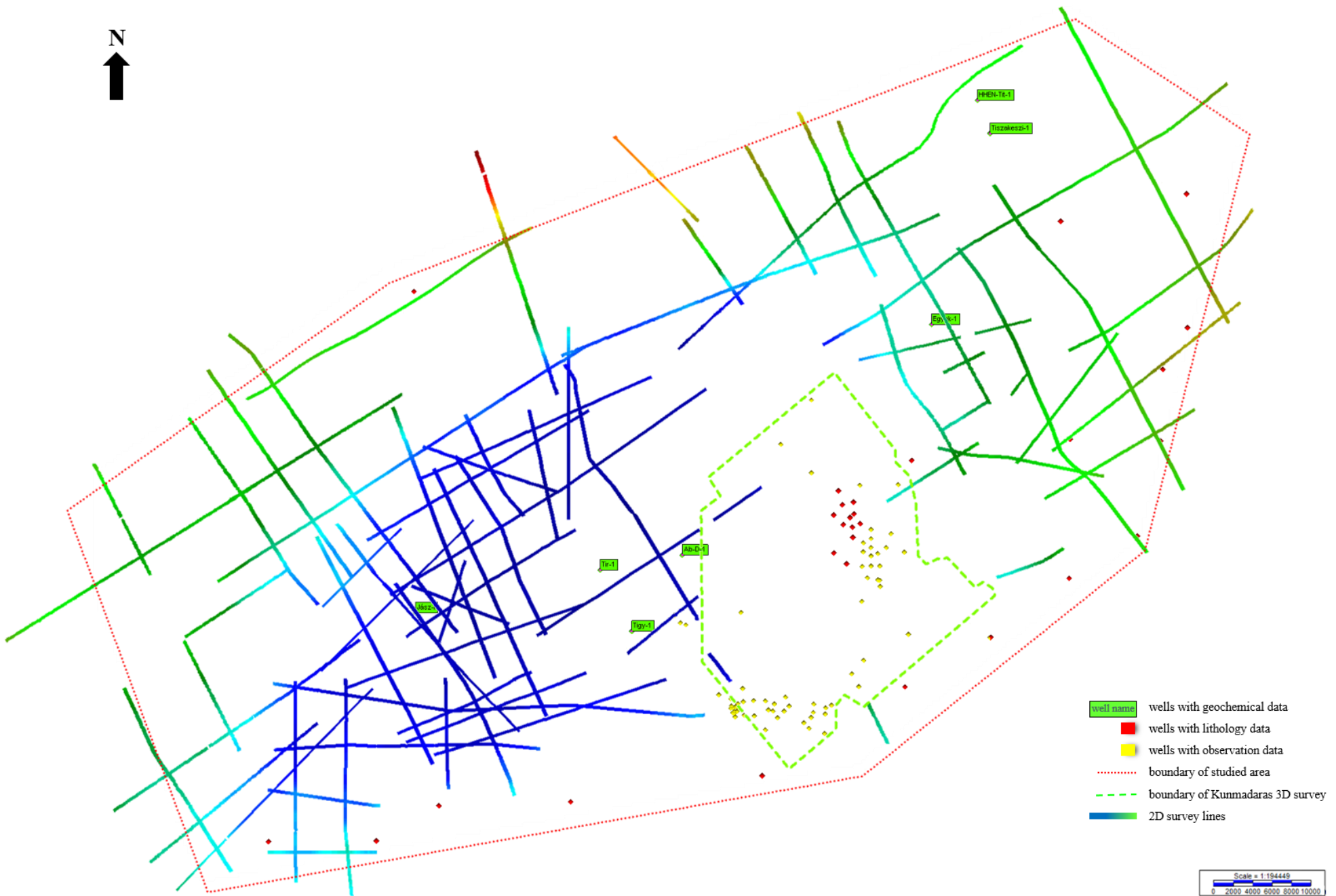


*Figure 4: Database overview of the studied area.*

## 4. GEOMODEL

The geomodel building is a method, which merge the result of seismic interpretation, depth map generation and well data gridding processes. In this part will be shown the methodology and results of 1D-, 2D modelling and an experiment to the probabilistic simulation runs. The method of basin modelling aims the geological events reproduction of at the most accurate way. It is a very common geological method, and helps a better to understanding processes, like the basin evolution on hydrocarbon generation and migration. The basin models are based on stratigraphic, tectonic, geophysical, geothermic and geochemical data, these data are coming mostly from wells, and exploration and research reports and studies. The approach provides three basic outcomes: the burial history, the thermal history and hydrocarbon generation models. This establishes the input data to migration modelling.

The methods of modelling, and the process of calibration can be **deterministic**, when the input are discrete values, or can be **probabilistic**, when the parameters has a range of varying values and the results are not discrete values but distribution. During the analysis the task is to choose the best fitting model scenario (Figure 5). The 1D- and 3D model is built by deterministic method and the principles of probabilistic modelling are discussed in Chapter 4.3 with an example.

Building a basin model allows us to investigate all the elements of presumed hydrocarbon systems. The aim of this tool/method is the control for possible existence and maturity of the source rocks, the timing, quality and quantity of the generated hydrocarbons – depending on software capabilities, thus the hydrocarbon migration scenarios can be investigated.

Based on data and software the models can be: 1D-, 2D-, or 3D dimensional. In case of 1D models the thermal - and subsidence history of the studied area is reconstructed based on well or pseudo-well locations using the well information. In case of 2D-, and 3D models the evolution history of a territory is restored on seismic data, which is vital. The input data can also be divided into three parts considering the accuracy. The measured data are the most accurate with possible errors related only to measurements. The derived data carry the possibility of calculation errors, while the estimated data is the least reliable. These were used only in case of full lack of measured data.

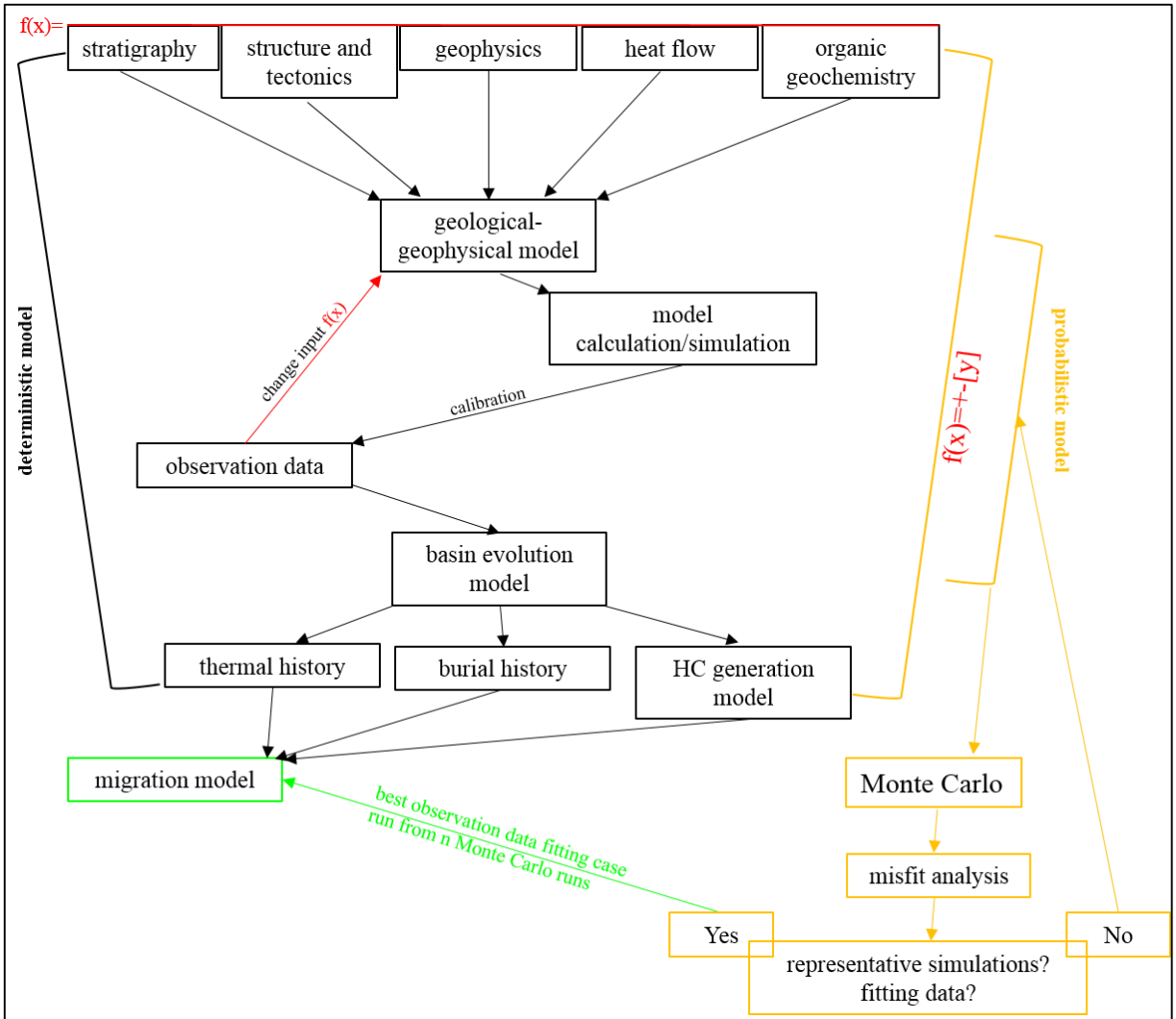


**Figure 5:** The modified diagram of basin modelling (Horváth et al., 1986), presenting the deterministic way of modelling (middle and left part of the flowchart) and the addition of uncertainties to the model by probabilistic methods (right part of the flowchart) where:

$f(x)$  – presents the set of varying parameters by each Monte Carlo run with  $+y$  value;

misfit analysis – represents the restriction of results of the Monte Carlo runs by statistical processes;

Two software packages were used in this study. To evaluate the potential properties of the possible source rocks and to assume a basic basin evolution 1D model the product of **Zetaware Genesis** was used. To build a 3D model, which exceeds the results of general basin models and focuses to the issue of migration, the **MigriX** (limited version) and **Migri** (full version) was used. The sketch of migration model building steps is as follows:

- data collection/seismic interpretation/depth map generation
- 1D model building with calibration
- by gridding: extrapolate the collected and modelled (1D) data to depth layers
- 3D model building: calibration/ evaluation/ series of simulation

## 4.1 Genesis Workflow-1D modelling

### 4.1.1 Data input

#### Well Data

Based on the available well data, 5-7 wells with temperature and thermal indicator data were selected to 1D modelling work. Two wells were treated as key wells (Jászladány-I, Abádszalók-D-1) since they contained calibration data. The calibration method in case of 1D models is based on the comparison of the measured and modelled vitrinite reflectance and temperature data. Four of the selected wells have Rock-Eval data, which helps us in the characterization of potential source rocks. The available data of wells is listed in Table 3.

Well Name	NS_UTM	EW_UTM	Total dept	KB [m]	Lithology	Temperature	Rock Eval	Ro%	other
Tiszakeszi-1	274343.41	797199.46	2144	90.4	y		y		
Abádszalók-D-1	231201.05	765604.49	3150	89.65	y	y	result	y	
Egyek-1	254811.92	791230.06	2900		y		y	y	
Tiszaroff-1	229696.48	757211.15	3200	92.66	y				y
Jász-I	225293.97	738247.11	3800	93.05	y	y		y	
Tiszatarján-1	277747	795920	2794		y		y		
Tiszagyenda-1	223411.79	760440.7	3161	93.17	y				y

Table 3: Used wells with the available data types.

#### Lithostratigraphy Input

The Genesis requires a less detailed lithostratigraphy column (which indicates a low impact factor for this input data) with formation tops or layers which are associated with exact chronostratigraphic tops. Since the Pannonian basin was filled with inter-fingering deltaic systems during the Late Miocene the lithological or facies changes cannot be related to exact ages. In order to fulfill the software requirements the age assignment defined in Table 1 was used. As a rough facies definition the lithology distribution shown in Table 4 was used.

Formation	Petroleum System Element	Lithology	Genesis Lithology
Quarter	sandstone (clay rich)	sandstone (clay rich)	shaly sand
Zagyvai Formation	seal rock	shaly silt	silt33/shale33/shaly sand33
Újfalúi Formation	reservoir rock	sandstone	sandstone80/silt10/shale10
Algyői Formation	seal rock	silty shale	shale80/silt20
Szolnoki Formation	reservoir rock	sand+shale	marl25/silt45/sandstone30
Endrődi Formation	source rock	marl	marl

Table 4: Large scaled lithology assignment used for Genesis input.

## Paleo Water Depth

The paleo water depths are considered as an important input data and can be estimated from well data and seismic interpretation. These data are used in Genesis for the burial history reconstruction. The changes of paleo water depths could be influenced by: accommodation space, eustatic sea level changes and sedimentation input rate.

In Pannonian basin the main factor of water level changing is the sediment input of prograding deltaic systems which has exceeded the rate of thermal subsidence of the basin(Juhász, 2007). The modelling study of the potential source rocks from presumed kitchen areas based on 2D seismic interpretation is not included in our case since several similar studies have already been published in this area (Csizmeg, Juhász, Milota, & Pogácsás, 2011). Therefore, the paleo water depth estimations were made using the previously mentioned studies, and took/used the USGS data and research results of Horváth et al. (1986).

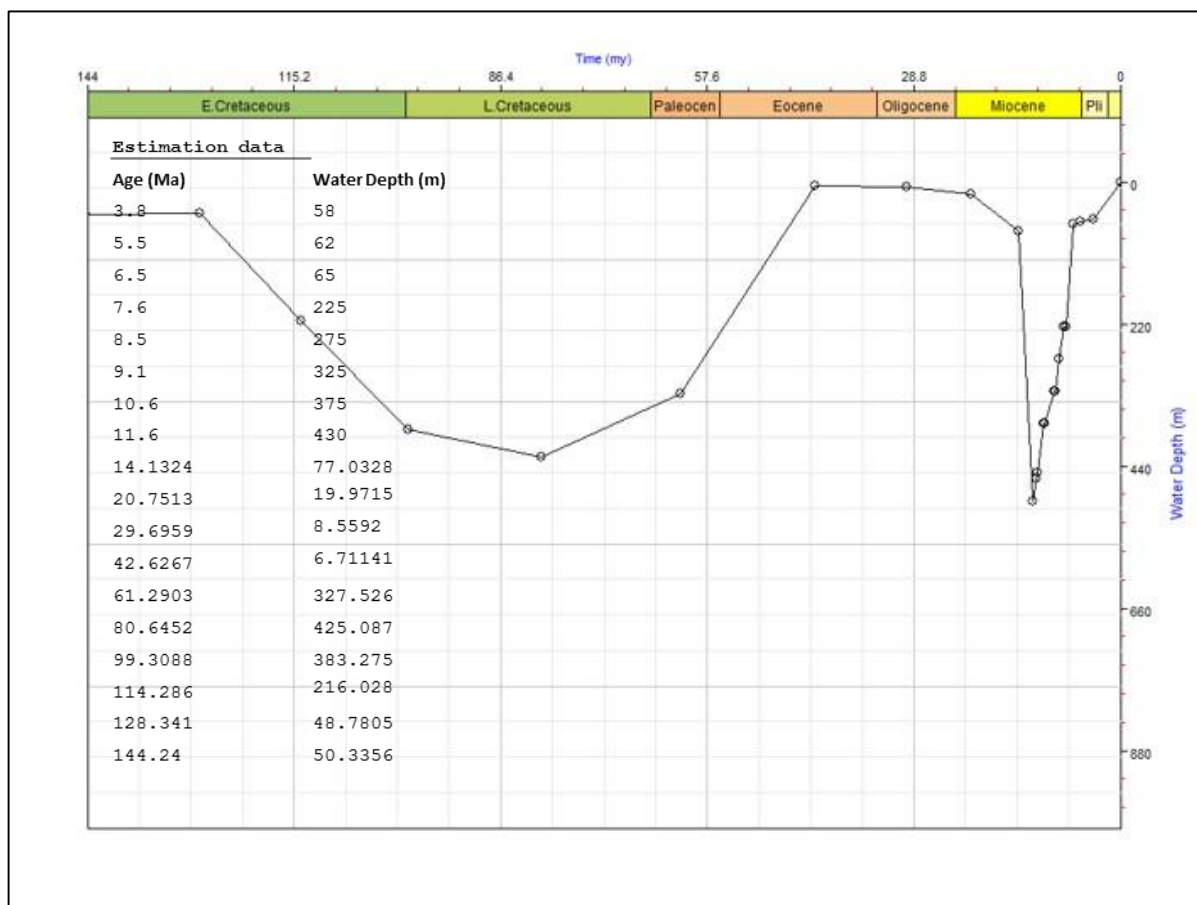


Figure 6: Estimated paleo water depth input for 1D model.

## SWIT/Paleolatitude

For upper boundary condition in Genesis the **Sediment Water Interface Temperatures (SWIT)** should be defined. It is a complex procedure where the exact paleoclimate conditions has to be restored. The Genesis unlike other basin modelling software does not contain a SWIT module therefore the results of the PetroMod surface temperature calculator (Wygrala, 1989) was applied for the studied area (Figure 7).

In a paleomagnetic research study Panaiotu (1998) determined and compared the timing of the rotation events and measured paleolatitudes in the Transylvanian Basin. The results of this study can be applied in the Transdanubian Central Range Domain and Pannonian Basin with a 95% confidence, and they were integrated in our model as a curve.

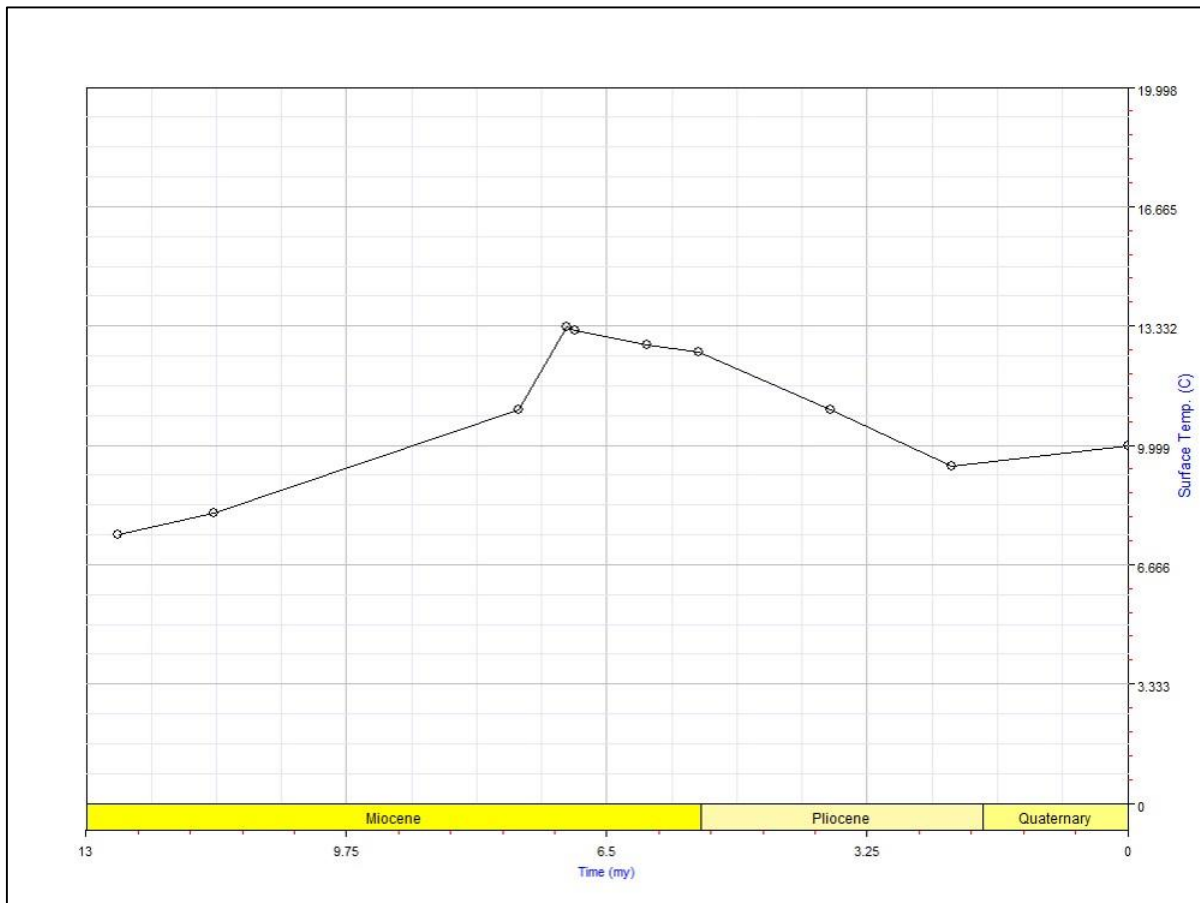


Figure 7: Applied Sediment Water Interface Temperature curve for 1D model.

#### 4.1.2 Heat Flow and Calibration

The heat flow is the most important factor which influences and controls the maturation of organic rich sediments and the hydrocarbon genesis. Heat flow is heat thought of as energy flowing from one substance to another; quantitatively, the amount of heat transferred in a unit time (McGraw-Hill Dictionary of Scientific & Technical Terms, 2003) The heat conductivity law states, that a temperature difference between two locations causes a heat flow **Q**. Its magnitude depends on thermal conductivity of the material and the distance between two locations.

$$Q = k * (T_k - T_o) / d,$$

**k**-layer heat conductivity, **T<sub>k</sub>**-layer temperature, **T<sub>o</sub>**-surface temperature, **d**-depth

The actual heat flow it is easy to calculate with the given equation, where the heat conductivity and temperatures of the layer is known at present day. Moving back through geologic time the calculation of heat flow is stressed with uncertainties and varying unknown factors that leads us to a detailed investigation and model calibration. The 1D model approach all heat flow vectors are directed vertically and this solution often provide a good estimate for temperatures. The terrestrial heat flow provides basic information at depth. Practically the heat flow analysis is subdivided into two problems: (1) the consideration of the crustal model to calculate the heat in-flux into the sediments and (2) the temperature calculation in the sediments afterwards (Hantschel & Kauerauf, 2009). Adsorbing in thermal history modelling the occurring heat flow types should be clarified this way we have to distinguish the:

- **Basal Heat Flow:** heat flow at base sediments
- **Heat Flux:** the heat flowing through on sediment successions/layers (depends on thermal conductivity of layer)
- **Surface Heat Flow:** the admixture of Basal Heat Flow and Heat Flux (measured at surface)

There are several temperature and conductivity measurements from the Pannonian basin which can support (Figure 8) the model calibration.

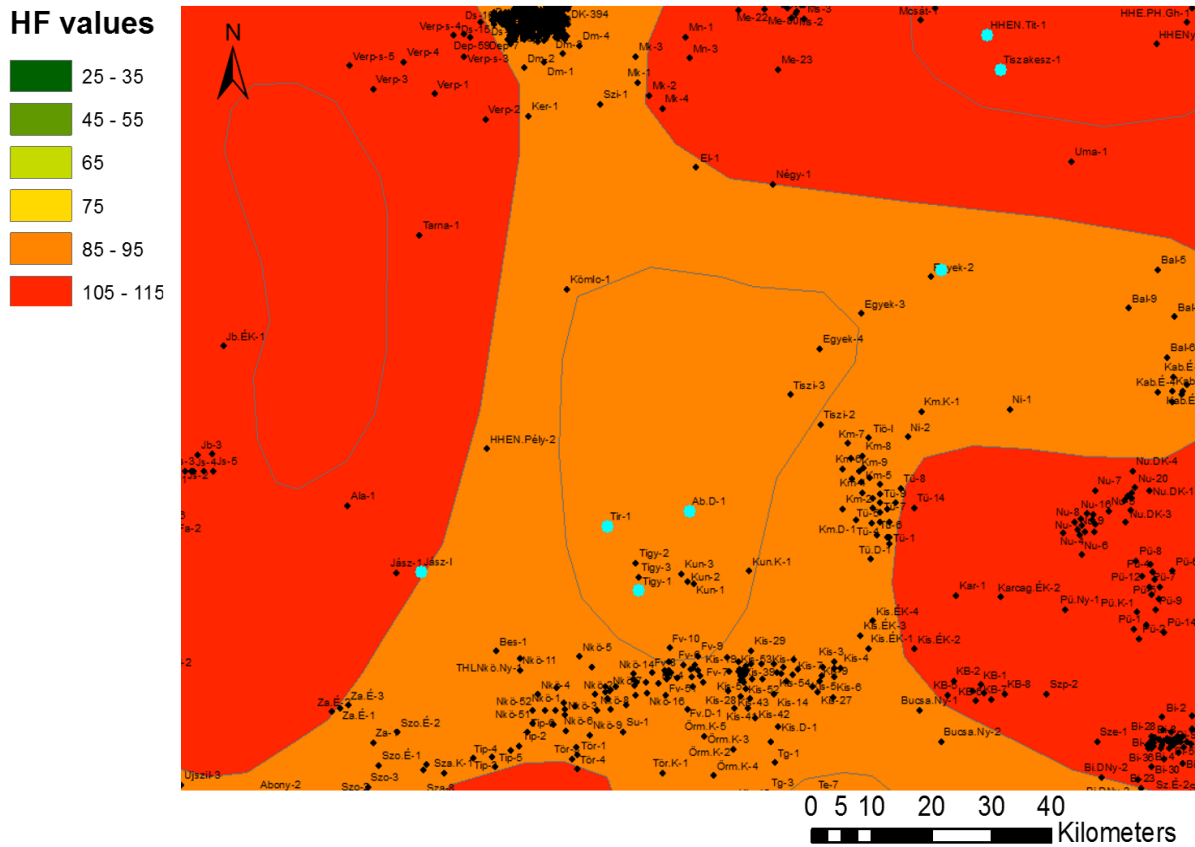


**Figure 8:** The digitized (Á., Boros) surface heat flow map of interested area based on Horváth et al. 2005 (corrected temperature data for thermal disturbance of drilling from 4600 boreholes)

The high heat flow in the Pannonian could be explained by the Middle Miocene extensional event (Royden & Horváth, 1982) which led to a crustal thinning (Tari et al., 1999) and normal faulting in Neogene basement (Horváth, 1993). The surface heat flow distribution in the Pannonian basin shows values varying between 50-130 mW/m<sup>2</sup> with a 100 mW/m<sup>2</sup> mean (Lenkey L., Dövényi P., Horváth F., Cloething & L., 2002). The rifting and heat flow modeling in Genesis will result lower heat flows through time because applies McKenzie (1978) model to the heat flow from mantle allowing the radiogenic heat from lithosphere to be reduced by stretching. Other software implementations applies the radiogenic heat flow from mantle without reduction to obtain the heat flow at time of rifting (ZetaWare, 2001).

The Genesis contains a well-developed thermal modelling module and handles five thermal models where can be used a wide range of input parameters (*T°C at base sediment, present day surface T°C, present day surface heat flow, heat flow at base lithosphere, heat flow at base sediments, thermal gradient, radioactive heat production and T°C at base lithosphere*) and multi-selection of input data is allowed. Hence a great deal of thermal model and input parameter variation was tried on the selected master wells – where the Ro% reflectance and

temperature calibration helped in assessing the calculated thermal history – and two applicable thermal models were selected besides establishing the fact that the heat flow curve modeled by Genesis always reflects the heat flow at base sediments.

The selected thermal models which indicates two outgoing scenarios (a higher and a lower heat flow adapted) after the calibration step are the next: Steady State Heat Flow model with Rift Thermal History variation (used in the following as SSRM) and Transient Heat Flow model at Fixed Temperature at Base Lithosphere (used in the following as TFBL). The role of thermal calibration is to adapt the best fitting thermal model for the selected area that carrying that one scenario will be endowed with kerogens. The steady state 1D models are the simplest solutions where all the time dependent factors like transient, convection or compaction effects are neglected. Supposing that the harmonic average of the corresponding single layer bulk thermal conductivities is equal with the average bulk thermal conductivity  $\lambda b$  the multilayer the 1D modelling can be directly derived from the heat flow equation:

$$q = \lambda b \frac{Tb - T_{swit}}{hl}, \quad \frac{hl}{\lambda b} = \frac{hm}{\lambda m} + \frac{hc}{\lambda c} + \frac{hs}{\lambda s},$$

where  $\lambda b$  - thermal conductivity of the lithosphere,  $hl$ -thickness of the lithosphere and the corresponding properties of the upper mantle  $\lambda m$ ,  $hm$ , the crust  $\lambda c$ ,  $hc$  and sediments  $\lambda s$ ,  $hs$  (Hantschel & Kauerauf, 2009).

The temperature of each layer can be calculated from surface temperature with the equation of thermal gradient. For thermal conductivity of the layers the Genesis's default properties were used because of the lack of thermal conductivity measurements from the wells. Using steady state solution because of the average bulk thermal conductivities expended to big scaled layers with constant thermal gradient a very rough approximation of heat flow could be modelled.

**SSRM**- Steady State Heat Flow model with Rift Thermal History variation

**TFBL**-Transient Heat Flow model at Fixed Temperature at Base Lithosphere

In practice, because of radioactive element content of the sediments the heat flow from the base upward does not remain constant, in Genesis is available a radioactive heat addition to the calculation, which simplified equation is the following:

$$\Delta q = (1 - \varphi) h Q_r,$$

where  $Q_r$  is the rock density dependent radioactive heat production with standard **U**, **Th**, and **K** concentration (Hantschel & Kauerauf, 2009),  $h$  is the thickness of the layer. This addition means an average **1mW/m<sup>2</sup>** per km sediment heat flow increase.

In case of SSRM model an estimated lithosphere and crust thickness adjustment has to be added besides the timing of rifting and the crustal stretching factor ( $\beta$ ) is also required. Crustal models describe the thermal processes of plate tectonics and are used to estimate basal sediment heat flow, which means the lower boundary condition of the thermal modelling. Referring to Tari, Posgay et al. (1999) and to our experimental settings on the studied area the next estimations were applied:

Upper Crust:	<b>8 km</b>
Lower Crust:	<b>19 km</b>
Rifting Started:	<b>17 Ma</b>
Rifting Ended:	<b>11 Ma</b>
$\beta =$	<b>1.8</b>

**Table 5: Applied crust, lithosphere and rifting properties in case of SSRM model.**

In Genesis using the TFBL the temperature at base lithosphere is the key input parameter which isotherm value (1333 °C) is applied in McKenzie (2005) model using the  $\frac{3}{4}$  part of the melting temperature of pyrolite.

## Calibration

The calculated thermal models can be calibrated with measured temperatures from wells and thermal maturity parameters among which is available, in our case, the vitrinite reflectance. The thermal parameters are time and temperature dependents and indicates spent interval of a rock on a constant thermal condition. The most widely used parameter is the vitrinite reflectance because it covers typical oil and gas maturity ranges. There are numerous technics to change the thermal parameters when the measured thermal parameters or temperature data differs from a model run.

**SSRM-** Steady State Heat Flow model with Rift Thermal History variation

**TFBL-**Transient Heat Flow model at Fixed Temperature at Base Lithosphere

In the case of SSRM model as initial thermal input, the measured temperatures were added which allows the paleo basal heat flow calculation. If the exact thermal conductivity of the layer would be known a basal to surface heat flow calculation could be a good control data. Back-calculating the modeled temperature (ex. 160 °C at 3740 m depth) with an average  $\lambda=2$  W/m/K thermal conductivity considered the layers as homogenous a **80 mW/m<sup>2</sup>** surface heat flow was resulted, which not including the radioactive heat addition satisfies the calibration concept in our case. For more detailed calibration the exact thermal conductivity of the layers should be known.

In the case of TFBL because of the complexity of differential equation the analytical back-calculation was not made. The correlation of measured and modelled data is shown on Figure 9 for the model SSRM respective on Figure 10 for the model TFBL.

**SSRM-** Steady State Heat Flow model with Rift Thermal History variation

**TFBL-**Transient Heat Flow model at Fixed Temperature at Base Lithosphere

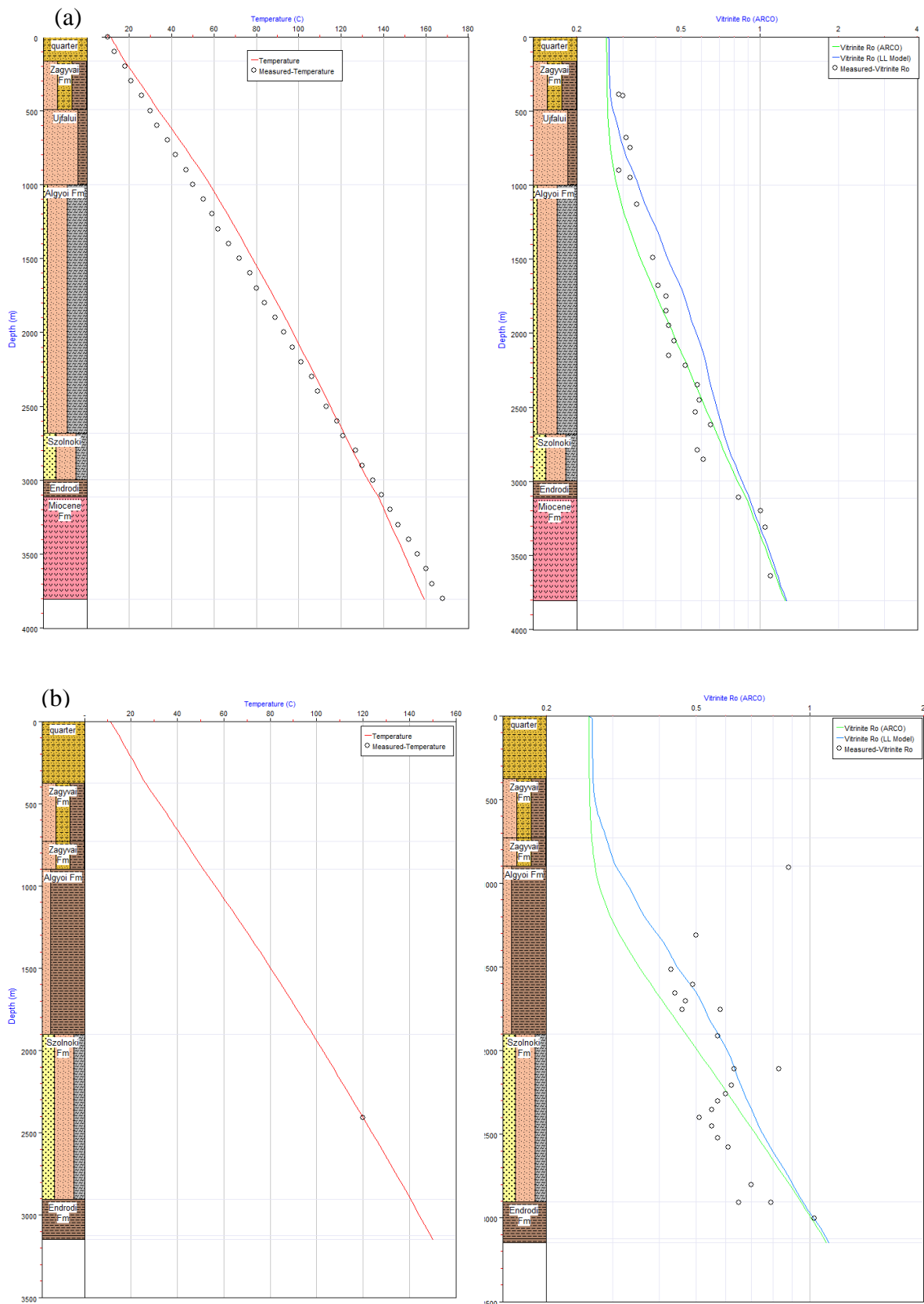


**Figure 9: SSRM model: measured (circles) versus modeled (lines) temperature (left) and Ro% (right) correlation; (a)-Jászladány-I, (b)-Abádszalók-D-1**

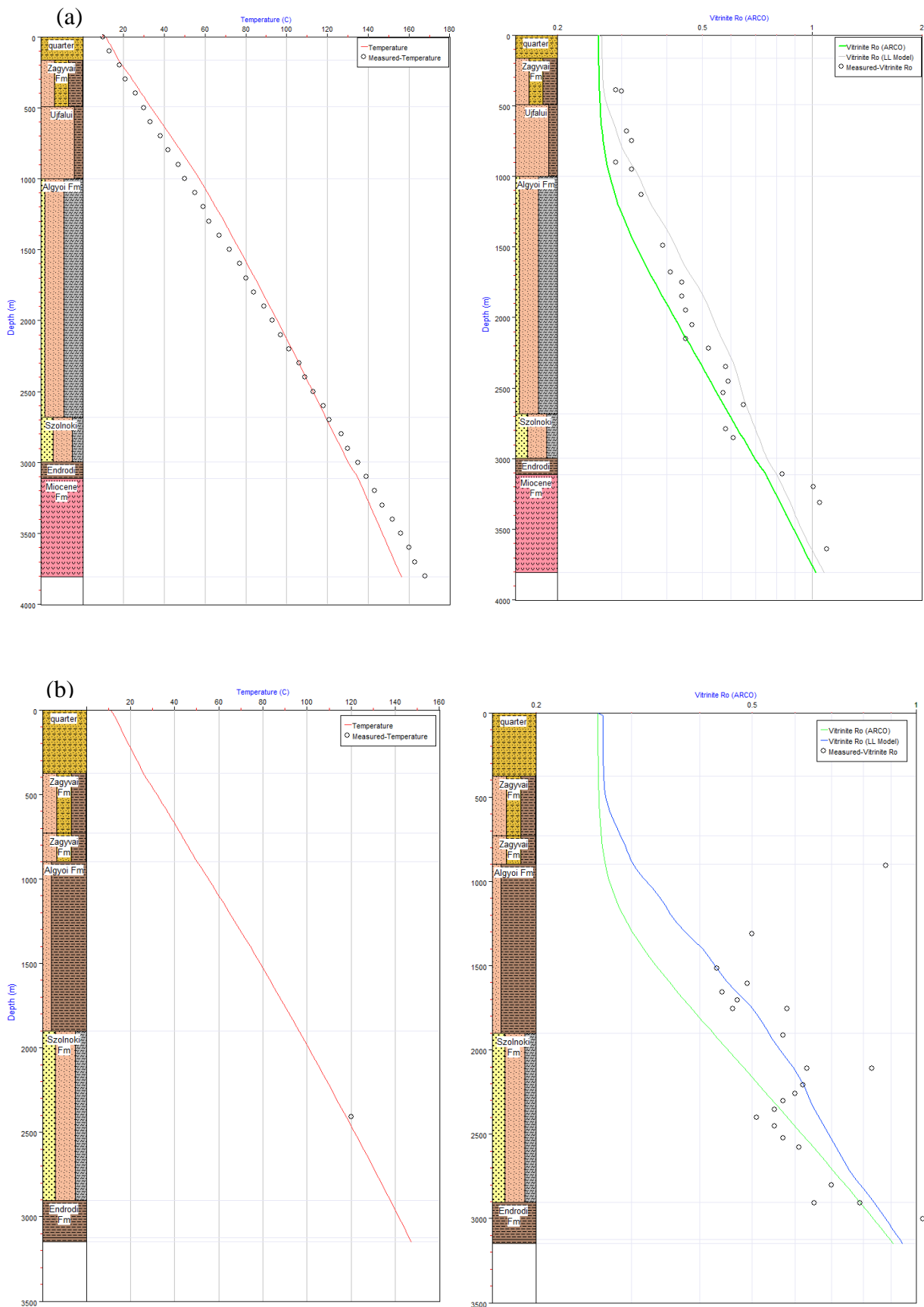


**Figure 10: TFBL model: measured (circles) versus modeled (lines) temperature (left) and Ro% (right) correlation; (a)-Jászladány-I, (b)-Abádszalók-D-1**

In each of two heat flow models the calculated temperature and Ro% reflectance data is correlating with measured. The TFBL model shows lower temperatures with 3-4 C which was expected considering the mentioned transient heat flow properties discussed in previous chapter.

In the studied area from two more wells is available Ro% reflectance data that lets us to specify the calibration and to choose the best fitting model. This Ro% data in one well are from cuttings and in both of wells is without measured temperature. So it can be stated that this calibration data is stressed with high uncertainty and the cutting data are not representative. In despite in TFBL model the calculated Ro% is not showing correlation with the measured data (Figure x) like in SSRM model. Summarizing, the SSRM model can be considered as applicable thermal model for the studied area.

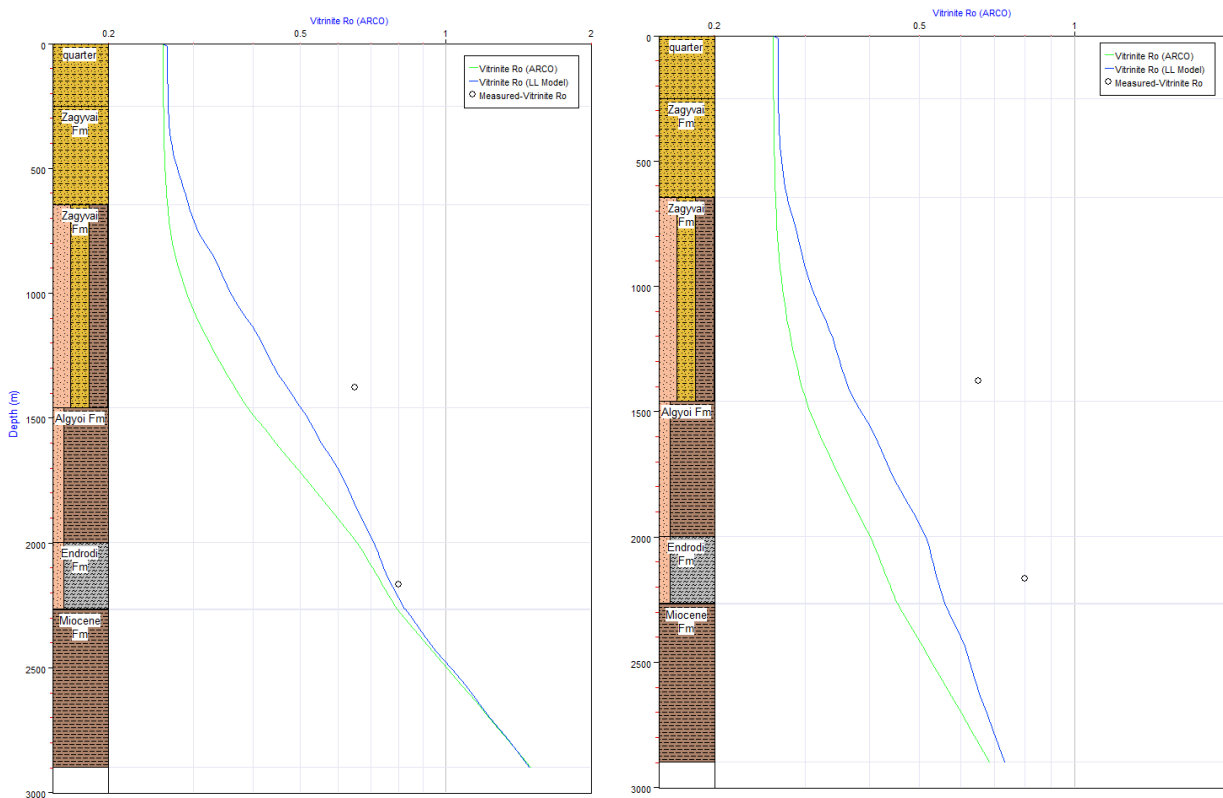


**Figure 11:** correlation of measured (circle) and modeled (line) vitrinite reflectance data in Egyek-1 well in SSRM model (left) and TFBL model (right).

The vitrinite reflectance data without measured temperatures like in case of Egyek-1 well should be considered as non-representative low confidence calibration data (Figure 11). The absence of measured temperature data from wells using the SSRM model make us to give as input a thermal gradient. It can be expressed easily from the equation of heat flow, knowing the actual surface temperature and the surface heat flow .The temperature at 100 m depth can be computed (with an average  $\lambda=2 \text{ W/m/K}$  thermal conductivity). The difference between the surface temperature and the calculated temperature results the requested geothermal gradient in

the well. Thus, the geothermal gradient of three wells was determined (Tiszakeszi-1, Tiszaroff-1, Tiszagyenda-1).

The model of *Easy%Ro* (for vitrinite reflectance in Genesis LL model) is generally accepted and only in case of Jászladány-I well can be discussed about trend and correlation between the measured and modelled temperature and vitrinite reflection data. Making a distinction between the previously compared two thermal models (SSRM and TFBL) can be stated that is no significant difference in modelled temperatures, but considering the SSRM model's better correlation, simplest numerical model with less uncertainty factors and with more adjustable options (e.g. thermal gradient), in summary the SSRM model settings applied on Jászladány-I well can be accepted as a master setting on the studied area.

#### 4.1.3 Organic Geochemistry

The organic matter included in sediments and source rocks is the most confident marker of hydrocarbon potential. The transformation and maturation of organic matter shown in Figure 12 can be subdivided into three phases: diagenesis, catagenesis and metagenesis (Tissot & Welte, 1984). In the process of transformation after the fast burial of organic matter rich sediments which are effected with a variable or constant heat flow by chemical reactions the genesis of the kerogen then the hydrocarbons are implemented. In case of hydrocarbon oversaturation the phase of migration is starting.

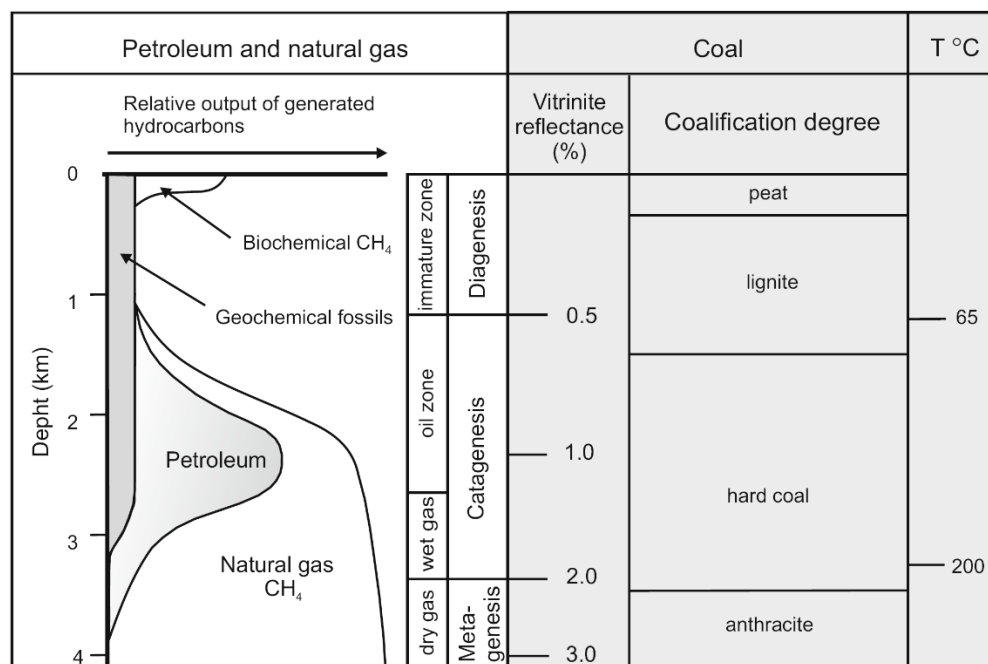


*Figure 12: The evolution of organic matter and the main phases after Bahlburg and Breitkreuz (2004).*

**SSRM**- Steady State Heat Flow model with Rift Thermal History variation

**TFBL**-Transient Heat Flow model at Fixed Temperature at Base Lithosphere

The rate of transformation depends mostly on depth and temperature the reason of detailed heat flow analysis can be found here. First the heavier petroleum components are generated then they are cracked into lighter components at higher temperatures in a so called oil window generally between 1 and 3 km depth.

## Petroleum Generation Kinetics

The total organic matter content of sediments is usually expressed in terms of the total organic carbon content (TOC) in mass%. This means the ratio of the mass of carbon atoms to the total mass of the rock matrix. To convert this value into generated and expelled petroleum the total rock mass of source rock has to be known. The petroleum kinetics are distinguished from cracking types, kerogen types and the number and type of generated petroleum. The generated kerogen can be subdivided according to van Krevelen diagram into type I-IV corresponding to its hydrogen and oxygen content (Figure 13, a, b).The kerogen types are assigned to depositional environments as follows after Tissot and Welte (1984) and Peters et al. (2005):

-**type I:** are generally originated from lacustrine algal matter in a few cases some source rocks deposited in marine settings are also dominated by this type. The HI of this type is the higher and the generated petroleum component is oil.

-**type II:** the most common kerogen type originated from marine algal matter indicating marine sedimentation in a reducing environment. This type of kerogen can generate heavy and easy petroleum components also.

-**type III:** with the highest oxygen content is derived from plant organic matter deposited in terrigenous environment

-**type IV:** is characterized with the smallest H/C ratio and hydrocarbon generation potential being originated from forest and peat bog organic matter.

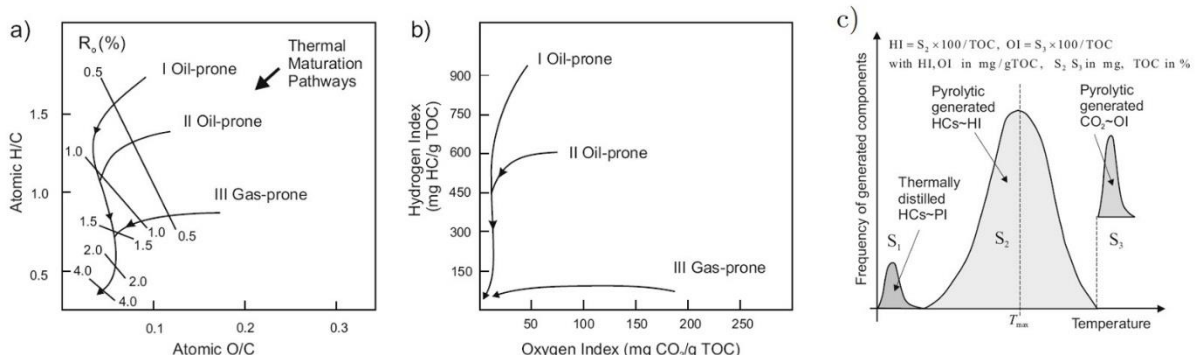


**Figure 13: Characterization of kerogen by van-Krevelen diagrams after Peters et al. (2005): (a) according to the abundance of the elements in kerogen in ratios of H/C and O/C, (b) according to the generative amounts of HC and CO<sub>2</sub> in Rock-Eval parameters HI (hydrogen index) and OI (oxygen index), (c) the process of Rock-Eval pyrolysis**

The maturation paths of decreasing H/C and O/C ratios can be related by simple mass balance calculations to the corresponding decrease in the generative masses of hydrocarbons (in following as HC) and CO<sub>2</sub> (Hantschel & Kauerauf, 2009). The above mentioned HC and CO<sub>2</sub> masses are measured with Rock-Eval pyrolysis expressed in HI and OI which leads to van Krevelen classification. The Rock-Eval method is developed by Espitalie et al. (1977) and is an open system pyrolysis. The organic rich rock sample (100 g) is heated from 300 °C to 600 °C with 5°C/minute and the released masses of HCs and CO<sub>2</sub> are measured. The next step is the Rock-Eval method related terminologies and will be used with the corresponding analogically conversions (Figure 13, c):

**S1:** corresponds to the residual (already generated and not yet expelled) bitumen and means the first HC peak during the thermally distillation

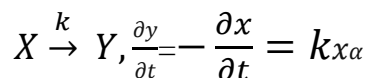
**S2:** the second peak of pyrolytic generated HCs and means the total generative mass and it is related to HI given in mg/gTOC.

**HI:** S2x100/TOC

**PI:** the production index is a measure of cracked kerogen which value varies between 0 and 1.  
PI=S1/(S2+S2)

**Tmax:** the oven temperature at the maximum HC generation rate for S2. This temperature can be used as maturity indicator of the kerogen sample and as thermal calibration parameter.

In the modelling softwares, including Genesis and Migris the complicated processes and reactions regarded to HC maturation are approached by kinetic way. For petroleum maturation kinetic simulation a great deal of models are created and applied but the basic conception is the unimolecular forward reaction from an initial reactant X mass of x to the product Y mass y (Hantschel & Kauerauf, 2009):



where  $\alpha$  is the reaction order,  $k$  is the reaction rate and  $t$  is the time (Tissot & Welte, 1984).

Hence every model is unique considering different type of parameters and effects like kerogen type, age or kerogen component. Referring to researches made from the interested area (Csizmegi et al., 2011) and considering the fact that the supposed source rock kinetics is not known the most common BP model was applied which is created by Pepper and Corvi (1995) based on vitrinite reflectance, considers all kerogen types and can be used in a large vitrinite reflectance range. In modelled wells the 33% type II and 66% type III kerogen distribution for the supposed source rock and for its following formation (Szolnok Formation) with the purpose of the study from the viewpoint of hydrocarbon generation.

That part of kerogen which can be converted to hydrocarbons is called labile component. The oil prone part of labile component gets converted to oil, the gas prone part of it to gas. In Genesis software/module the gas prone fraction is about 15% of marine or lacustrine kerogens and about 50% of terrestrial kerogens (“ZetaWare,” 2001). The above mentioned HI parameter measures the labile component content of a kerogen. HI is all the labile component divided by all the carbon in the kerogen (mg HC/TOC). Higher HI source rocks produce more hydrocarbons per unit TOC.

For the expulsion of hydrocarbons from kerogens into porosity of the source rock is generally accepted the process of adsorption. If the quantity of generated hydrocarbons exceeds the saturation limit of kerogen, the additional hydrocarbon fluids will be expelled into the pore system. If the pore system is dominated by fine grained water wet clay minerals, it stores very little oil or gas before they are expelled from the source rock into a carrier bed.

In Genesis the formula of calculating the expelled hydrocarbon from kerogen is given by the next context:

**Volume expelled (per unit area) =  $H \cdot (HI \cdot Tr \cdot (1 - G_0) - S \cdot C_i) \cdot TOC \cdot r_r/r_o$ , where:**

**H** – thickness of source rock,

**r<sub>r</sub>** – density of source rock,

**r<sub>o</sub>** – density of oil,

**HI** – hydrogen index,

**Tr** – transformation ratio,

**G<sub>0</sub>** – initial gas prone fraction (fraction of the total initial that is gas generative) = **GOGI/(1+GOGI)**,

**TOC** – total organic carbon,

**S** – sorption capacity for oil or gas, for example, 100 mg/gTOC for oil and 20 mg/gTOC for gas.

**C<sub>i</sub>** – the fraction of inert carbon.

It is believed that the software is considering the available and added measurements to determine the expelled HCs parameters.

#### **4.1.4 Results of 1D modelling**

The goal of 1D modelling of the Jászság-basin is to identify the possible source rock from basin and largely determine the boundary conditions of hydrocarbon genesis in studied area. Therefore, a 2D model interpretation and an experimentation with the possible kerogen types was not made. This can be argued referring to the main goal of the thesis. The obtained source rock properties and thermal settings are added by gridding into Migris interface. The results of 1D modelling in Genesis will be discussed shortly from 3 viewpoints well by well: heat flow and temperature, Ro% and oil window, expelled HCs. The lithology and the presence/thickness of possible source rocks and formations was estimated and slightly modified by lithology descriptions of wells.

#### **Jászladány-I well**

The modelled thermal history of well shows a maximum  $80 \text{ mW/m}^2$  basal heat flow around 12 Ma (Figure 14, a). This relatively high heat flow effect ( $70\text{-}60 \text{ mW/m}^2$ ) during the burial of the supposed source rock formation led the sediments to reach the boundary of oil maturity window at 2400 m depth around 8 Ma (Figure 14, b). The oil generation rate reached its maximum at 6 Ma and the source rock became saturated around 5 Ma, when the increasing oil expulsion started (from 2 to 6 mg/gRock HC). Beside the *Endrődi Formation* the model shows the *Szolnok Formation* as possible source rock also, regarding its younger position and differing lithology it is characterized by lower HC generation and expulsion rate. The generation of gas started at 2600 m around 7 Ma with a low generation and expulsion rate (<1 mg/gRock HC) (Figure 14, c).

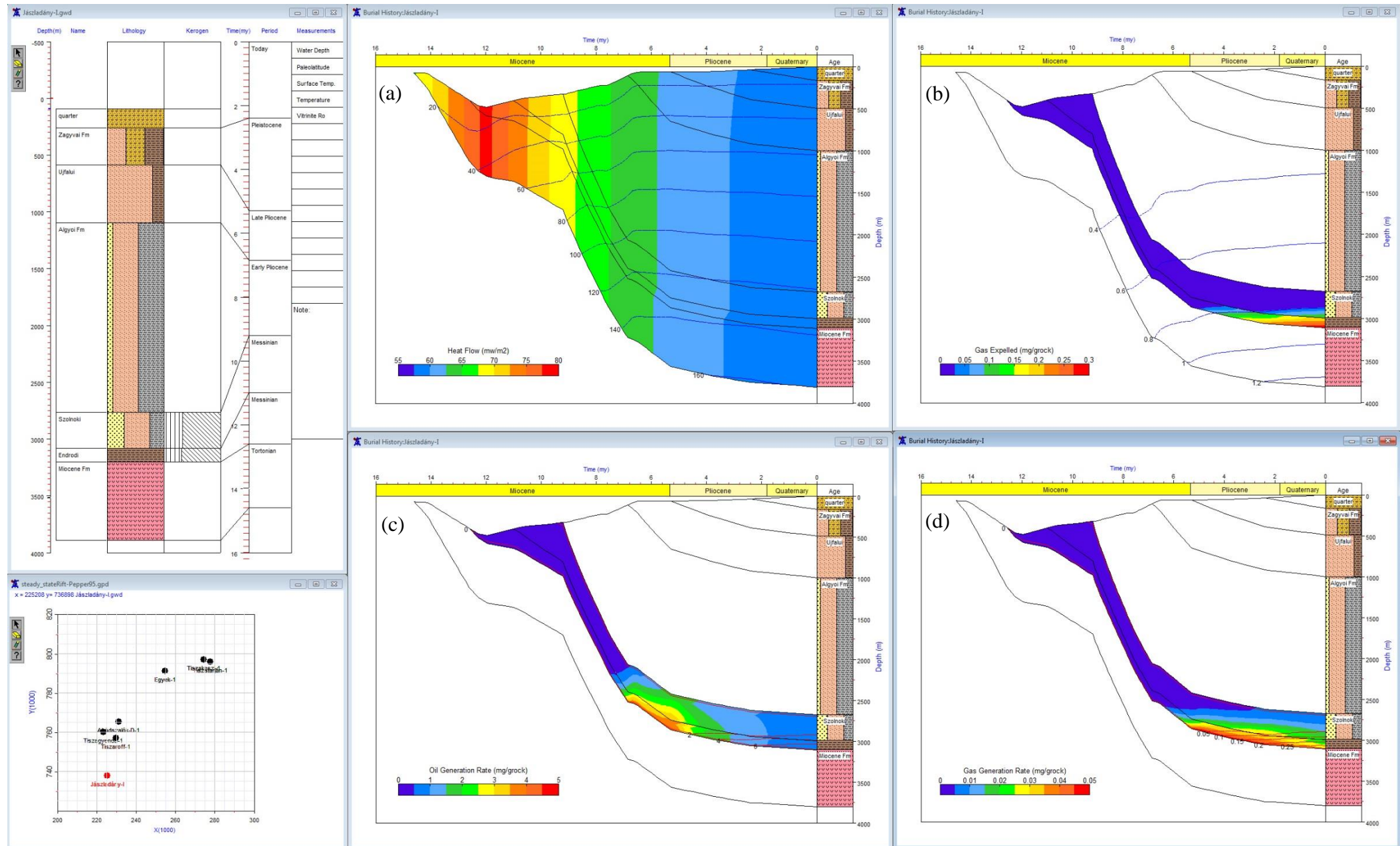


**Figure 14: Jászladány-I well SSRM burial history.** (a) heat flow vs. temperature diagram, (b) expelled gas vs. vitrinite reflectance (blue line – Easy %Ro) diagram, (c) oil generation rate vs. expelled oil (red line) diagram, (d) gas generation vs. expelled gas (red line) diagram.

## Tiszagyenda-1 and Tiszaroff-1 wells

The only difference between two wells referring to model input parameters is in their lithology. At Tiszagyenda-1 well (Tigy-1) the *Endrődi Formation* is present and the *Szolnoki Formation* is sandier than in Tiszaroff-1 (Tir-1) well, where the main source rock is missing and the *Szolnoki Formation* is situated deeper containing mostly siltstone. Therefore, the two wells can be discussed together thus obtaining information about the behavior of model according to lithology.

Because of the lack of temperature and vitrinite reflectance data as thermal indicator of these wells the calculated geothermal gradient ( $4.8\text{ }^{\circ}\text{C}/100\text{m}$ ) was used. This indicates a high paleo temperature with  $110\text{-}115\text{ mW/m}^2$  maximal basal heat flow (Figure 15, a). The oil window situated at 1800m depth (Tigy-1), respective at 2300m (Tir-1) around 9 Ma and the high oil generation plus expulsion rate (Figure 15, b) can be connected to the modeled high temperatures ( $90\text{ mW/m}^2$  at the start of oil window). Probably because of the lithology the modeled HC generation of *Szolnoki Formation* is not meaningful/important in quantity/ in the case of Tigy-1 well. In contrast the silty *Szolnoki Formation* of Tir-1 represents the main source rock of the model (Figure 16, c)

The model behavior, considering the lithology, can be examined with comparing the HCs generation and expulsion rates. In case of Tigy-1 well the source rock characterized by marls in a shallower position generates twice more HCs (e.g.  $20\text{ mg/gRock oil}$ ) than the source rock of Tir-1 well. The probably source rock of Tir-1 can be characterized by silts and it is situated deeper with the same thermal conditions like the source rock of Tigy-1 well. Thus the importance of temperature and rock type can be highlighted referring to key model input parameters.

The gas generation started around 8-9 Ma at Tigy-1 and around 7 Ma at Tir-1 with a relative low rate ( $0.05\text{-}0.3\text{ mg/gRock HC}$ ), which is decreasing toward the present while the saturation of source rock is increasing that indicating a growing expulsion rate ( $0.75\text{ mg/gRock HC}$ ) (Figure 16, d).

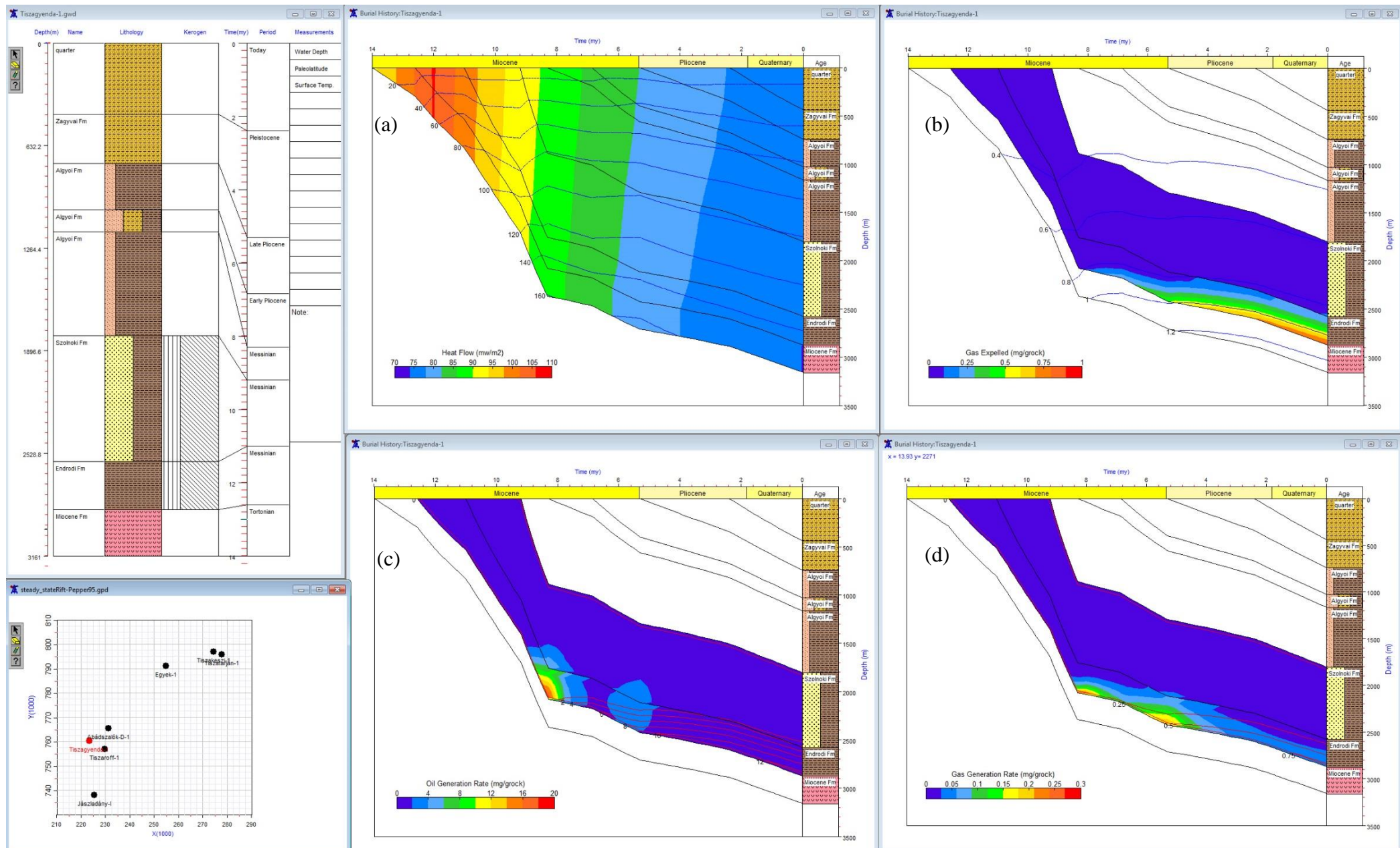


**Figure 15: Tiszagyenda-1 well SSRM burial history.** (a) heat flow vs. temperature diagram, (b) expelled gas vs. vitrinite reflectance (blue line – Easy%Ro) diagram, (c) oil generation rate vs. expelled oil (red line) diagram, (d) gas generation vs. expelled gas (red line) diagram.

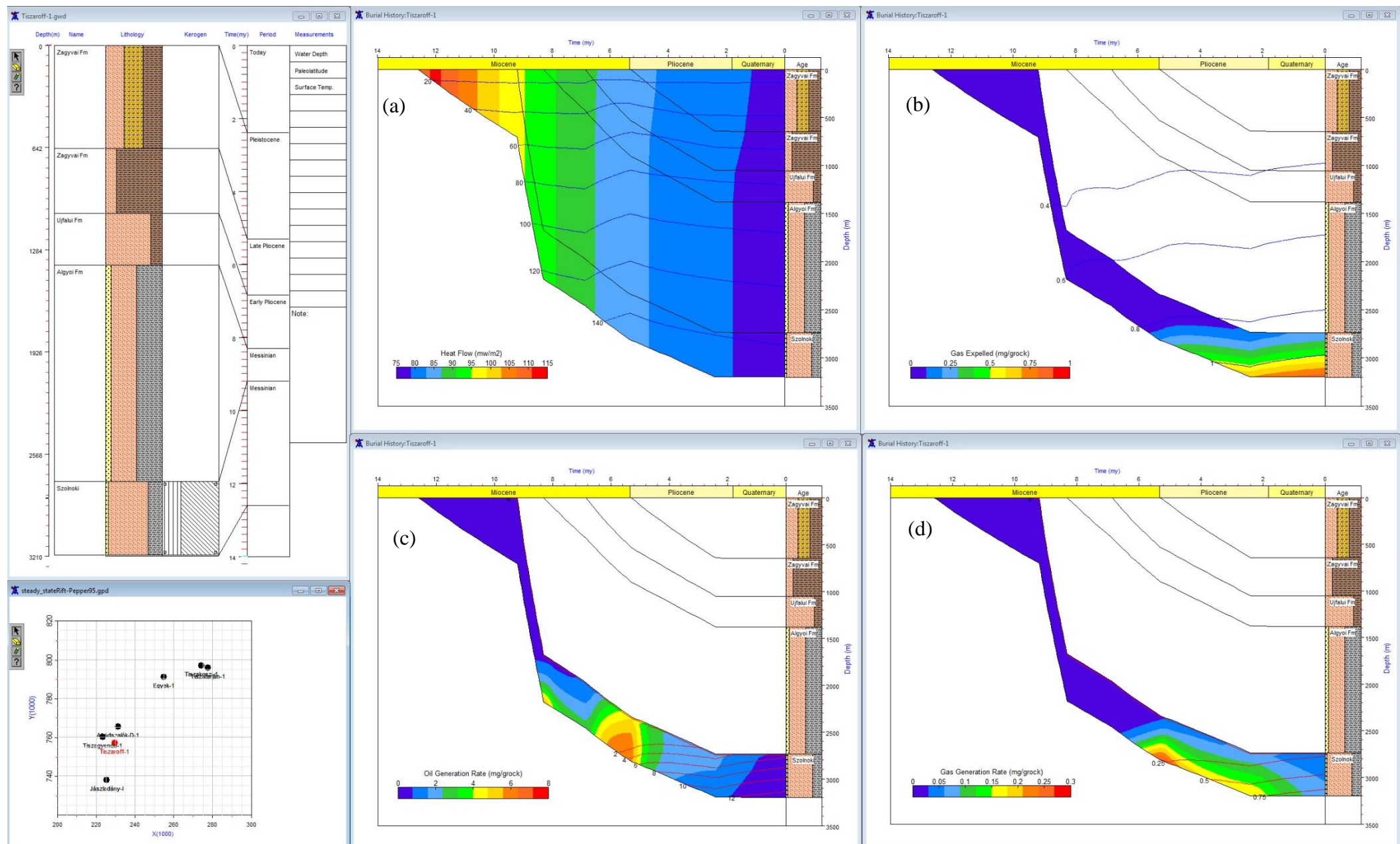


Figure 16: Tiszaroff-1 well SSRM burial history. (a) heat flow vs. temperature diagram, (b) expelled gas vs. vitrinite reflectance (blue line – Easy%Ro) diagram, (c) oil generation rate vs. expelled oil (red line) diagram, (d) gas generation vs. expelled gas (red line) diagram.

## **Abádszalók-D-1 well**

As thermal input parameter, for this well, the measured temperatures were used. The thermal history of well shows a lower temperature range than the above discussed wells without measured control data, which means an  $85 \text{ mW/m}^2$  maximal basal heat flow. The oil window is situated at 2200 m depth around 9 Ma and this point is characterized with a  $65-70 \text{ mW/m}^2$  heat flow (Figure 16, a). The maximum phase of oil generation rate is located around 7 Ma with a relatively high rate ( $10 \text{ mg/gRock HC}$ ) and this stage means the start of gas generation phase also. The maximum of gas expulsion is modelled to present day time-step with a  $1 \text{ mg/gRock HC}$  rate. In this case the *Szolnoki Formation* is also characterized as possible source rock with very low HC generation rates.

## **Egyek-1 well**

In this case the key input parameter is the measured Rock-Eval data. For thermal indicator the calculated geothermal gradient was used which generated a high paleo heat flow with a  $110 \text{ mW/m}^2$  maximum value. In this case is available measured vitrinite reflectance data which is highly stressed with uncertainty. Hence, the oil window is situated at very high position (1600 m depth around 11 Ma) which causes a poor HC generation model. In addition for the supposed source rock at 2160 m depth is related a low HI ( $130 \text{ mgHC/TOC}$ ) measured value. These conditions led to a low HC generation rate which main phase is around 5 Ma with a  $1.5 \text{ mg/gRock HC}$  rate in case of the oil. In the case of Egyek-1 well the saturation of source rock is not realized (Figure 17, c, d).

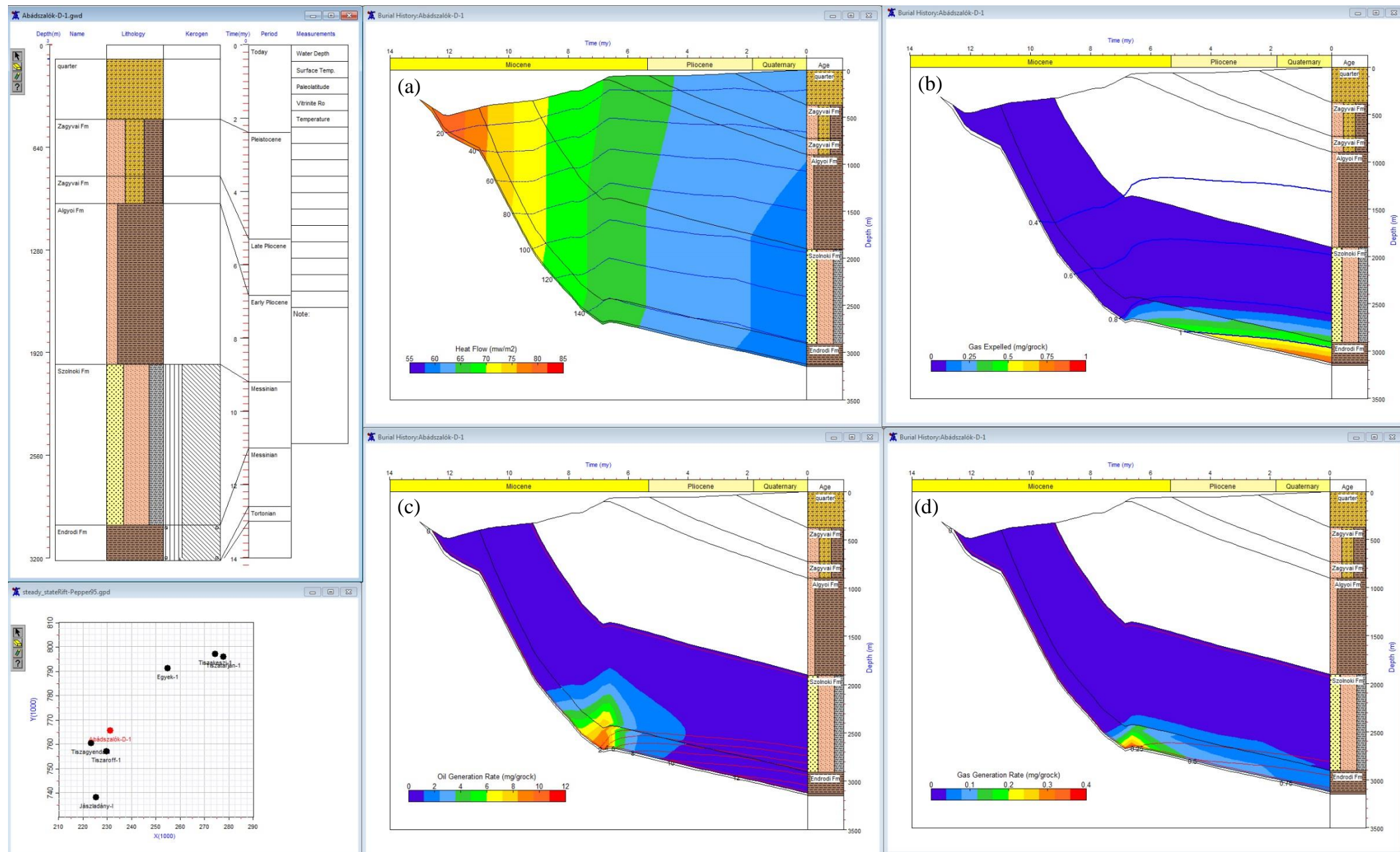


Figure 17: Abádszalók-D-1 well SSRM burial history. (a) heat flow vs. temperature diagram, (b) expelled gas vs. vitrinite reflectance (blue line – Easy%Ro) diagram, (c) oil generation rate vs. expelled oil (red line) diagram, (d) gas generation rate vs. expelled gas (red line) diagram.

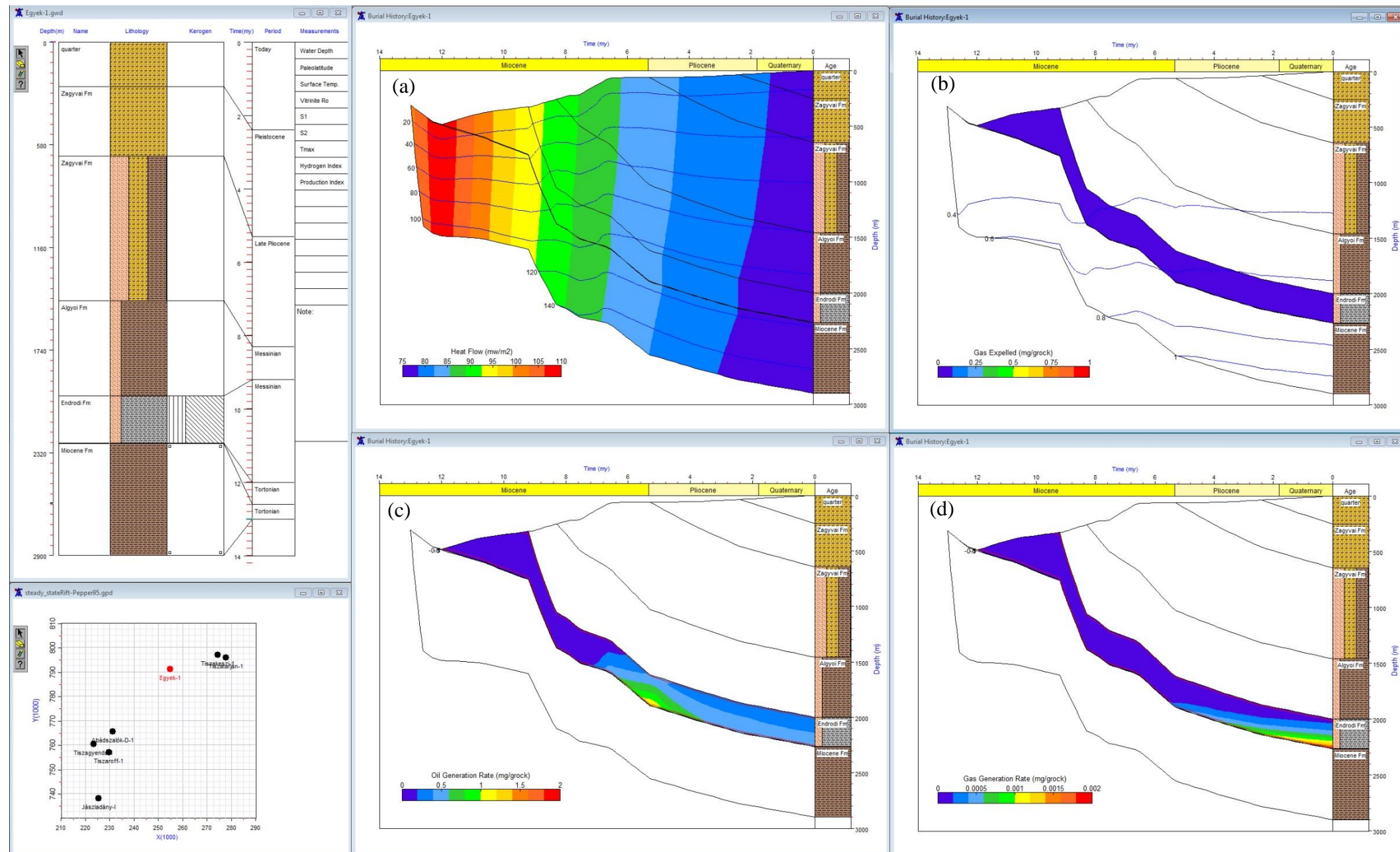


Figure 18: Egyek-1 well SSRM burial history. (a) heat flow vs. temperature diagram, (b) expelled gas vs. vitrinite reflectance (blue line – Easy%Ro) diagram, (c) oil generation rate vs. expelled oil (red line) diagram, (d) gas generation vs. expelled gas (red line) diagram.

## **Tiszakeszi-1 and Tiszatarján-1 wells**

These two wells are situated at the edge of Jászság basin (Figure 4) and were selected because of Rock-Eval data content. The supposed source rock can be found only in Tiszakeszi-1 well. With the aim of checking the accuracy of the modelling method in Tiszatarján-1 well the silty-shaly *Algyői Formation* was endowed with kerogens. Despite of modelled high paleo heat flow (Figure 19, a) and relatively deep oil window (Tiszatarján-1 well), none of cases shows the possibility of HC expulsion.

At Tiszakeszi-1 well for the supposed source rock a 1 - 1.6% TOC was measured while the superposing *Szolnoki Formation* contains 4-5%TOC values. In case of Tiszatarján-1 the TOC% values range is between 0.6-2.2% (Figure 20, d). The oil generation started in both of the formations around 8 Ma at 1500 m depth with a medium rate (1-3 mg/gRock HC) but the saturation of kerogen rich rocks could not be realized because of the lithology of sandy *Szolnoki Formation* and silty *Algyői Formation*. This lithology indicates a high porosity and requires a higher generation rate. None of the two models reached the level of gas generation probably because of the high position and low kerogen quality of the sediments.

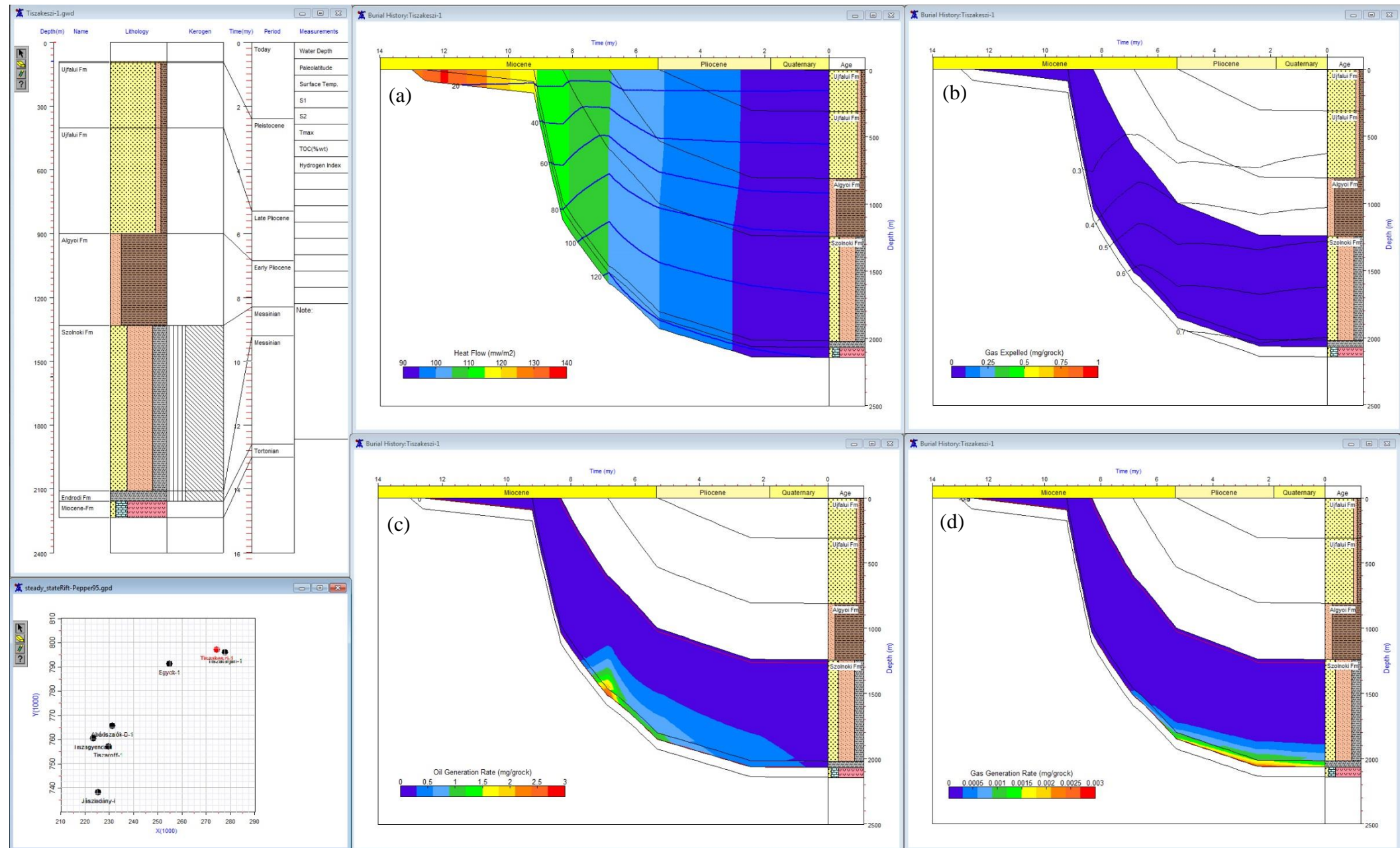


Figure 19: Tiszakeszi-1 well SSRM burial history. (a) heat flow vs. temperature diagram, (b) expelled gas vs. vitrinite reflectance (blue line – Easy%Ro) diagram, (c) oil generation rate vs. expelled oil (red line) diagram, (d) gas generation vs. expelled gas (red line) diagram.

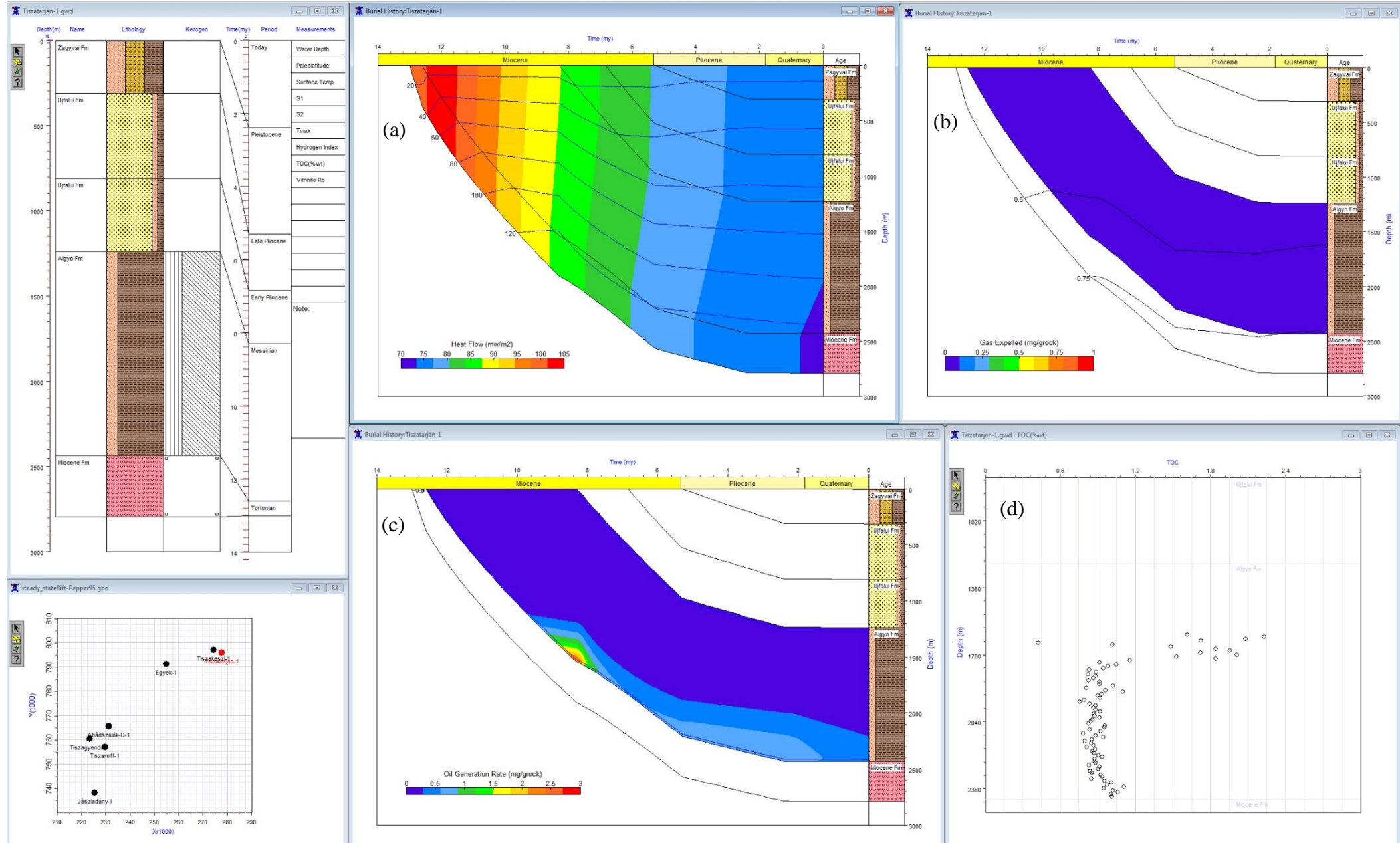


Figure 20: Tiszatarján-1 well SSRM burial history. (a) heat flow vs. temperature diagram, (b) expelled gas vs. vitrinite reflectance (blue line – Easy%Ro) diagram, (c) oil generation rate vs. expelled oil (red line) diagram, (d) measured TOC % values.

## **4.2 Migri Workflow-3D modelling**

The Migri simulates and visualizes the migration of hydrocarbon through 3D models. The basin modelling software combines innovative migration modelling processes (Sylta, 2004) with probabilistic Monte Carlo techniques. The software is also able to simulate leakage effects and the spill from the traps. In Migri the simulation is realized through a series of time-steps for which the geometry is reconstructed, the geological and flow properties are calculated and the generated and expelled hydrocarbon amount is estimated (Migri-AS, 2016).

The accuracy of Migri model depends on the resolution of data set and on the extension of studied area. The number and extension of used layers/depth maps in the model depends on the scale of seismic interpretation, and the fill up of layers with properties. It also depends on gridding resolution in function of available data. Thereby a Migri model can vary from basin to prospect scale. Regarding the available data and the aim of study a basin scaled model was built.

The main purpose of using Migri in this work is to study and describe the uncertainties of migration pathways. To reach this stage, building a migration model in Migri, all steps of basin modelling are required, which steps will be shown in distinguishing three main phases: (1) data input; (2) simulation and calibration; (3) results. For each part selected purposeful examples will be attached which reflect the most significant properties or differences in model.

### **4.2.1 Data Input**

#### **Geometries**

In the process of building a Migri model, the first step requires the setting up the geometries, which is the loading of depth maps and assigning for each an age. The same age assignment was used as in case of seismic interpretation and 1D model building (Table 1).

The user can define the number of desired sub-layers to involve in simulation. Only the age assigned layers are able to adopt properties and reflect results as surfaces. The sub-layers always carry the well-proportioned averages of the top layer and in purpose of simplicity just in certain cases are displayed (Figure 21). In this study for each layer 10 sub-layers were assigned. The faults are handled as fault planes loaded in the geometry.

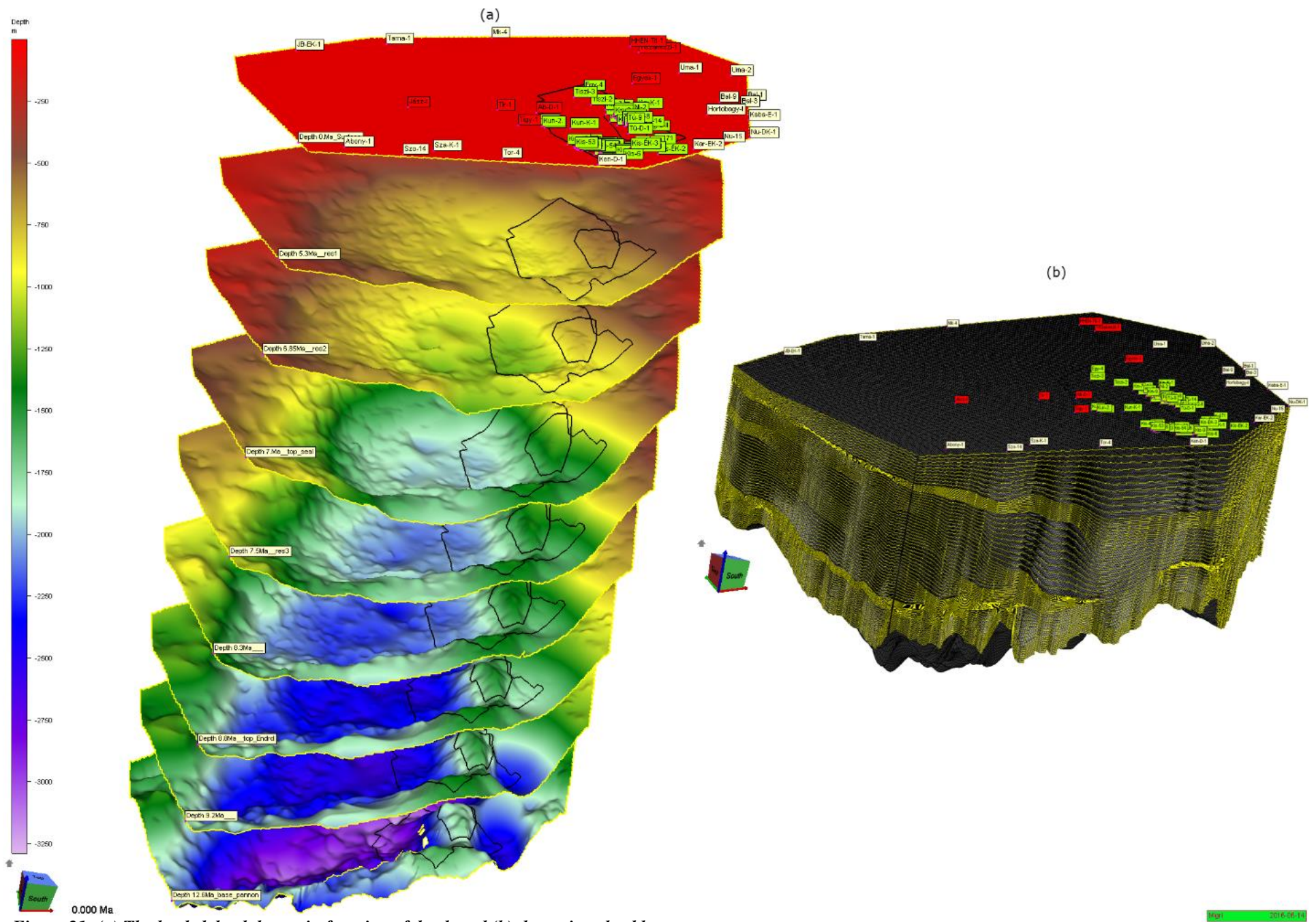


Figure 21: (a) The loaded depth layers in function of depth and (b) the assigned sublayers.

Because of the complexity of a fault related geomodel requires a higher level of investigation, which does not fit in the framework of a thesis, two fault planes were loaded and investigated with demonstration purposes (Chapter 4.3).

## Lithologies

The software uses a small set of default lithologies to define the default layer property. The list of default lithologies contains: *salt*, *shale*, *shaly silt*, *silt*, *silty sandstone*, *calcareous sandstone*, *arenitic carbonate*, *carbonate*, *argillaceous carbonate*, *shaly carbonate*, *calcareous shale* - each of these lithologies being defined with a standard shale fraction ( $V_{sh}$ ), carbonate fraction ( $V_{ca}$ ), permeable carbonate fraction ( $V_{cp}$ ) and sandstone fraction ( $V_{ss}$ ).

The complexity and changes in lithology can be applied by loading lithology property grids for each layer, which influences the fraction content and distribution of loaded default lithology. Thus can be stated that the lithology resolution and accuracy depends on the available data and gridding method.

For the purpose of lithology refinement and in function of available well data in our case 41 wells were used to create lithology grids (~26 lithology grid) for each main layer. These grids reflects the fraction changes of  $V_{sh}$ ,  $V_{ca}$  and  $V_{ss}$  of each layer. Two examples are shown in Figure 22. For the intersection points of the well and layer lithology fraction were estimated by the average lithology fraction content of the lithology column between two layers. Three examples of lithology definition by fraction is shown below (Table 6):

Lithology	$V_{sh}$	$V_{ca}$	$V_{ss}$
<i>Shale</i>	0.95	0	0.05
<i>Sandstone</i>	0.05	0	0.95
<i>Calcareous shale</i>	0.75	0.25	0

Table 6: Examples of lithology definition by fractions in Migri.

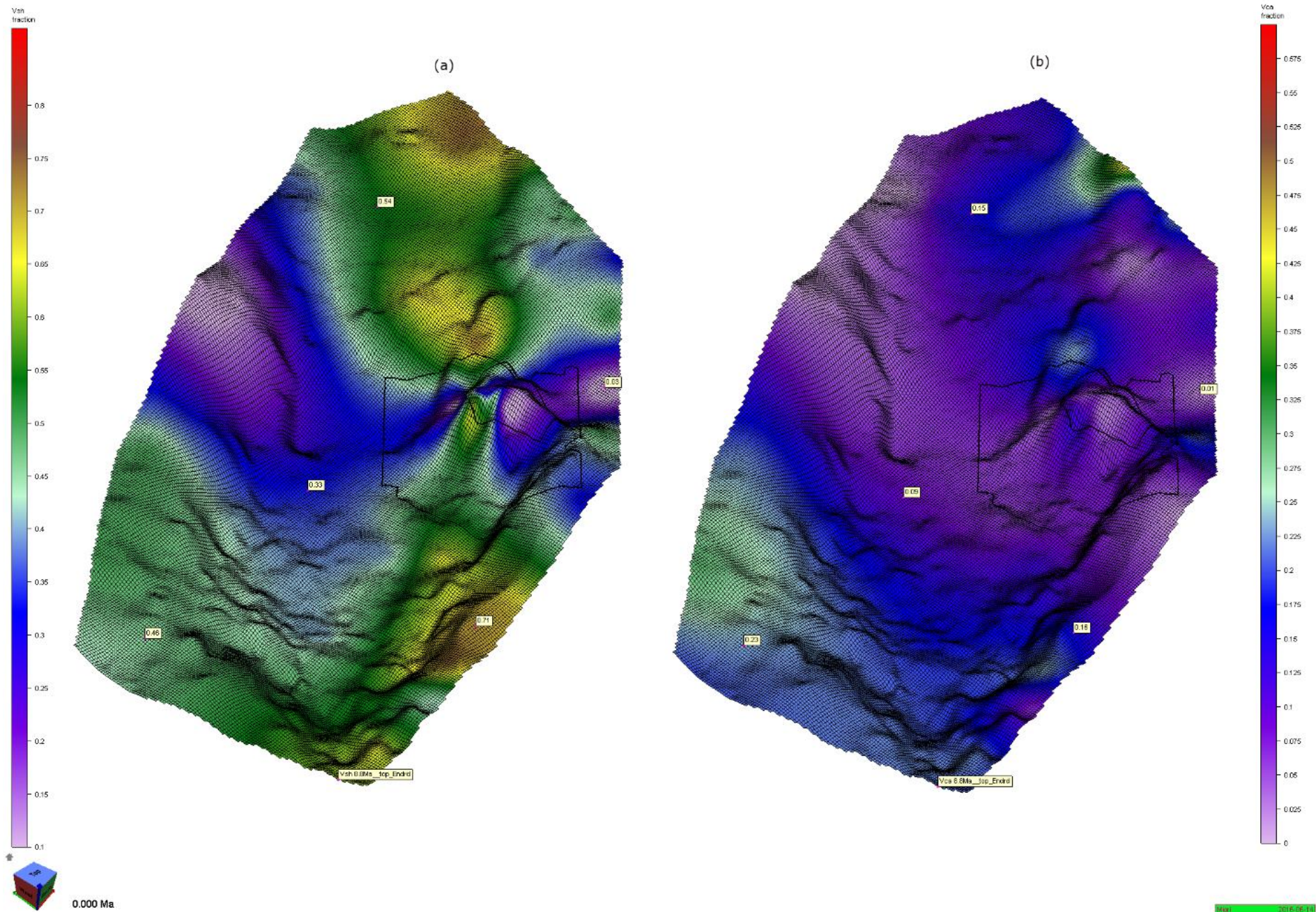


**Figure 22:** (a) Distribution of shale fraction ( $V_{sh}$ ) and (b) of carbonate fraction ( $V_{ca}$ ) on the top of the supposed source rock (Endrődi Formation).

## Temperature Histories

Migri provides a mechanism as input for handling history property. The history property is build up by of a series of grids-for each time-step, which describes the evolution of that property for one layer/unit over the modelled history of the basin. The input temperature in Migri is crucial for HC generation modelling. Two TDL (Time at Deposition of Layer) parameters are available to set up temperature conditions for the model: to use a simple surface temperature or to use geothermal gradient. The input data for each deposition time of the layers were provided by the temperature history results of 1D modelling (Chapter 4.1). Defining the thermal conditions of the model both of the parameters was used. The method was the kriging process: to pick the intersection value of depth layer and proper well temperature, then extrapolate for the surface of the layer. Thus for each depth layer the TDL geothermal gradient and temperature surface was determined. Two examples are shown in the Figure 23.

## Source Rock Potential

The source parameters are used to specify the richness of source rock intervals. Selecting from the Migri options the available source rock parameters the *thickness*-, the *initial TOC%*-, the *initial HI*- and the *kinetic scheme* of source rock was determined in this model. The source rock thickness was calculated by the subtraction from the supposed source rock depth map the underneath depth layer, using the grid mathematics function in IHS Kingdom. In our case three layers were considered as possible source rocks (*h9.2 Ma–h8.8 Ma–h8.3 Ma*), assuming that the model recognizes the insufficient source rock parameters thus not overestimating the source rock coverage/quantity. To define the supposed source layers TOC% distributions from 34 well were data available. For the not covered areas by TOC% data, an average 1.5% TOC value (Badics & Vető, 2012) was estimated for the *Endrőd Formation*. We introduced lower values for TOC in case of the superior layers above. The back-calculation method for the initial TOC% values is detailed in Chapter 3. The difference between back-calculated and measured TOC% is approximatively 0.5% which is not a significant error in iteration. The TOC% input distribution of one possible source layer is shown on Figure 24.

After Pepper & Corvi (1995) for the **HI** average a 333 mg HC/TOC value was applied for the source layers- and the kinetic model, using kerogen type III.

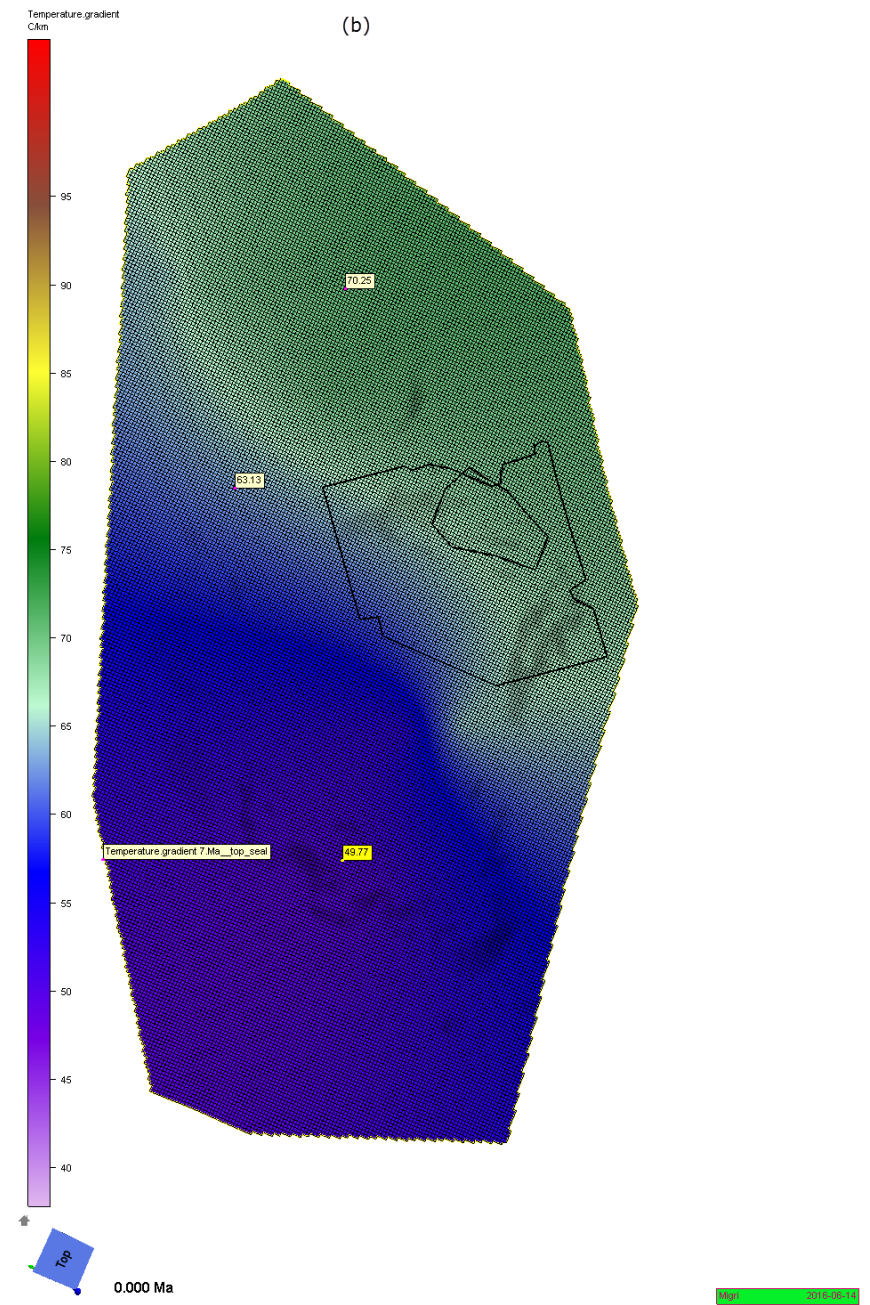
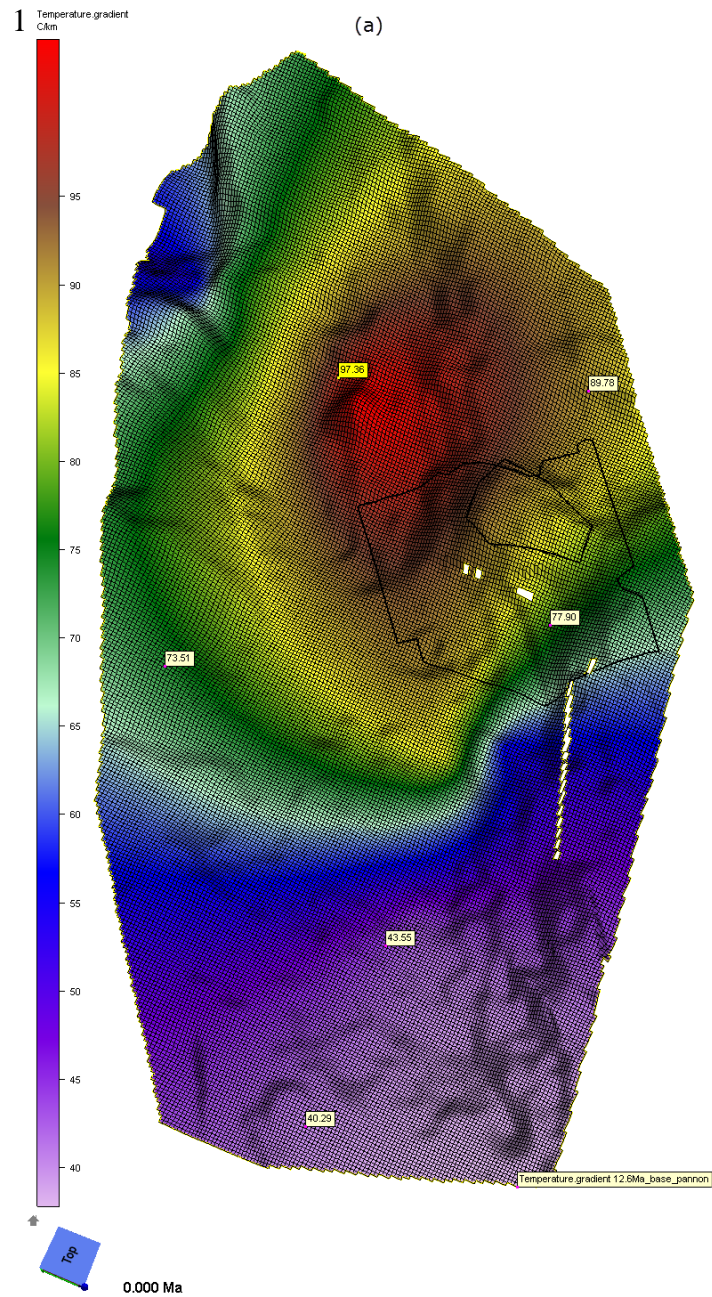


Figure 23: The resulted TDL temperature gradient grids from 1D modelling for the (a) base of Pannonian layer and for the (b)  $_{\text{h}}7$  Ma layer.

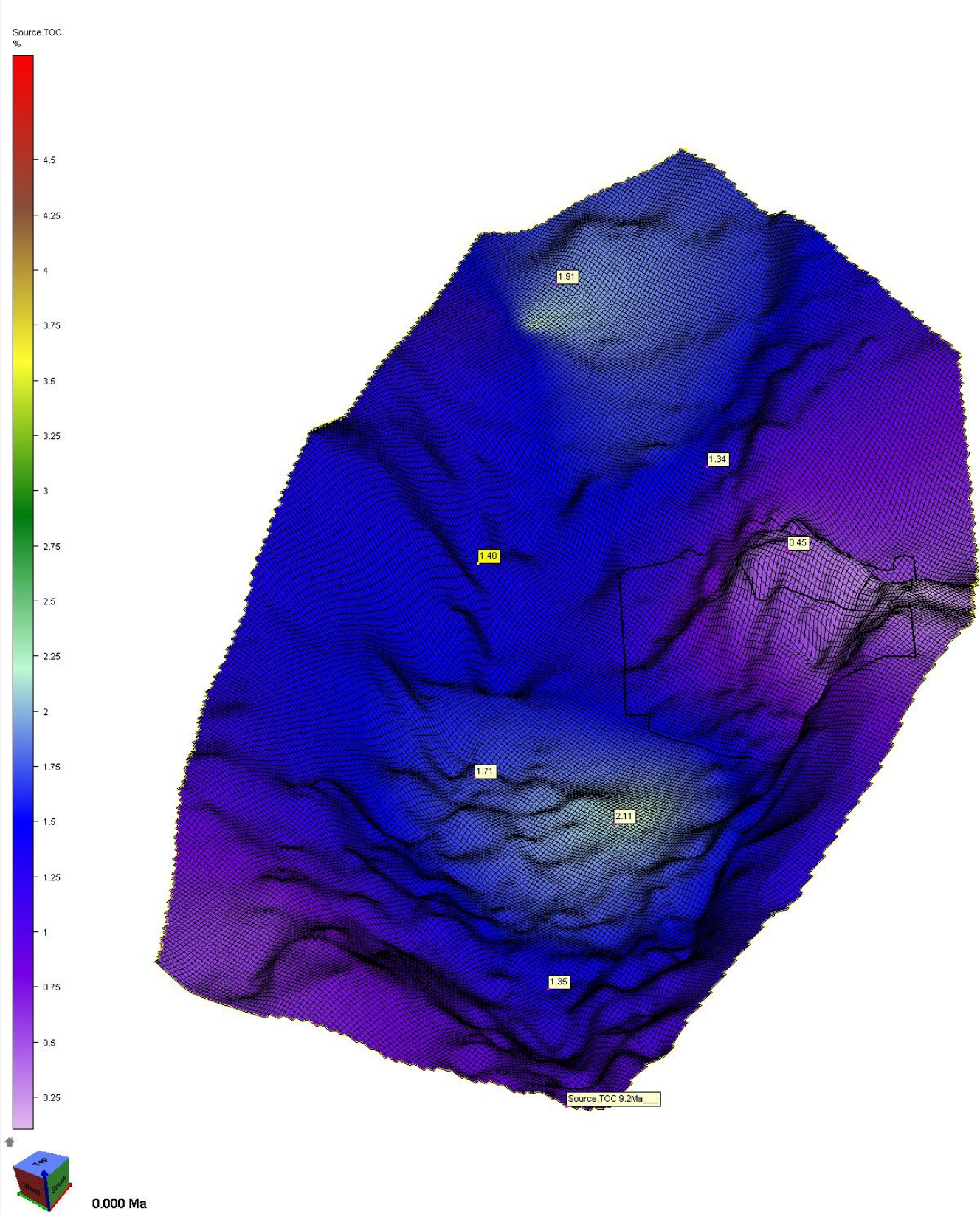


Figure 24: The back-calculated (TDL TOC% values from measured and estimated) TOC% data on the  $h9$  Ma source layer.

#### 4.2.2 Calibration and Simulation

The calibration of the model was realized by deterministic method, which is the same as in case of 1D models, and it means the refining of input thermal parameters with iteration until the modelled temperatures and vitrinite reflectance data fits to the measured. The calibration was based on the two master wells (Jász-I, Ab-D-1) with involving the highly uncertain data of Egyek-1 well. The comparison was made on the two lowermost layer and the thermal parameters were set up to the model. Applying the configuration of these settings, the best fitting cases were carried out shown in Table 7.

wells	Jász-I				Ab-D-1				Egyek-1			
layers	depth [m]		measured	modelled	depth [m]		measured	modelled	depth [m]		measured	modelled
<i>h 9.2 mA</i>	2416	T°C	111	110.6	2250	T°C	x	112.8	1369	T°C	x	70
		%Ro	0.58	0.58		%Ro	0.61	0.51		%Ro	0.6	0.2
<i>h 12.6 mA</i>	2955	T°C	130	133	2490	T°C	119	121	2164	T°C	x	108
		%Ro	0.77	0.75		%Ro	0.55	0.6		%Ro	0.8	0.7

Table 7: Comparison of measured and modelled temperature and vitrinite reflectance data on two layers.

Considering the low data quality and quantity for calibration, and accepting the fact that a 3D model with varying depths and lateral changes is forced to be calibrated by 2-3 values, the differences between measured and modelled data can be considered as a good calibration. To except better calibration the accuracy of depth conversion and the quantity of observation data should be increased. In our case this was not realizable. A higher level of thermal- and maturity calibration can be also done with probabilistic methods, where a range of varying parameters and settings is run and the best fitting options are restricted and chosen. This application of method will be the aim of another study.

A 10-20% limit error is accepted in this deterministic calibration and the Egyek-1 less reliably data is demonstrated, as it was supposed in the case of 1D models.

This part of work deals with the deterministic simulation method. This is realized by using the mean of the input parameters (grids and standard values).

### **4.2.3 Results of 3D Migration Modelling**

The results represents the conditions in basin at present day (as in the most of the cases will be shown), but can be viewed at each time-step.

#### **Maturity and Expelled Volumes**

In Migri model a kinetic scheme was applied to generate hydrocarbons because the main aim of the work is to investigate the processes of migration and not to define the possible geochemical scenes and expelled hydrocarbon volumes. This approach can be confirmed by three reasons:

- (1) the barely positive thermal conditions and the small amount of hydrocarbon expulsion of the source rocks was demonstrated by 1D models;
- (2) similar reference work was not founded which can be compared regarding to expelled volumes and the used control fields are supposed to contain biogenic gas also;
- (3) the issue of migration is strongly related to expelled volumes which are not considered as driving force, thereby not hindering the investigation;

Considering the above confirmations the expelled volumes will be not detailed. The present day oil window and expulsion window is shown on Figure 25 with the present day maturities in terms of *Easy%Ro* and maturity windows.

The oil window started the development ~8.5 Ma in ~2100 m depth and the present day conditions can be characterized with a 3150 m maximal depth and maximal 145°C temperature.

The basin during its subsidence did not achieved the phase of gas window (proven by the 1D-, 3D models and measured Ro% data), however a minimal gas expulsion is shown. An explanation of this result can be the initial gas generation during the late oil window phase. The oil generation in basin is present in the same spatial distribution as the expelled gas amount is shown in the Figure 25, but it differs with one order of magnitude from that.

The expulsion of hydrocarbons started ~8 Ma in case of the oil (T=70°C; Depth=900 m) and ~6 Ma in case of gas (T= 120°C; Depth=2000 m).

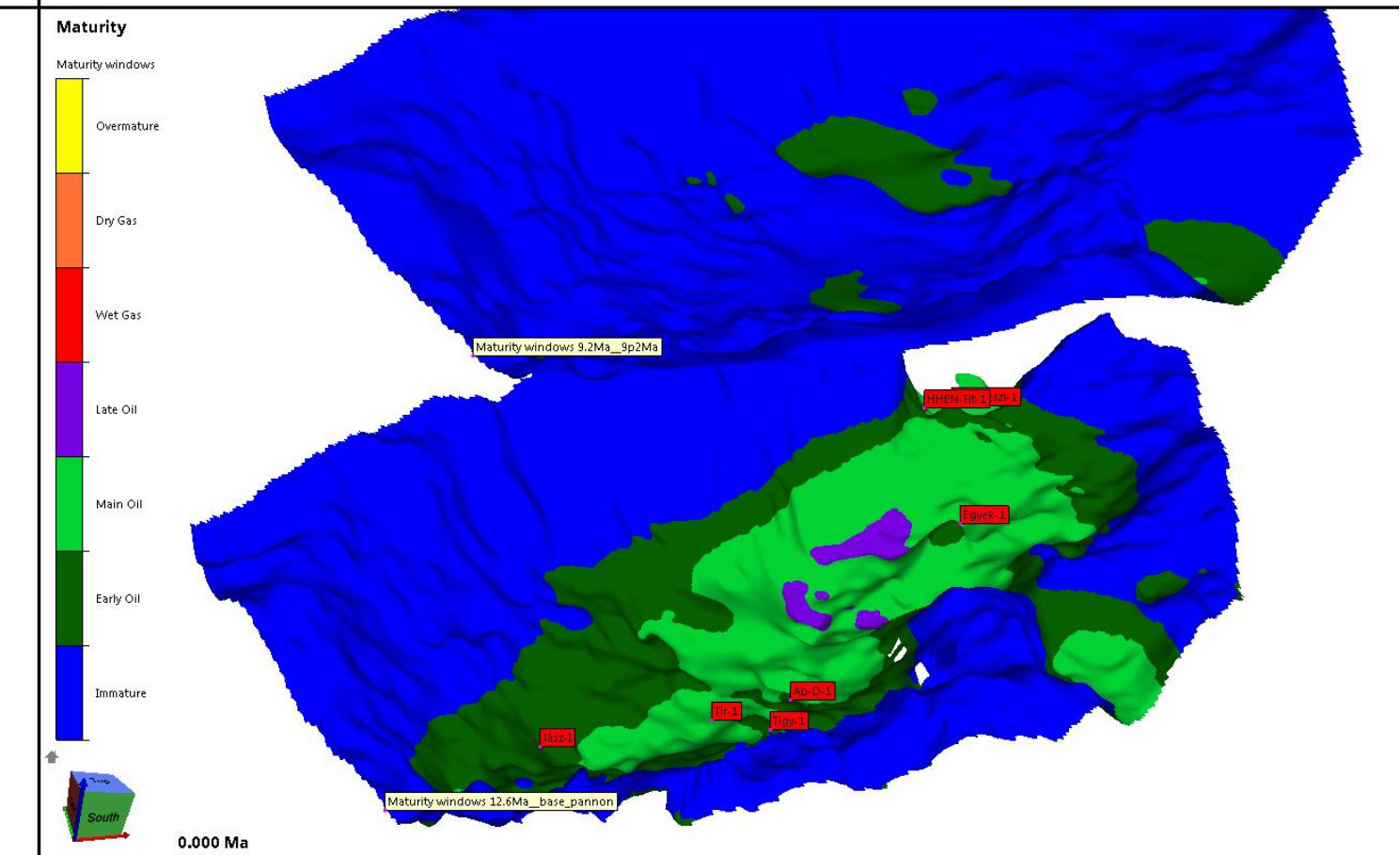
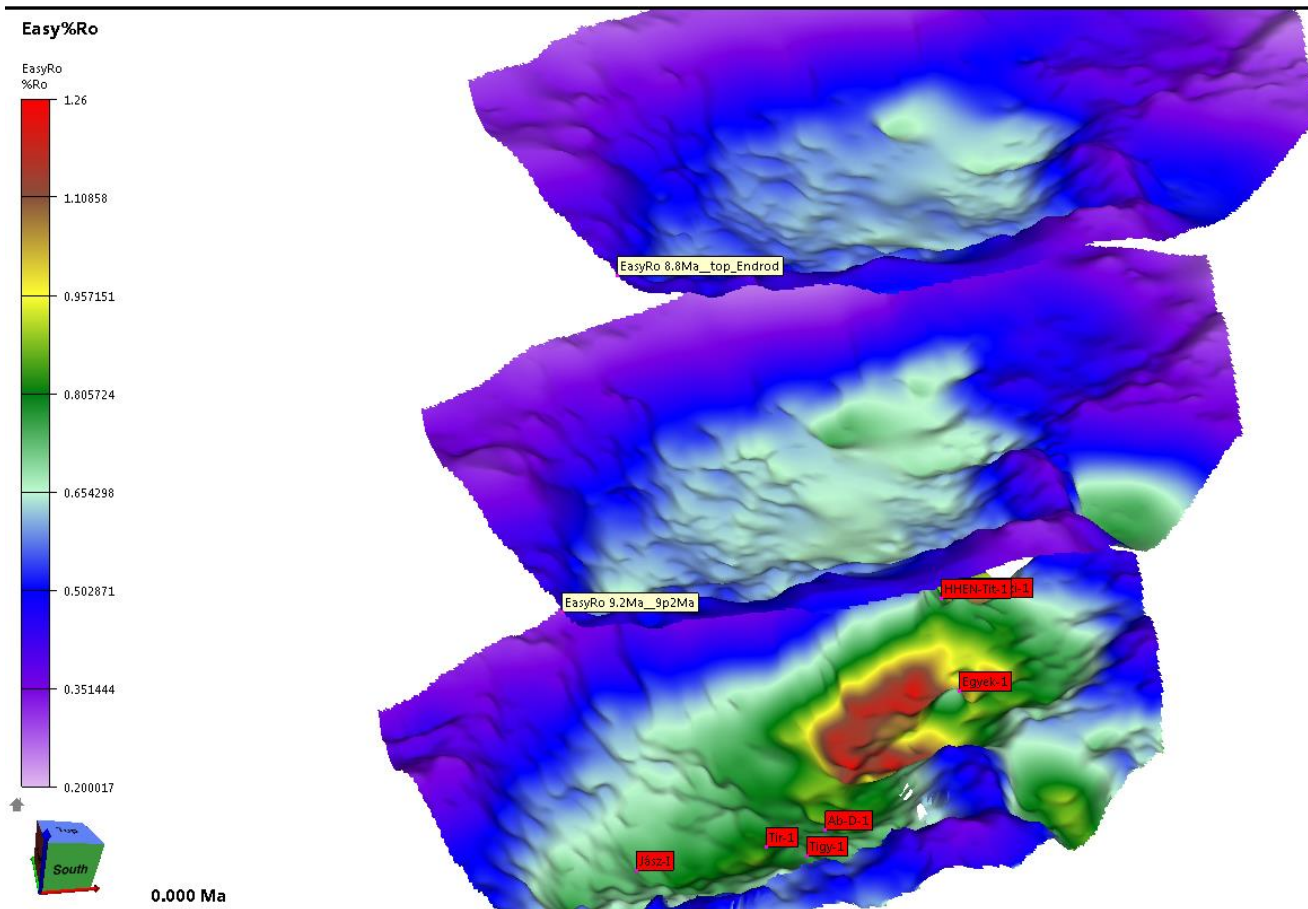
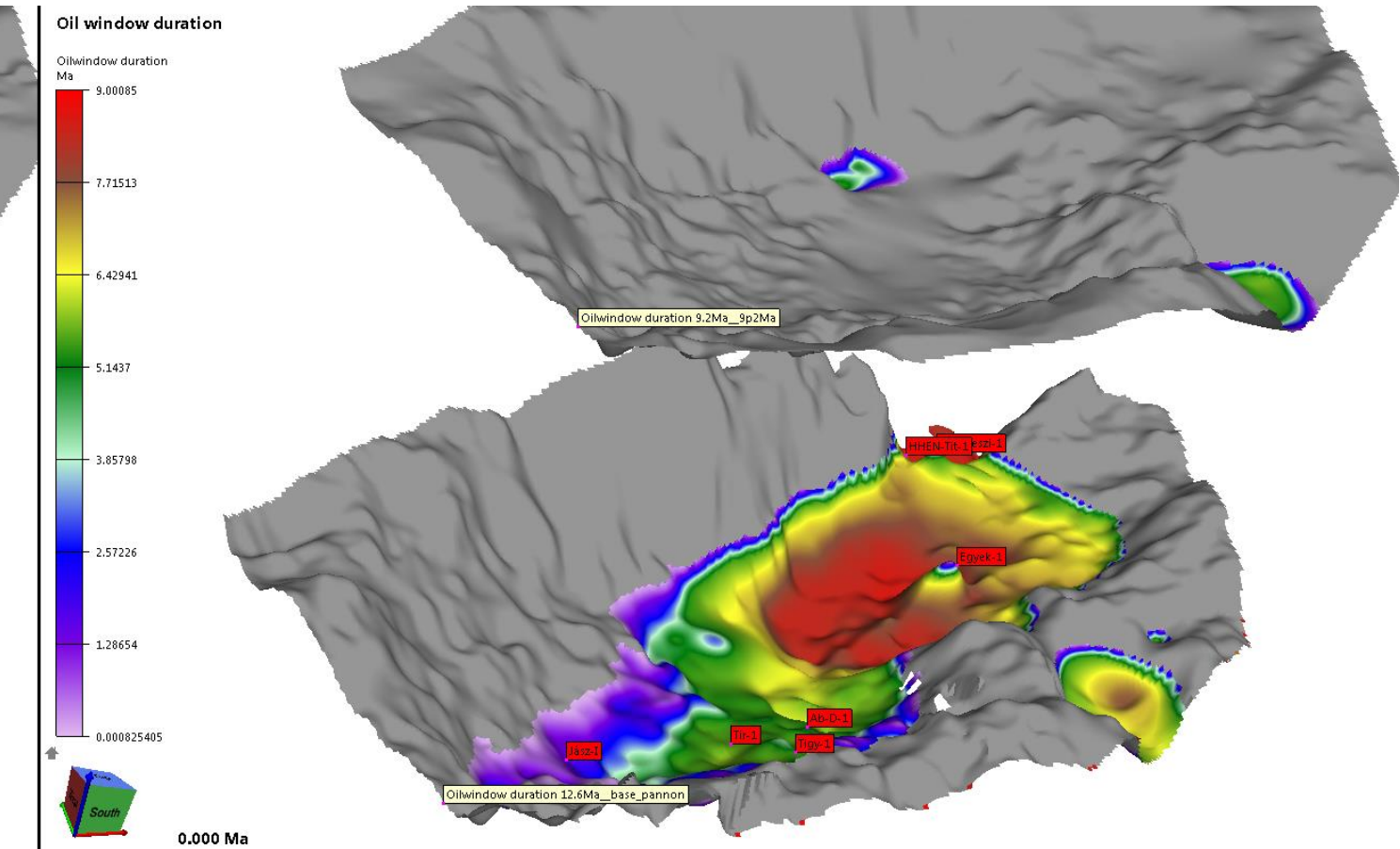
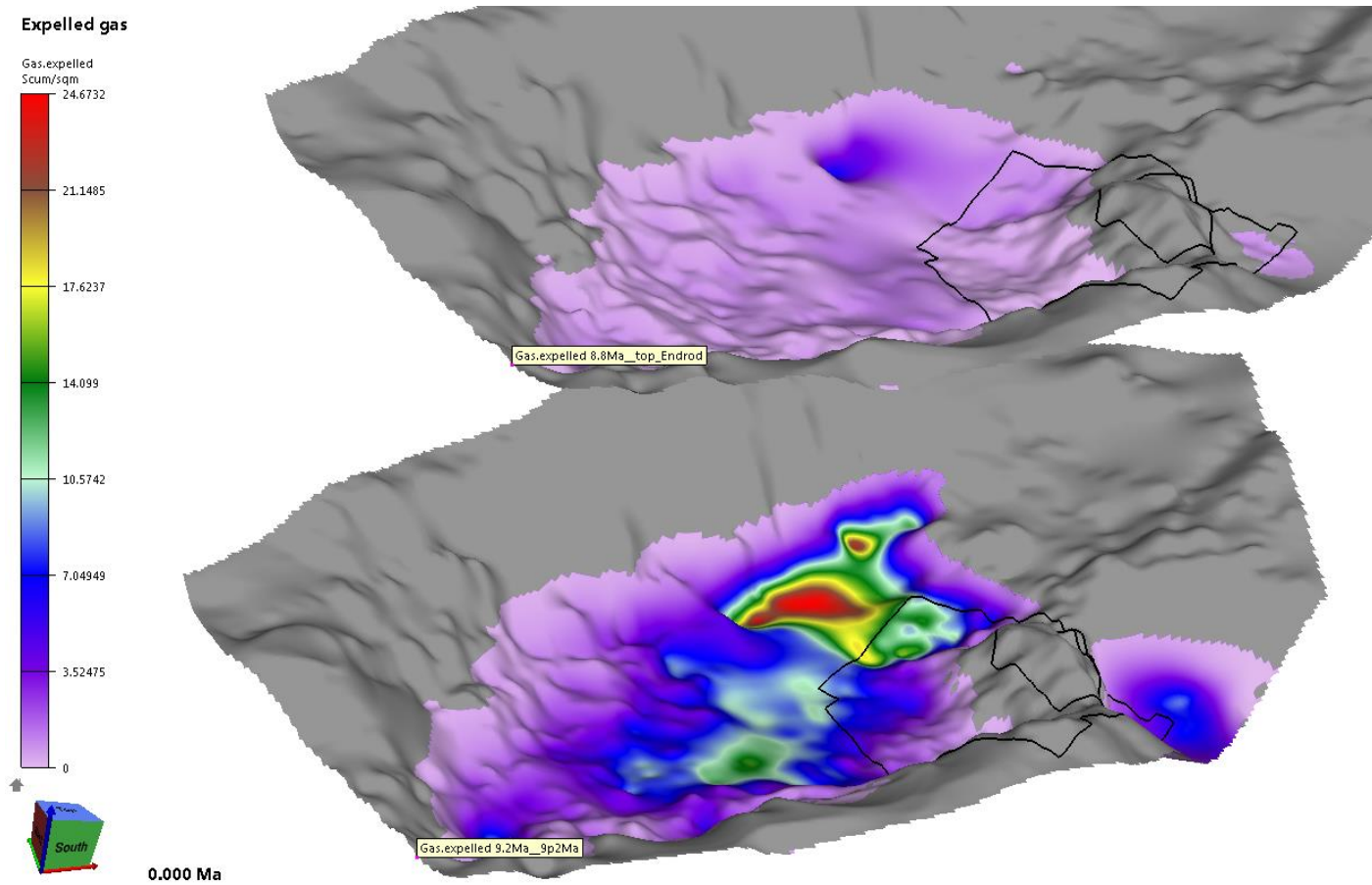


Figure 25: The present day maturity conditions of the studied area. The color bar and displayed property are shown on the left side of the figures.

## Migration

The main processes of hydrocarbon migration, which are still under debate and not very well understood, are as follows:

-primary migration: expelling of hydrocarbons from the source rocks;

-secondary migration: migration of hydrocarbons in the carrier rock to the trap;

-tertiary migration: the leakage of the traps.

Several different processes aim to describe the above processes, which show a wide alteration in the function of sedimentary basin and geological conditions. A large scale, basin wide, simulators with integrated fluid flow modelling tool are applied successfully to model the hydrocarbon migration. The engine of this simulators is based on the multi-phase Darcy flow law (Hantschel & Kauerauf, 2009). This method as an extrapolation by differential equation through geologic times and varying geological conditions reproduces the flow processes of hydrocarbons. The driving forces of fluid flow are potential differences of pressure, which is defined as:

$$u_p = p - \rho_p g z,$$

with  $\rho_p$  the density of fluid phase,  $p$ ,  $g$  the gravitational acceleration, and  $z$  the depth.

Darcy's law states that a potential difference causes a flow according to

$$V_p = \mu_p \frac{\Delta u_p}{\Delta l},$$

Where  $V_p$  is the velocity of flow of phase  $p$  and  $\mu_p$  its mobility. The  $\Delta u_p$  indicates a potential difference over a distance  $\Delta l$  in space. The flow direction is from high to low pressure potential. Timing of the fluid flow is included and quantified via the introduction of flow velocities. The mobility in multi-phase fluid systems is usually split into three factors: relative permeability, effective permeability and intrinsic permeability – equation description after Hantschel & Kauerauf (2009).

Similar to the majority of the basin modeler softwares, Migri uses multi-phase Darcy flow equation to describe and simulate the process of migration. Migration is modeled to occur in

regular or irregular mesh elements and can be influenced by sealing faults close to the seismic scales in resolution (Migri-AS, 2016).

Based on the profound doctoral thesis of Sylta (2004) the processes of migration will be discussed combined with some of the results of 3D modelling highlighting the most important geological parameters.

## Buoyancy and Hydrodynamics

The most important processes in hydrocarbon migration is considered the buoyancy and hydrodynamics, and they are related to overpressures and barriers. Buoyancy influences the hydrocarbon migration because of the density difference between the water and hydrocarbon phases. If the temperature is the most important factor in the hydrocarbon generation process than the pressure is the driving force for the migration process.

Based on experiments (Ibrahim, 1970) a general exponential relationship between capillary entry pressures and permeability values is given as follows:

$$P_{ce} = a(k/k_0)^b,$$

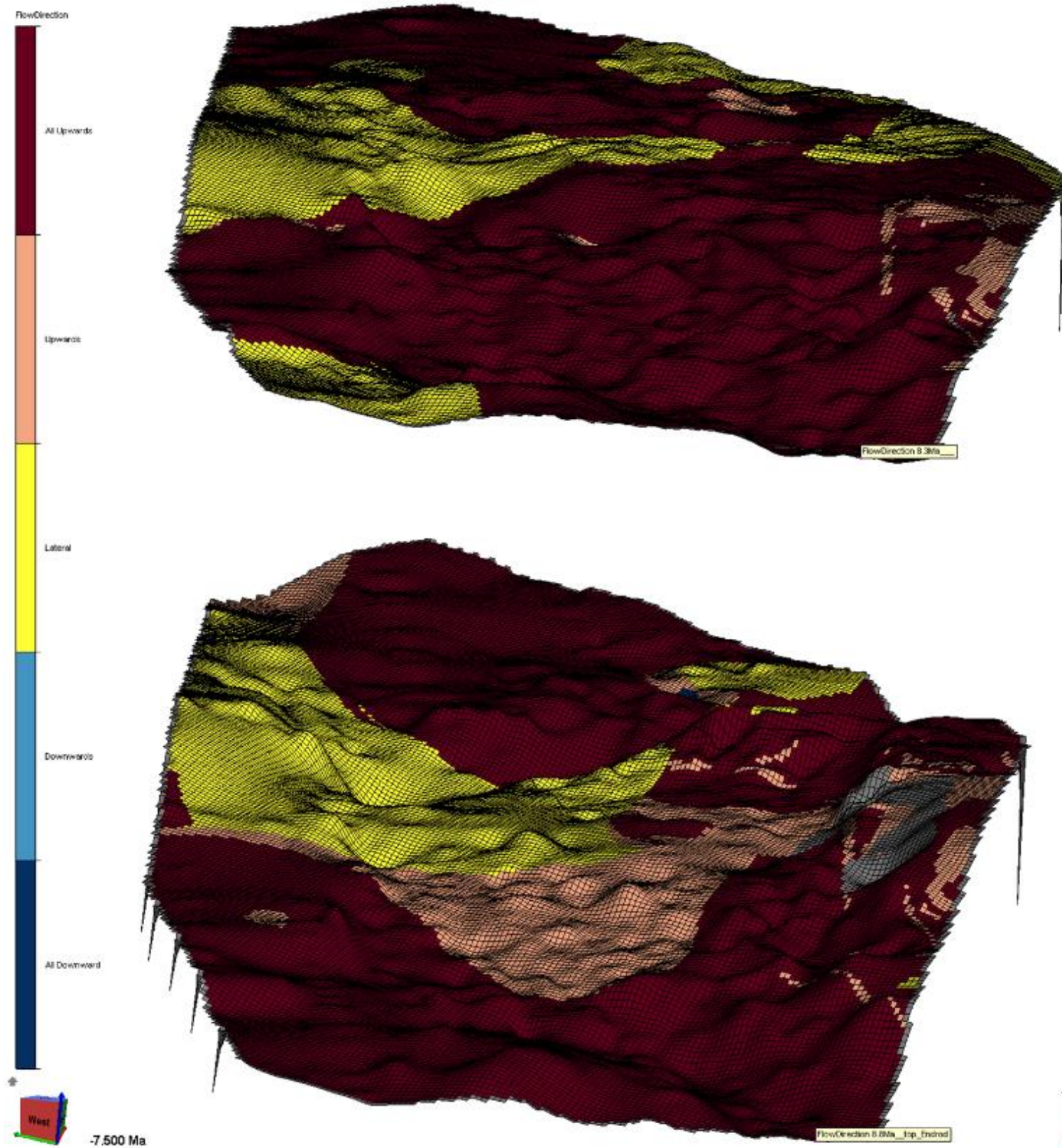
where  $P_{ce}$  is the capillary pressure,  $a = 0.548 \text{ MPa}$ ,  $b = -0.33$ ,  $k_0 = 1 \text{ mD}$ ,  $k$ =permeability.

Because of the lack of pressure data the pressure input of the model was untouched. Thus, the most general migration flow direction are influenced by permeability which is lithology dependent. The permeability values are computed from a depth dependent function which considers the  $Vca$  and  $Vsh$  lithology fractions.

In our case the buoyancy- and hydrodynamics parameters of the model are set by default and calculated with mean values. The only parameter, which is typical for the basin and influences the flow directions of the model are the permeability values derived from lithology.

The influence of the pressure is well showed on the Figure 26, where the flow direction of main source layer ( $\sim 8.8 \text{ Ma}$ ) – at the time-step ( $\sim 7 \text{ Ma}$ ) of the starting gas expulsion – is lateral and upwards while the present days (from the time-step 5.3 Ma) flow direction shows downward components.

(a)



(b)

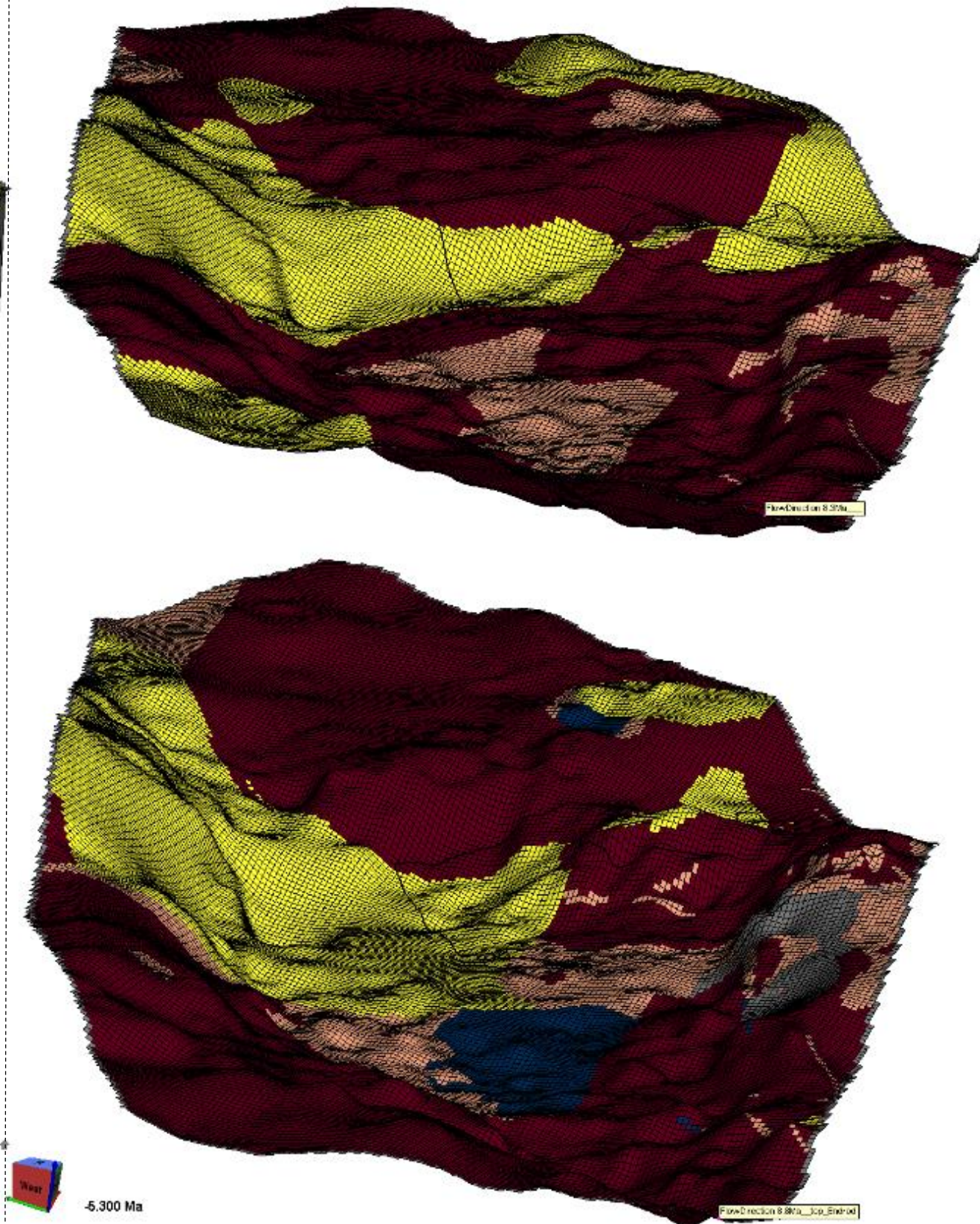


Figure 26: The flow directions of layers which present the top of Endrődi Formation by different time steps: (a) at 7.5 Ma time step; (b) at 5.3 Ma time step. The change of flow directions (e.g. the appearance of downward direction at 5.3 Ma) is related to the pressure increase by the burial of sediments.

## **Primary Migration and Flowpaths**

The primary migration in mud-mud rich sediments is a process with low losses of hydrocarbons. For this process the prior expulsion phase is definitely required (Chapter 4.2). The effects of primary migration using geochemical methods was investigated by many authors, but as the most commonly process to describe it, the Darcy flow was accepted. Because of low permeability values (nano-Darcy range) which a mud-rich source rock carries the migration rates in shales is shown a very low flow. This can lead to high hydrocarbon saturations migrating in extremely focused flow paths. The flow path is the velocity of hydrocarbon flow, expressed from Darcy's law as follows:

$$v = -\frac{\mathbf{k}kr}{\nu} \nabla u,$$

with permeability tensor  $\mathbf{k}$ , relative permeability  $kr$ , viscosity  $\nu$  and overpressure gradient  $\nabla u$ . A low estimation in carrier rocks is  $v=180\text{km/My}$  and velocities up to  $1000\text{km/Ma}$  have been reported in the literature (Sylta, 2004).

## **Secondary Migration and Traps**

The analysis of flowpaths is mostly related to the secondary migration process, when the hydrocarbon within a permeable carrier system into the traps is measurable. The condition of flow, because of good permeability values, can be imagined as the oil flow occurs during the production. Accepting the capability of hydrocarbons to migrate long distances it is considered that the migration in carriers continues until a trap is reached. During the secondary migration the chance of hydrocarbon losses is increasing with the occurrence of low permeability rocks (e.g. siltstones), but the possibility of appearances of micro-accumulations is given. The micro-traps can be considered as hydrocarbon losses but in the case of a complex geology and numerous accumulation this losses can gain significance. The flowpaths help to visualize the migration. In Migri the flowpaths are displayed as flowrates in function of hydrocarbon phases. These flowpaths end at the local heights of the carrier indicating the end of the migration and the process of trapping. Flowpaths are reconstructed from geometric analysis and indicate the direction of flow. In Migri each flowpath of a grid point from layer can be visualized in form of animated streams also. Several flowpaths can form a single stringer and ends at one local high forming a trap. The detailed analytics of flowpath modelling is too complex to detail in a thesis work.

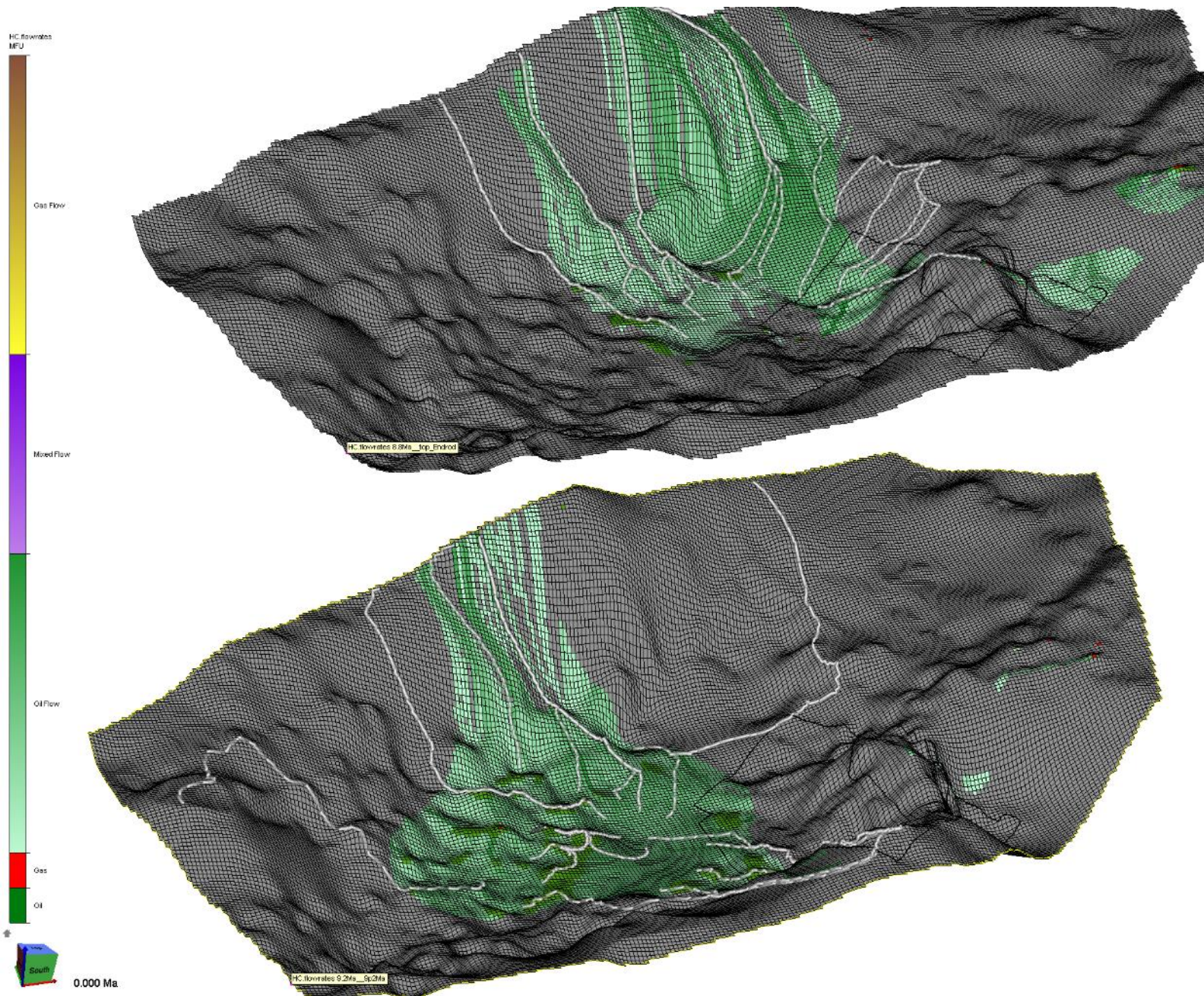


**Figure 27: Animated flowpaths. The path of each picked stringer can be investigated separately.**

The traps can be investigated from multiple views. The Migri offers a series of tools, which help to determine almost all properties of a trap. The drainage area of the trap, the spillnodes of the trap, the HC column and HC phase of the trap, and the dimension of the vertical closure can be investigated. In the **trap viewer tool** the amount and physical condition (PT, moving/leaking) of trapped hydrocarbons can be compared and analyzed. The accumulation of hydrocarbon in traps requires four-way closure by seals which facilitates the preservation. The issue of barriers, of seals and the related leakages need a complex high resolution analysis which is not included in this study. To analyze seals and trap leakages the scale of modeling requires prospect dimension with more detailed lithology, pressure and permeability input. To consider the faults and predict the fault sealing properties a probabilistic approach could be applied

(Chapter 4.3). By deterministic method a couple of scenarios can be set and without statistical analysis the evaluation this remains just a guess. Thereby in case of the model the identified maps should mean/represent four-way closures interpreted.

### **Trap-A\_216**

The filling history of each trap can be investigated individually using the wide tool palette of Migri to display the result of migration modelling. As observation data the production wells of Kunmadaras field were chosen. In this deterministic model scenario from the best reservoirs of field (Km-1, Km-3, Km-4, Km-5) the grid point of Km-3 well shows a hydrocarbon accumulation. Is known as the Kunmadras field contains mixed gas which are trapped in depth ~1100 m.

The trap is situated on layer generated from  $\mu 5.3Ma$  seismic horizon, which is set to carry the lithology of *Zagyvai Formation* (seal) and *Újfalui Formation* (reservoir). Each grid point of layer reflects the summarized properties of the relating sublayers, to define the depth and accurate position in space of the trap needs a higher resolution prospect scale model. However, an overview scenario of the trap filling can be established. In section AB (Figure 28) is shown that the migration direction of hydrocarbons is upward until the reservoir layer/formation is not reached. The lateral migration of hydrocarbons is realized across this layer while the migration streams shows the most favorable pathways (related strongly to geometry) to accumulate and migrate. The stringer which theoretically fills the trap A\_216 joining with other stringers and moving forward in the direction of a higher and larger structural closure.

Not tending to detail the amount of trapped gas, but considering the low hydrocarbon generation of basin and the presence of biogenic gases, the next solution seems acceptable: In case of trap A\_216 the thermogenic gases probably was generated in late oil phase. During the migration processes, they contributed in filling up the four-way closure in form of micro-traps, thus representing the thermogenic portion of the trap. The leakage of the trap is shown possible, but to make approximate conclusions a deeper investigation is needed.

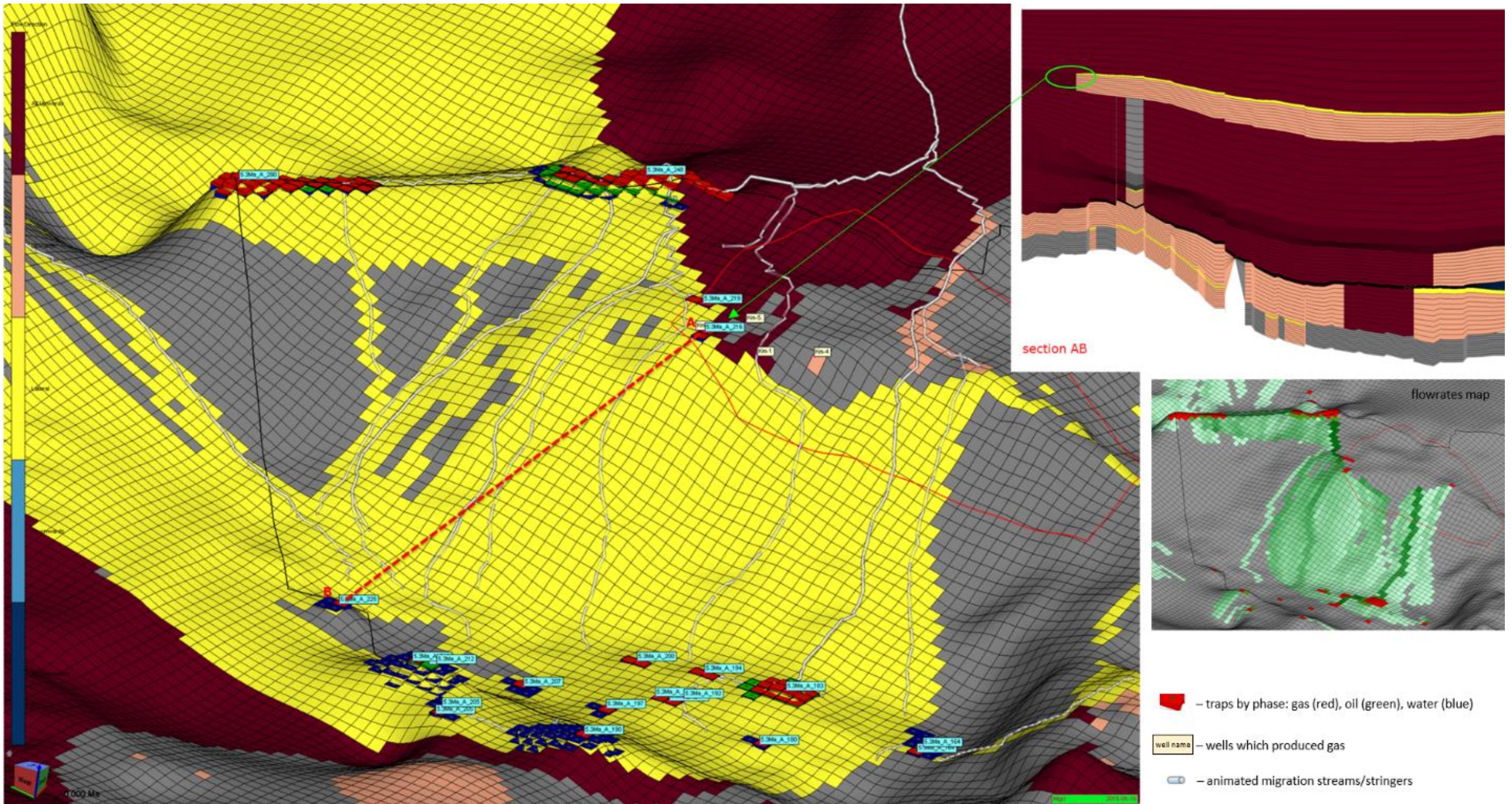


Figure 28: Displayed traps and migration streams in function of flow directions on layer n5.3Ma. The investigated Trap\_A\_216 is shown on layer in point A and on section AB with green circle. The flow directions related to trap can be viewed in section AB (legend on the left side).

### 4.3 Probabilistic Approach

During the model building no faults were considered. Involving faults in the geometry of the model, increase the uncertainty factor and the possible outgoing of a simulation. Complex geological situations barely can be solved by deterministic methods which – regarding to the time limit and technical limits of a project – offer a small amount of outgoing scenarios without extreme values, among which one is accepted as best solutions. Thus a series of questions remains opened: What is the chance of having real scenarios? Which parameter influences which result/outcome? What is the impact uncertainties and changing parameters in the model?

In case of one trap related fault, a basic question can be provided: The fault is sealing or leaking? Thinking on deterministic way a couple of scenarios can be set and modelled: the fault is totally sealing, the fault is leaking, and the fault is semi-closed. What if the results are similar, and two of the three scenarios fill up the trap? How can be chosen and applied the sealing properties of the fault supposing that it has a great influence in hydrocarbon accumulation? An example for a similar situation is given on Figure 29, where in case (a) the fault is totally closed and in case (b) is opened but in either cases the trap-A is filled. The scenario with closed faults indicates the presence of alternative traps.

The probabilistic modelling can restrict the unanswered questions. Requires a backward thinking approach: in function of observed data (hydrocarbon show maps, well testing data, temperature data, maturity data) thousands variation of changing parameters are tried by Monte Carlo analysis to a given geological situation, and after a series of data analysis the best fitting scenario is accepted. The probabilistic migration modelling and the consideration of uncertainties is widely researched by Sylta (2004).

In Migri the simulation method can be switched from deterministic to stochastic, which means the introduction of uncertainties into the model. The stochastic simulation can be done by using Monte Carlo simulation. Monte Carlo methods are algorithms that rely on repeated sampling of a known distribution to obtain numerical results. The starting point for a Monte Carlo simulation is a reference model and a list of uncertainties belonging to the data. The reference model is based on a parameter set within the limits of these uncertainties which represents a best first guest. So the Monte Carlo simulation means a set of random numbers according to the distributions is drawn and a simulation run with this parameter set is performed (Hantschel & Kauerauf, 2009).

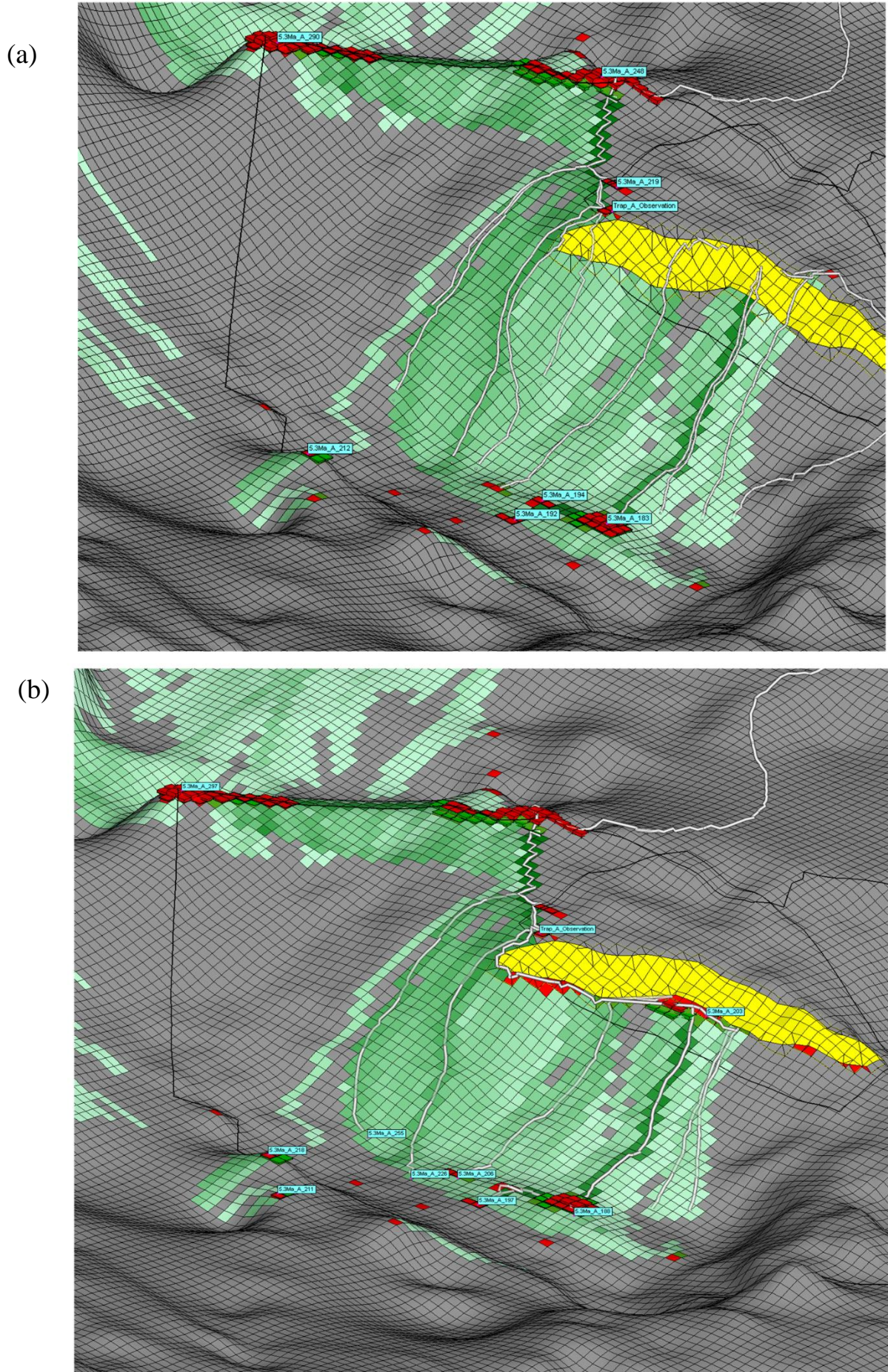


**Figure 29:** Two possible cases for a fault (yellow surface): (a) leaking fault; (b) sealing fault. The migration streams shows the possible pathways and alternative hydrocarbon accumulations (red grid points, case B, trap A\_203).

To demonstrate the method and the achievable results, a stochastic simulation case was set up in this work. The goal of the simulation was to restrict the offset (if it exists) of the demarcated/considered fault identified on 3D seismic. The fault is defined on the  *$h5.3Ma$*  layer which represents the summed up properties of the possible reservoir layer (Figure 29). Having no information about this fault and its sealing conditions, a randomly best first guess was applied, supposing that the fault has offset.

The prior mentioned observation data in our case is the height/thickness of the tested and produced reservoir bodies defined in just one well (for simplicity) Km-3. The reference model of stochastic case is represented by the thermally calibrated deterministic model with its parameters defined by grids and standard values.

Almost for every parameter can be set uncertainty. Regarding to the experimental nature of this simulation, uncertainty was assigned as follows:

Property	Mean	Uncertainty
<i>Vsh</i> (shale fraction)	grid	[+0.018] %
<i>Vca</i> (carbonate fraction)	grid	[+0.02] %
<i>HI</i> (Hydrogen index)	grid	[+100] mgHC/TOC
geometric <i>fault offset</i>	120	[+60] m

*Table 7: The varying parameters and the assigned uncertainties during the stochastic simulation.*

The stochastic simulation can be made in Migri or with the background simulator called MigriBee. The MigriBee process is running without visualization component and simulates the defined number of runs determined by user. In our case 2400 runs was proceeded with the varying values of the above parameters.

The analysis of resulted simulations is in Risk Chart tool where with many methods the comparison of runs can be made (misfit analysis, distribution/deviation analysis). Thus the extreme parameters which shows the highest misfit to the observed data can be filtered, and with the refined range of parameters a new iteration can be run. This procedure is repeated while the results – which are based on statistically measurable quantities – fits to the observed data. After the first iteration run the average misfit of the simulations was [-2.7] which means that the model is underestimated by one parameter. A new iteration was set by changing those parameters which deviation exceeded with more than 0.3 the mean value of the parameter calculated from 2400 run. Hence the deviation of HI parameter was restricted which solved the underestimation of the model, regarding to hydrocarbon column heights. The obtained result from 1500 run with the second iteration shows a good calibration with an acceptable [-0.02] average misfit.

The possibility to analyze the risk is given by the software during simulation. Thus the risk map of the parameter can be generated and the probabilities calculated. An example for realizing the probabilities of the hydrocarbon flow is shown on Figure 30 and the risk of phase is shown on figure 32.

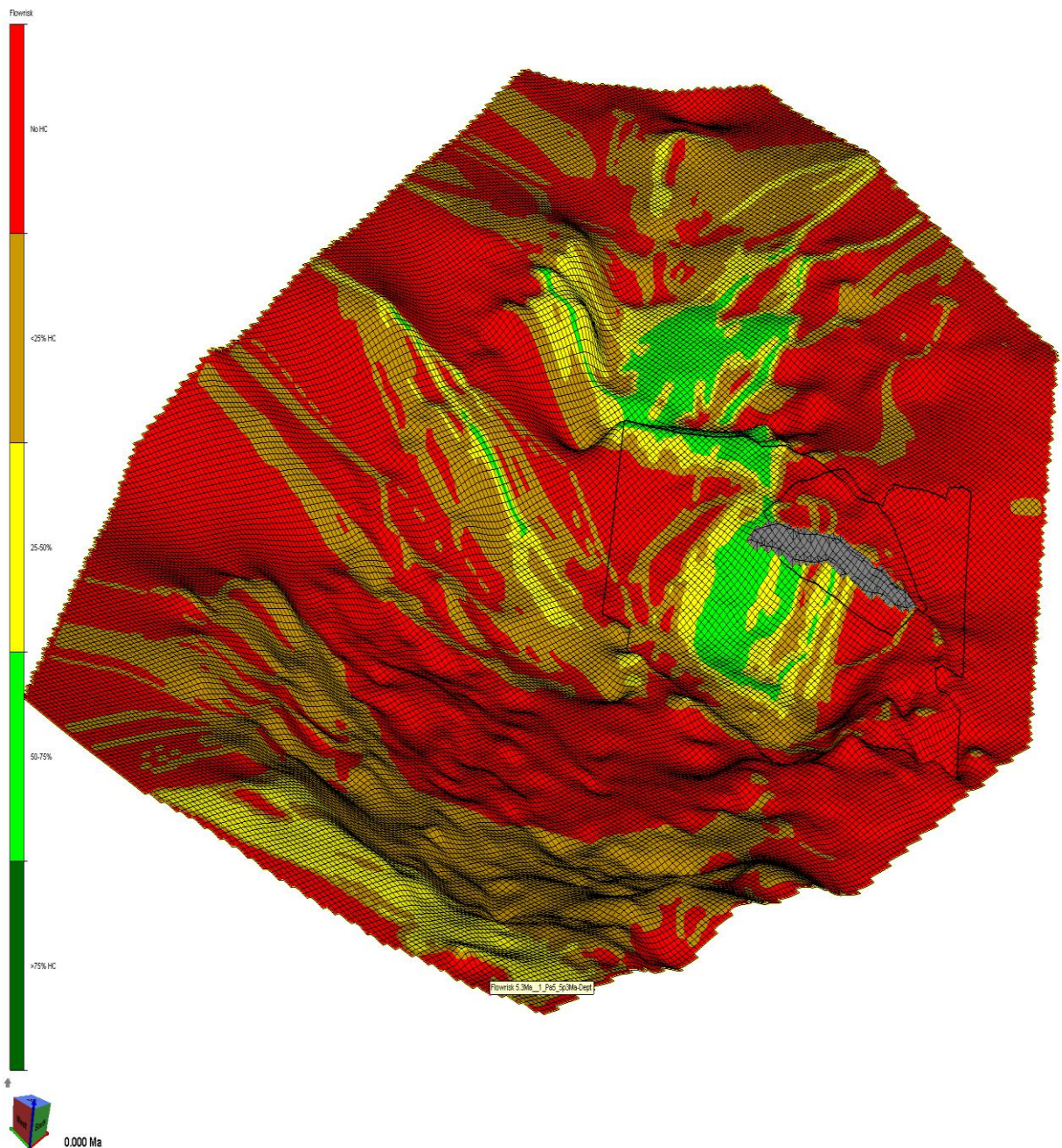


*Figure 30: The resulted hydrocarbon flow-risk map of the stochastic simulation based on more than 3000 runs.*

Thereby, the relation of a supposed throwing fault with the observation data can be determined and the next statues accepted to this case:

- The filling of observed traps could be realized within a throwing fault, which maximal throw does not exceed the 80m (Figure 31)

- based on more than 3000 simulation runs the probability of hydrocarbon flow in the direction of trap is 50-75%

- if the migration has been realized the probability of gas phase is ~65%

Summarizing, the main steps of the stochastic method are presented above, and this method is the base of the model calibration related to maturity and thermal history also. Introducing the uncertainties in modeling the complexity can increase, but the handling of varying parameters (which give a good approach to reality) is the way to estimate the real risks of hydrocarbon systems.

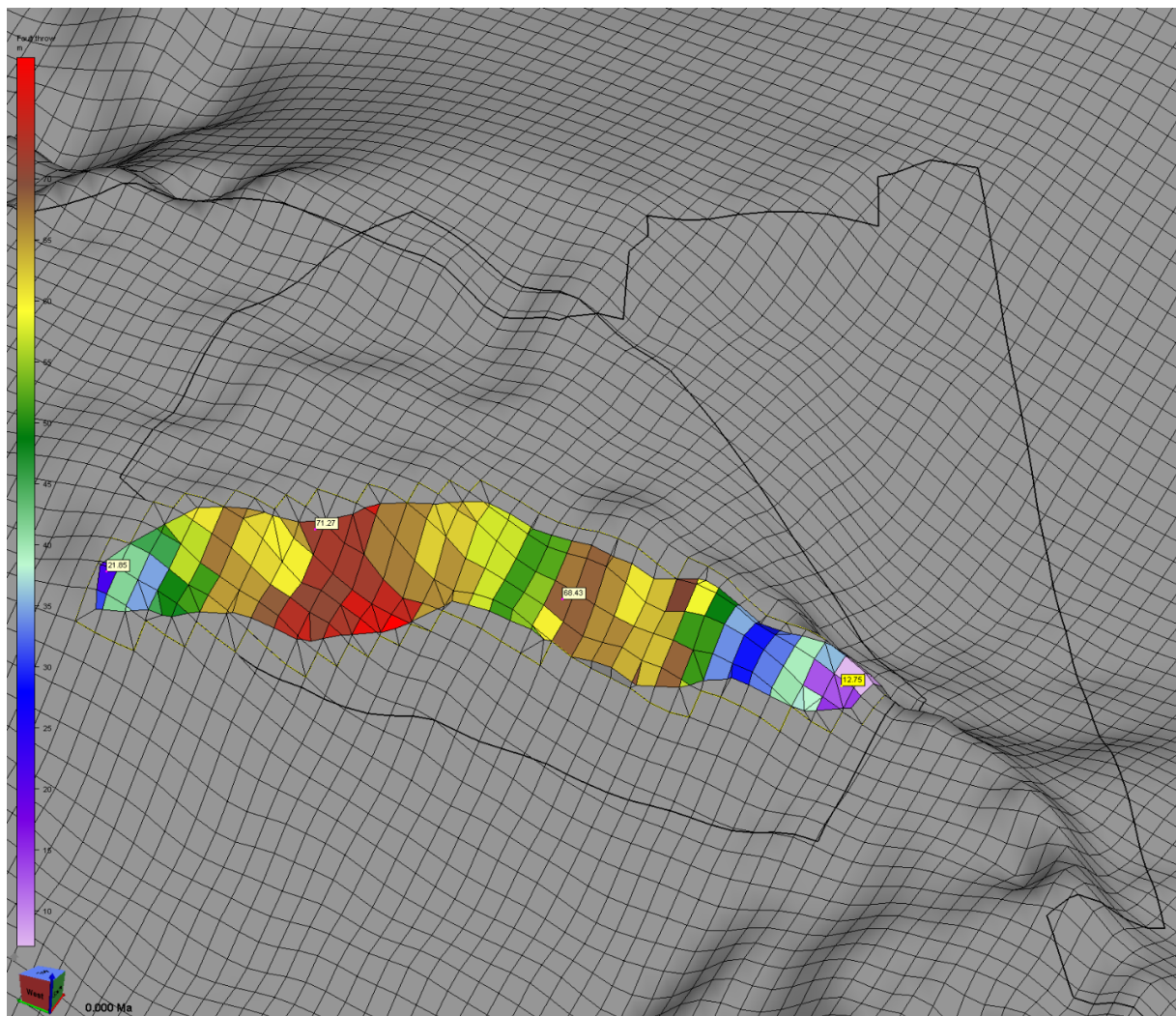


**Figure 31: The modeled fault offsets with picked values. This setting gives the best fitting case of the applied configuration – 120 m mean offset and [+60] m uncertainty – to fill the investigated trap.**

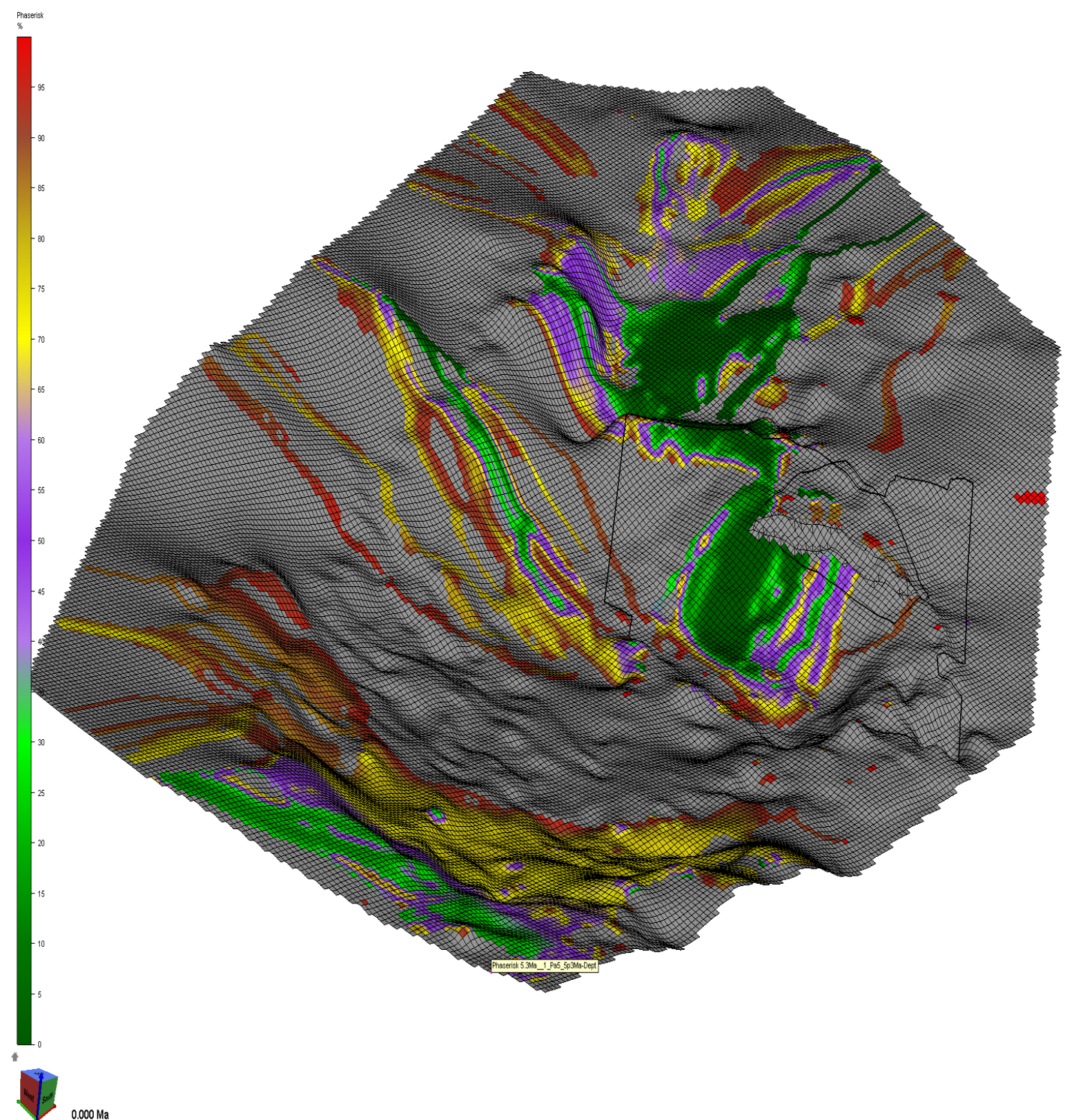


**Figure 32: Probability of gas phase, if migration takes place (100%-all simulations give gas, 50%-50% of simulations give gas and 50% give oil).**

## 5. CONCLUSIONS

By many modelling processes and software packages, the migration modelling is considered and included as a result of general basin modelling. They do not emphasize properly the role and risk of these in exploration workflow. The complexity of multi-phase fluid flow generation and modelling requires the separation and discussion of migration modelling as an overall risking method.

As first conclusion can be considered that the work achieved its goal in terms of studying the methods of modelling. The migration related to deterministic 3D model was built by proceeding through steps of 1D modelling. Both of models demonstrated the low hydrocarbon generation rate of the Jászság-basin and defined the thermal and maturity conditions of it. The driving forces of migration are presented and discussed in (Chapter 4.2.3).

The most widely distributed modelling techniques contains the thermal modelling and source rock generation modelling to investigate the possible hydrocarbon potential of the prospects. Besides, the aim of subsidence and burial modelling is included. The thermal evolution of source rocks are realized generally using heat flow histories and sediment surface temperatures. The generation of oil and gas phases are computed from thermal history related to the kinetic models. The primary migration of generated hydrocarbons can be modelled using the Darcy flow method. This approach of modelling is mostly used in deterministic studies where the results of one or a very few simulation are considered as best case scenarios for geological risk assessments.

As second conclusion can be stated that the accuracy, thus the relation to reality of the model depends mostly on three parameters: (1) scale of the model; (2) amount and resolution of input data; (3) calibration method. The accuracy of model could be increased with the introduction of probabilistic calibration methods, where the thermal and maturity parameters are defined by Monte Carlo simulations and calibration based on input data statistics. In the study the deterministic calibration approach was used. Thus, necessarily has to be stated that the model carries uncertainties.

In modelling workflow the non-consideration of alternative cases increases the risk of not including the correct geological scenario (Sylta, 2004). Thereby, referring to the many reasons (lack of data, lack of experience, uncertainty of using the results of the analysis) why well calibrated 3D models are not used in exploration projects and the method of hydrocarbon migration investigating is ignored (Figure 33).

The principle of migration modelling in probabilistic ways, thus enabling the concept of risk analysis related to exploration campaigns, was investigated widely by *Dr. Philos Øyvind Sylta* (Sylta, 2004). His approach was followed in this study. In exploration workflow, beside the mainly used seismic interpretation, the processed based (probabilistic methods) modelling of geological events can be used as independent decision criteria for exploration works.

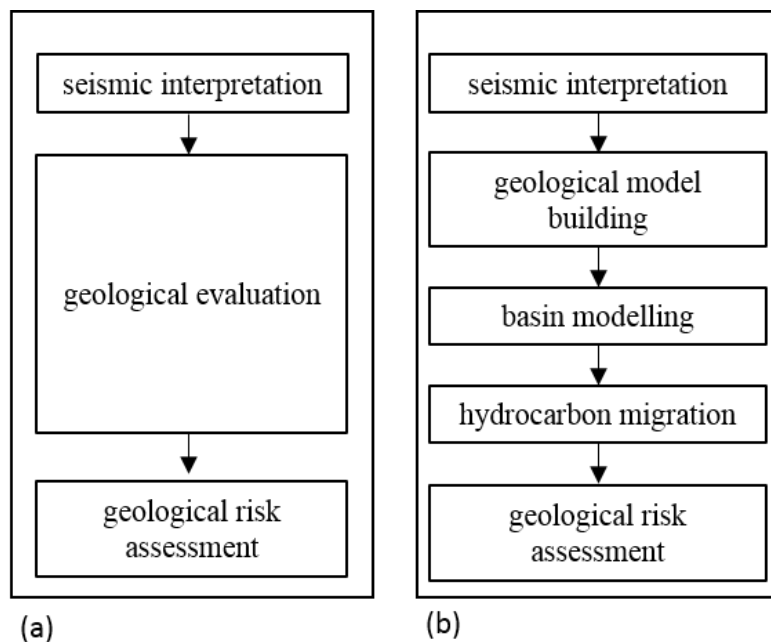


**Figure 33: Overview of hydrocarbon exploration workflow: (a) without and (b) including geological modelling tasks (Sylta, 2008).**

As third conclusion, in thesis is introduced the idea of stochastic based hydrocarbon migration modelling. This could be the tool to investigate the uncertainties of a geological model, to restrict the parameters and define the most probably scenarios for a poorly understood geological situation thereby decreasing the risk of exploration. With this goal an experimental case was run, with a low amount of varying parameters and simulation runs. Analyzing the result the risk map of geological events can be made. It is important to emphasize the experimental nature of this part. The probabilistic modelling counts with tens of varying parameters and thousands of runs.

The development of the work broadly can be sketched with the following ideas:

- to increase the data input and the resolution of seismic mapping (number of depth surfaces)
  - to accurate the depth conversion
  - to enlarge the input data types: pressure, permeability, porosity, anomalies, burial and expulsion histories
  - to calibrate with stochastic methods the thermal and maturity conditions
  - to enlarge the hydrocarbon observation data involving the use of HC show maps

## REFERENCES

- Bada, G., Horváth, F., Dövényi, P., Szafián, P., Windhoffer, G., & Cloetingh, S. (2007). Present-day stress field and tectonic inversion in the Pannonian basin. *Global and Planetary Change*, 58(1-4), 165–180. <http://doi.org/10.1016/j.gloplacha.2007.01.007>
- Badics, B., & Veto, I. (2012). Source rocks and petroleum systems in the Hungarian part of the Pannonian Basin: The potential for shale gas and shale oil plays. *Marine and Petroleum Geology*, 31(1), 53–69. <http://doi.org/10.1016/j.marpetgeo.2011.08.015>
- Bahlburg, H., & Breitkreuz, C. (2004). *Grundlagen der Geologie* (second edi). Muenchen: Elsevier GmbH.
- Balla, Z. (1984). The Carpathian loop and the Pannonian basin: a kinematic analysis. *Geophys. Trans.*, 30(4)(313-353).
- Bérczi, I. (1988). Preliminary sedimentological investigation of a Neogene depression in the Great Hungarian Plain. In L. Royden & F. Horváth (Eds.), *The Pannonian Basin. AAPG Memoir 45* (pp. 107–116). AAPG.
- Csató, I. (1993). Neogene sequences in the Pannonian basin, Hungary. *Tectonophysics*, 226(1-4), 377–400. [http://doi.org/10.1016/0040-1951\(93\)90128-7](http://doi.org/10.1016/0040-1951(93)90128-7)
- Csizmeg, J., Juhász, G., Milota, K., & Pogácsás, G. (2011). Subsidence , Thermal and Maturity History of Late Miocene to Quaternary Formations in the Pannonian Basin \*, 10367.
- Csontos, L., Nagymarosy, A., Horváth, F., & Kováč, M. (1992). Tertiary evolution of the Intra-Carpathian area: A model. *Tectonophysics*, 208(1-3), 221–241. [http://doi.org/10.1016/0040-1951\(92\)90346-8](http://doi.org/10.1016/0040-1951(92)90346-8)
- Dolton, G. L. (2006). Pannonian Basin Province, Central Europe (Province 4808)—Petroleum Geology, Total Petroleum Systems, and Petroleum Resource Assessment. *USGS Bulletin*, 2204-B(Province 4808), 1–47.
- Espitalie, J., Tang, Y., Vandenbroucke, M., & Behar, F. (1997). Thermal cracking of kerogen in open and closed systems: determination of kinetic parameters and stoichiometric coefficients for oil and gas generation. *Organic Geochemistry*, 26, 321–339.
- Faupl, P., Császár, G., Mišik, M. (1997). Cretaceous and Palaeogene sedimentary evolution in the Eastern Alps, Western Carpathians and the North Pannonian region: An overview. *Acta Geologica Hungarica*, 40/3, 273–305.
- Fodor, L., Csontos, L., Bada, G., Görfi, I., & Benkovics, L. (1999). Tertiary tectonic evolution of the Pannonian Basin system and neighbouring orogens:

a new synthesis of palaeostress data. *Geological Society, London, Special Publications*, 156(1), 295–334.  
<http://doi.org/10.1144/GSL.SP.1999.156.01.15>

Hantschel, T., & Kauerauf, A. I. (2009). *Fundamentals of basin and petroleum systems modeling. Fundamentals of Basin and Petroleum Systems Modeling.* <http://doi.org/10.1007/978-3-540-72318-9>

Horváth, F. (1993). Towards a mechanical model for the formation of the Pannonian basin. *Tectonophysics*, 226, 333–357.

Horváth, F. (1995). Phases of compression during the evolution of the Pannonian Basin and its bearing on hydrocarbon exploration. *Marine and Petroleum Geology*, 12(8), 837–844. [http://doi.org/10.1016/0264-8172\(95\)98851-U](http://doi.org/10.1016/0264-8172(95)98851-U)

Horváth, F., & Royden, L. (1981). Mechanism for the formation of the intra-Carpathian basins: a review. *Earth Evolution Sciences*, 1, 307–316.

Juhász, G. (1994). Magyarországi neogén medencerészek pannoniai s.l. üledéksorának összehasonlító elemzése. *Földtani Közlöny*, 124(3), 341–365.

Juhász, G. (1998). Lithostratigraphy of the Pannonian s.l. formations of Hungarian Neogene deep basins in Hungary. In I. Bérczi & Á. Jámbor (Eds.), *Magyarország geológiai képződményeinek rétegtana* (pp. 469–483).

Juhász, G. (2007). Óriáskanyon-rendszer szeli át a pannóniai üledékeket? *Földtani Közlöny*, 137(3), 307–326.

Juhász, G., Pogácsás, G., Magyar, I., & Vakarcs, G. (2007). Tectonic versus climatic control on the evolution of fluvio-deltaic systems in a lake basin, Eastern Pannonian Basin. *Sedimentary Geology*, 202(1-2), 72–95. <http://doi.org/10.1016/j.sedgeo.2007.05.001>

Lenkey L., Dövényi P., Horváth F., Cloething, S., & L., A. P. (2002). Geothermics of the Pannonian basin and its bearing on the neotectonics. *European Geosciences Union Stephan Mueller Special Publication Series*, 3, 29–40.

Magyar, I., Geary, D. H., & Müller, P. (1999). Paleogeographic evolution of the Late Miocene Lake Pannon in Central Europe. *Palaeogeography, Palaeoclimatology, Palaeoecology*, 147(3-4), 151–167. [http://doi.org/10.1016/S0031-0182\(98\)00155-2](http://doi.org/10.1016/S0031-0182(98)00155-2)

Mattick RE, Rumpler J, Ujfalusy A, Szanyi B, N. I. (1994). *Sequence stratigraphy of the Békés basin. In: Teleki PG, Mattick RE, Kókay J (szerk) Basin Analysis in Petroleum Exploration. A case study from the Békés basin, Hungary.* Dordrecht: Kluwer Academic Publishers.

McGraw-Hill Dictionary of Scientific & Technical Terms, 6E (2003).

- McKenzie, D. (1978). Some remarks on the development of sedimentary basins. *Earth and Planetary Science Letters*, 40, 25–32.
- Migri-AS. (2016). Migri. Trondheim.
- Mucsi, M., & Révész, I. (1975). Neogene evolution of the southeastern part of the Great Hungarian Plain on the basis of sedimentological investigations. *Acta Mineralogica-Petrographica*, 22(1), 29–49.
- Panaiotu, C. (1998). Monograph of Southern Carpathians , Reports on Geodesy. In *Africa* (Vol. 7).
- Peters, K. E., Walters, C. C., & Moldwan, J. M. (2005). *The Biomarker Guide, volume 1 and 2* (second edi). Cambridge: Cambridge University Press.
- Piller, W. E., Harzhauser, M., & Mandic, O. (2004). Miocene Central Paratethys stratigraphy – current status and future directions. *Stratigraphy*, 4(2/3), 151–168.
- Pogácsás, G. (1984). Seismic stratigraphic features of Neogene sediments in the Pannonian Basin. *Geophysical Transactions*, 30, 373–410.
- Révész, I. (1980). Az Algyő-2 telep földtani felépítése, üledékföld - tani heterogenitása és ösföldrajzi viszonyai. *Földtani Közlöny*, 11ö(3-4), 512–539.
- Rögl, F. (1998). Palaeogeographic Considerations for Mediterranean and Paratethys Seaways ( Oligocene to Miocene ). *Annalen Des Naturhistorischen Museums in Wien*, 99A(April), 279–310.
- Royden, L., & Horváth, F. (1982). *The Pannonian Basin: A Study in Basin Development*, AAPG Memoir 45. AAPG.
- Sacchi, M., Horváth, F., & Magyari, O. (1999). Role of unconformity-bounded units in the stratigraphy of the continental record: a case study from the Late Miocene of the western Pannonian Basin, Hungary. In *Geological Society, London, Special Publications* (Vol. 156, pp. 357–390). London: Geological Society. <http://doi.org/10.1144/GSL.SP.1999.156.01.17>
- Sclater, J. G., Royden, L., Horváth F., Semken, S., Stegna, L. (1980). The formation of the intra-Carpathian basins as determined from subsidence data. *Earth and Planetary Science Letters*, 51, 139–162.
- Sylta, Ø. (2004). *Hydrocarbon migration modelling and expolration risk*. The Norwegian University of Science and Technology (NTNU), Trondheim, Norway. <http://doi.org/T14034>
- Sylta, Ø. (2008). Analysing exploration uncertainties by tight integration of seismic and hydrocarbon migration modelling. *Petroleum Geoscience*, 14(3), 281–289. <http://doi.org/10.1144/1354-079308-767>
- Sztanó, O., Magyar, I., & Horváth, F. (2007). Changes of water depth in Late

Miocene Lake Pannon revisited: the end of an old legend. *Geophysical Research Abstracts*, 9, 38897836.

- Sztanó, O., Szafián, P., Magyar, I., Horányi, A., Bada, G., Hughes, D. W., ... Wallis, R. J. (2013). Aggradation and progradation controlled clinotherms and deep-water sand delivery model in the Neogene Lake Pannon, Makó Trough, Pannonian Basin, SE Hungary. *Global and Planetary Change*, 103, 149–167. <http://doi.org/10.1016/j.gloplacha.2012.05.026>
- Tari, G., Dovenyi, P., Dunkl, I., Horvath, F., Lenkey, L., Stefanescu, M., ... Toth, T. (1999). Lithospheric structure of the Pannonian Basin derived from seismic, gravity and geothermal data. *The Mediterranean Basins: Tertiary Extension within the Alpine Orogen*, 156, 215–250. <http://doi.org/10.1144/GSL.SP.1999.156.01.12>
- Tari, G., & Horváth, F. (1992). Styles of extension in the Pannonian Basin. *Tectonophysics*, 208, 203–219.
- Tissott, B. P., & Welte, D. H. (1984). *Petroleum Formation and Occurrence*. Springer–Verlag (Second Edi). Berlin.
- Uhrin, A., Magyar, I., & Sztanó, O. (2009). Az aljzatdeformáció hatása a pannóniai üledékképződés menetére a Zalai-medencében. *Földtani Közlöny*, 139(3), 273–282.
- Uhrin, A., & Sztanó, O. (2012). Water-level changes and their effect on deepwater sand accumulation in a lacustrine system: a case study from the Late Miocene of western Pannonian Basin, Hungary. *International Journal of Earth Sciences*, 101(5), 1427–1440. <http://doi.org/10.1007/s00531-011-0741-4>
- Vakarcs, G., Vail, P. R., Tari, G., Pogácsás, G., Mattick, R. E., & Szabo, A. (1994). Third-order Middle Miocene-Early Pliocene depositional sequences in the prograding delta complex of the Pannonian Basin. *Tectonophysics*, 240(1-4), 81–106. [http://doi.org/http://dx.doi.org/10.1016/0040-1951\(94\)90265-8](http://doi.org/http://dx.doi.org/10.1016/0040-1951(94)90265-8)
- Wygrala, B. P. (1989). *Integrated study of an oil field in the southern Po basin, Northern Italy: Ph.D. dissertation*. University of Köln, Berichte Kernforschungsanlage Jülich 2313.
- ZetaWare. (2001). Retrieved from <http://www.zetaware.com/products/genesis>